Ubiquitin-specific Protease 7 Plays a Critical Role in Control of Lytic Infection and Cell Transformation by Human Adenovirus Type 5

Dissertation

Zur Erlangung des akademischen
Grades eines Doktors der
Naturwissenschaften (Dr. rer. nat.)

am Department Biologie
der Fakultät für Mathematik, Informatik und Naturwissenschaften
an der Universität Hamburg

Vorgelegt von
Emre Koyuncu
Aus Kayseri

March, 2009

Genehmigt vom Department Biologie
der Fakultät für Mathematik, Informatik und Naturwissenschaften
an der Universität Hamburg
auf Antrag von Professor Dr. T. DOBNER
Weiterer Gutachter der Dissertation:
Herr Professor Dr. W. DEPPERT
Tag der Disputation: 20. März 2009

Hamburg, den 04. März 2009

Professor Dr. Jörg Ganzhorn
Leiter des Departments Biologie

DR AVRIL ARTHUR-GOETTIG

Specializing in editing, writing, translations for biotechnology
molecular medicine and
life sciences

Roemerstrasse 25
80801 Muenchen
Germany
Tel: +49 (0)89 337 696
Fax: +49 (0)89 337 696
Email: avril@bioxpress.de

www.bioXpress.de

09.02.09

RE: the thesis submitted to the University of Hamburg
for the degree of DOCTOR OF PHILOSOPHY
by **Emre Koyuncu**

I hereby declare as a native English speaker and professional scientific writer that I have checked this thesis for grammatically correct English and the scientific quality of the language.

Signed,

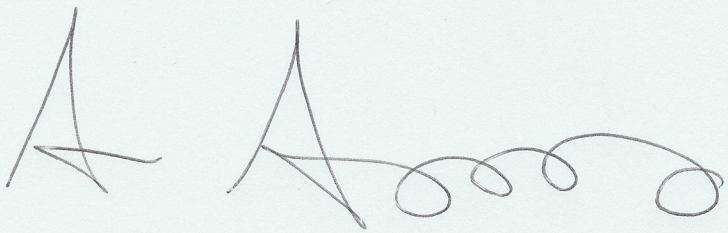

Dr. Avril Arthur-Goettig

Table of Contents

Abbreviations

Ad5	Adenovirus type 5
APS	Ammonium persulfate
aa	Amino acid
bp	Base pairs
BSA	Bovine serum albumin
Chx	Cycloheximide
C-terminus	Carboxy-terminus
dd.	Double distilled
DMSO	Dimethylsulfoxide
DTT	Dithiothreitol
EDTA	Ethylenediamine-tetraacetate
ffu	Fluorescence forming units
fw	*forward*
g	gravitational force
h	hour
h p.i.	hours post infection
Ig	Immunoglobulin
kb	Kilo base
kbp	Kilo base pair
K/ kDa	Kilo dalton
min	minute
moi	multiplicity of infection
MOPS	Morpholinopropansulfonic acid
nt	Nucleotide
N-terminus	Amino-terminus
OD	optical density
orf	open reading frame
PBS	phosphate buffered saline
rev	*reverse*
rpm	round per minute
RT	room temperature
s	second
SDS	sodium dodecyl sulfate
TEMED	N, N, N`, N`-Tetramethyl-ethylenediamine
Tris	Tris-(hydroxymethyl)-aminomethane
U	unit
vol	volume
v/v	volume per volume
w/v	weight per volume
wt	wild-type

1 Abstract

The ubiquitin-specific protease 7 (Usp7), also known as herpesvirus-associated ubiquitin-specific protease (HAUSP) is a critical component of the p53-Mdm2 stress response pathway and acts as a specific de-ubiquitinase for both p53 and Mdm2 and thus is important for p53 regulation. In addition, Usp7 was shown to interact with immediate-early proteins from Herpes simplex virus type 1 (Icp0) and Epstein-Barr virus (EBNA1), indicating that Usp7 may play an important role in the life cycle of several DNA viruses.

In the present study, Usp7 was identified as a novel interaction partner of the adenovirus type 5 (Ad5) E1B-55K protein. Similar to Icp0 and EBNA1, E1B-55K is a key regulator of Ad5 replication, and is required for maximal virus production. *In vitro* and *in vivo* binding assays demonstrated that E1B-55K binds to Usp7 with high affinity. The binding region mapped to a highly conserved motif located in the amino-terminal region of the Ad5 protein. Phenotypic analyses and functional studies using an Usp7-binding deficient E1B mutant virus and stable Usp7 knockdown cell lines, showed that Usp7 regulates E1B-55K lytic functions and contributes to efficient virus replication by increasing the stability of the viral protein. Surprisingly, these studies also demonstrated that Usp7 additionally contributes to Ad5 replication by an E1B-55K-independent mechanism. This activity of Usp7 involves the binding to and stabilization of the Ad5 DNA-binding protein (DBP). It appeared that binding to DBP occurs in the context of Usp7-positive PML-containing nuclear bodies (PML bodies), which form the origin of viral microenvironments of viral DNA replication and transcription. Finally, one-step growth curve experiments demonstrated that efficient virus growth is directly proportional to the Usp7 steady-state concentrations of the host cell. Thus, Usp7 is a key factor that is required for maximal virus production in permissive host cells, by

promoting the formation of viral transcription and replication centers through its interaction with E1B-55K and DBP in the context of PML bodies.

In addition, to its role in promoting virus replication, E1B-55K provides functions necessary for oncogenic transformation of primary mammalian cells in culture. It is generally considered that E1B-55K contributes to complete cell transformation by antagonizing apoptosis and growth arrest, which primarily result from the induction and metabolic stabilization of the tumor suppressor protein p53 by adenovirus E1A. These growth-promoting activities correlate with its ability to act as a transcriptional repressor that is targeted to p53-responsive promoters by binding to p53. Nonetheless, it has been hypothesized that the mode of action of E1B-55K during transformation may involve additional functions and other protein interactions. To test this model the role of Usp7 and p53 on E1A- plus E1B-mediated cell transformation was investigated by using an RNA interference approach. Similar to virus infected cells, the results of these experiments showed that Usp7 is required for efficient cell transformation of primary rat cells by affecting both p53 and E1B-55K steady-state concentrations indicating that Usp7 is an essential factor for Ad5 E1A and E1B-55K-mediated oncogenesis.

2 Introduction

2.1 Adenoviruses

2.1.1 Classification

Adenoviruses (Ads), belonging to *Adenoviridae* family, are known to infect a wide range of hosts including mammalian and other vertebrate species. The *Adenoviridae* family covers over 100 different Ad serotypes that are basically divided into two large genera according to the hosts they infect: *Aviadenoviruses* and *Mastadenoviruses* that infect birds and mammals, respectively. In addition, three smaller genera that infect a broader range of hosts were identified recently: *Atadenovirus* infecting avian, reptilian and ruminant hosts (Benkö and Harrach, 1998), *Siadenovirus* infecting amphibians, and the most recently identified from fish; *Ichtadenovirus* (Benkö et al., 2002). Human Ads comprise 52 different serotypes, and based on their oncogenicity in immunosuppressed experimental animals, hemagglutination properties and DNA sequence homologies, they are classified into 7 subgroups ranging from A to G (Berk, 2007) as summarized in Figure 1. Adenovirus type 2 and type 5 (Ad2 and Ad5) belonging to subgroup C are the most widely studied serotypes due to their non-oncogenic nature (Shenk, 2001).

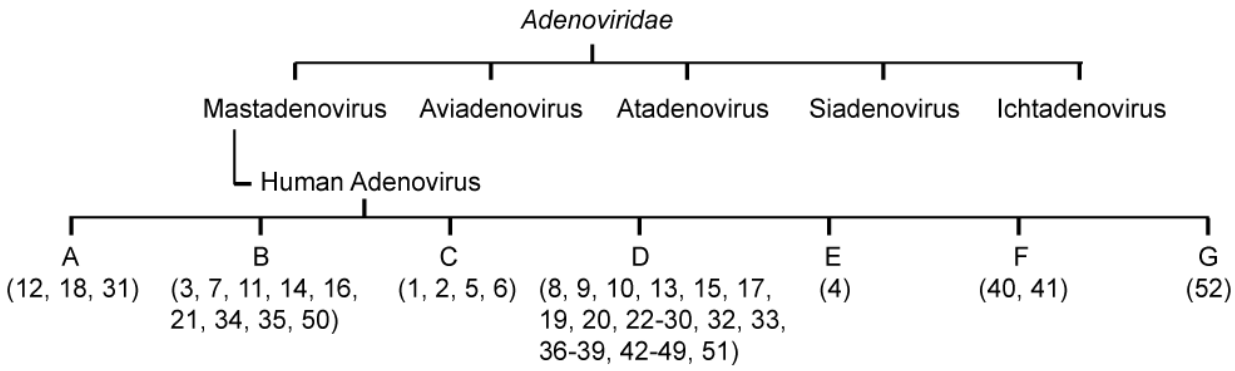

Figure 1. Classification of human Ad serotypes. Schematic representation of the *Adenoviridae*

family and its members. Serotypes belonging to each subgroup are indicated in parenthesis.

2.1.2 **Pathogenesis**

Human Ads cause lytic and persistent infections. Although most Ad infections are asymptomatic, some serotypes cause mild symptoms that are generally respiratory and gastrointestinal (Table 1). The diseases that have been associated with human Ads are acute respiratory disease (usually), pneumonia (occasionally), acute follicular conjunctivitis, epidemic keratoconjunctivitis, cystitis, and gastroenteritis (occasionally). In infants, pharyngitis and pharyngeal-conjunctival fever are common (Baron, 1996). Ads are also the second main causative agent of childhood diarrhea. The symptomatic Ad infections are usually observed in young children and followed by long-term effective immunity. Nevertheless, severe Ad infections may occur in immunosuppressed patients. In particular, Ad-induced hemorrhagic cystitis is a recognized cause of morbidity and mortality following allogeneic hematopoietic stem cell transplantation (Abe et al., 2003).

Table 1. The diseases that have been associated with different Ad serotypes.

Subgroup/Serotype	Clinical Syndromes
A, E	Acute respiratory illness, conjunctivitis, pharyngitis, pneumonia, acute/chronic appendicitis, respiratory tract infections
B (3, 7, 14, 21)	Fever, pharyngitis, acute respiratory illness, meningitis
C (1, 2, 5, 6)	Respiratory illness in children, rare in adults
D (8, 19, 37)	Epidemic keratoconjunctivitis
E (4)	Fever, pharyngitis, acute respiratory illness
F, G (40, 41)	Gastroenteritis

2.1.3 **Structure and genome organization**

Ads comprise an 80-110 nm large icosahedral protein capsid made up of 252 capsomeres: 240 hexons forming the faces and 12 pentons at the vertices. Each penton

extrudes a slender fiber (Baron, 1996). Ads are non-enveloped viruses containing a linear, double-stranded DNA genome within their capsid (Fig. 2). The genome is associated with two major core proteins and carries a terminal 55-kDa protein (TP) covalently attached to the 5′ end of each strand. These TPs are thought to protect the viral DNA. An important characteristic of an Ad capsid is the antenna-like extensions protruding from each corner of the icosahedron (i.e. 12 protrusions). These extensions take part in the absorption of the virus by the host cell receptor and are also responsible for the hemagglutination (Philipson, 1961). The prime receptor for human adenovirus is identical to that for coxsackie B virus and has been named the coxsackie/adenovirus receptor (CAR). After the attachment step, interaction between the penton base and αv integrins on the cell surface leads to internalization of the virus through endocytosis. Once inside the cell, and with help from the penton base, the virus escapes the endosome and translocates to the nuclear pore complex, where the viral DNA is released into the nucleus and transcription begins (Howitt et al., 2003).

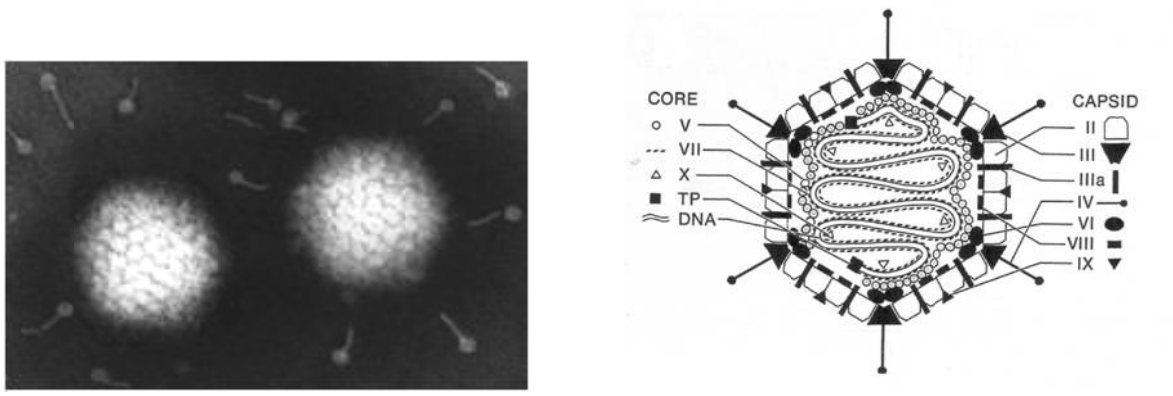

Figure 2. Electron microscopic image and schematic representation of adenovirus. An electron microscopic image of adenovirus (left) and a schematic representation of the adenovirus virion organization (right) (Stewart et al., 1993).

Human Ad serotypes have the same genomic organization and express a similar set of RNAs. The viral chromosome of the most widely studied subgroup C Ad serotypes 2 and 5 have characteristic linear, double-stranded DNA genomes of 36 kb in length (Shenk, 2001). The genome of Ad5 carries 9 different transcription units that encode 40

different polypeptides and two small RNAs (virus associated RNAs, VA RNAs). The genome of Ad5 is organized into early and late genes. Early genes are designated as E1-E4, and late genes, which are under the control of major late promoter (MLP), are designated as L1-L5. In addition, two RNAs encoded from the IX and IVa2 genes are observed at intermediate times of infection (Fig. 3).

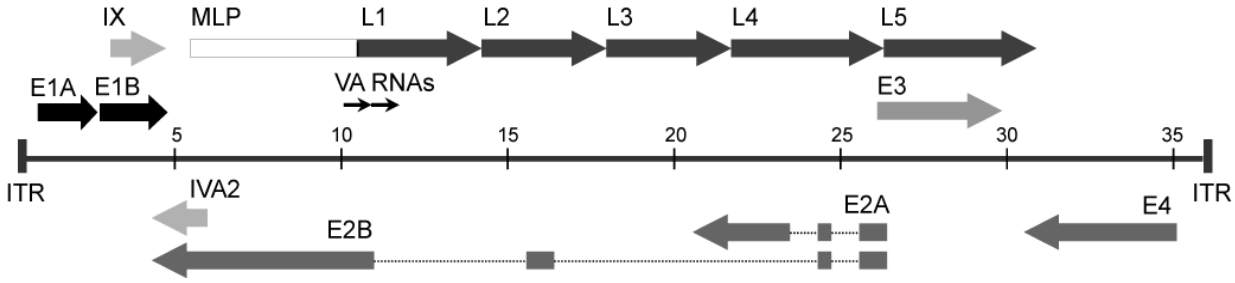

Figure 3. Genome organization of adenovirus type 5. The position of the early (E1A, E1B, E2A/B, E3, E4, IX und IVa2) and late genes (L1-L5), major late promoter (MLP), virus-associated RNAs (VA RNAs), and inverted terminal repeats (ITR) are shown. Numbers indicate the genomic coordinate in kb.

2.1.4 **Productive infection cycle**

Ads are able to infect a wide range of cell types, but their primary target is post-mitotically resting epithelium cells of the neck, nose, and throat area, the lungs and the digestive tract. In addition, Ads can also infect different types of cultured tumor and primary cells. Human Ads usually go through a productive (lytic) infectious cycle in human cells, which results in the death of these cells (Modrow, 1997; Shenk, 2001). As with most DNA viruses, the Ad infectious cycle is organized into early and late phases (Dobner and Kzhyshkowska, 2001). The early phase of infection is characterized by the production of viral mRNAs from the early transcription units, E1A, E1B, E2, E3 and E4. These transcription units produce multiple differentially spliced and polyadenylated mRNAs encoding a variety of distinct polypeptides.

Early viral gene products function in transcriptional and posttranscriptional regulation of viral and host RNA production, induce cell cycle progression, and

antagonize a variety of antiviral defense mechanisms, such as apoptosis and the immune response. Expression of early genes is required to establish an optimal environment for efficient viral DNA replication and the subsequent expression of the late genes. Following the onset of viral DNA replication, the late phase of infection starts. Ad late transcription is activated at three different transcription units, which encode structural polypeptides or are involved in packaging of viral genomic DNA. The Ad late coding regions are organized into a single large transcription unit, called the major late transcription unit (MLTU). The MLTU is controlled by the MLP and generates a large primary transcript that is processed by differential splicing into different mRNAs grouped into 5 families, L1-L5. Within a few hours of the onset of the late phase, several complex metabolic changes occur that ensure preferential synthesis of viral proteins and efficient assembly of progeny virions. The lytic cycle is completed approximately 24-36 hours after infection by the production of about 10,000 virus particles per infected cell. A schematic representation of the Ad productive infectious cycle is shown in Figure 4.

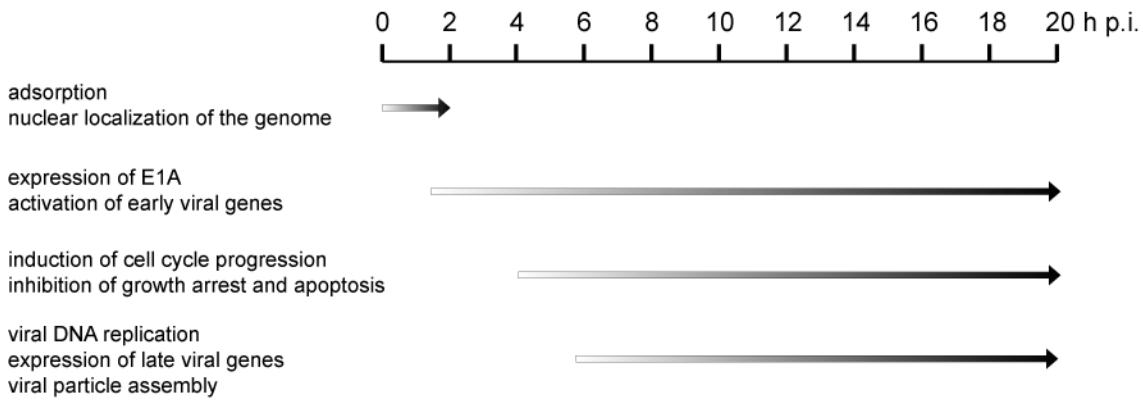

Figure 4. Adenovirus life cycle. Schematic representation of events during productive adenovirus infection. Time scale of each event is represented by an arrow. Corresponding time is indicated above as hours post infection (h p.i.).

2.1.4.1 **Adenovirus E1B-55K protein**

The Ad E1B region is required for efficient virus replication. At least five different gene products are encoded by this region during Ad5 infection (Sieber and Dobner, 2007). Among these, the large E1B product, E1B-55K is a 496 amino acid long

multifunctional phosphoprotein that is required for maximal virus production. It plays critical roles in both the early and late phase of adenovirus infection, and controls several processes including the inhibition of host cell defense responses and selective transport of late viral transcripts (Dobner and Kzhyshkowska, 2001). Multiple lytic activities of E1B-55K result from posttranslational modifications, continuous nucleocytoplasmic shuttling, and interactions with a variety of cellular and viral factors (Flint and Gonzalez, 2003).

In the early phase, E1B-55K contributes to the inhibition of apoptosis by interacting with p53. The expression of E1A causes the induction and stabilization of the tumor suppressor protein p53. E1B-55K binds to p53 and alone has the ability to block p53 mediated transcriptional activation (Kao et al., 1990; Sarnow et al., 1982a; Shen et al., 2001; Yew and Berk, 1992; Yew et al., 1990). In infected cells, the vast majority of E1B-55K is found in a complex with a small 34 kDa protein encoded by the E4 region, E4orf6. These two proteins promote the proteasomal degradation of p53 by forming a Cullin 5 based E3-ubiquitin ligase complex (Blanchette et al., 2004; Querido et al., 2001). This ubiquitin ligase complex is similar to previously characterized E3 ligase SCF complexes (Zheng et al., 2002) and VBC (Kamura et al., 2001). This complex also functions in targeting other proteins for degradation.

Infected cells recognize Ad double-stranded DNA genomes as double-strand breaks (DSBs) and actively attempt to repair them. One of the functions of E1B-55K is to inactivate DSB repair pathways (Weitzman and Ornelles, 2005). The E1B-55K/E4orf6 induced E3-ubiquitin ligase complex is responsible for degrading DNA repair pathway elements such as Mre11 of the MRN DNA DSB repair complex (Stracker et al., 2002) and DNA ligase IV, a protein essential for DNA repair in non-homologous end-joining (Baker et al., 2007). E1B-55K is thought to recognize target substrates for degradation, while E4orf6 appears to be important for the formation and assembly of the complex (Blanchette et al., 2004; Querido et al., 2001).

The late functions of E1B-55K mainly involve the simultaneous inhibition of host cell mRNA export and promotion of late viral mRNA transport from the nucleus to the cytoplasm (Beltz and Flint, 1979). Although the precise mechanism is still not clear, the ubiquitin ligase activity of the E1B-55K/E4orf6 complex has also been shown to be essential for selective late viral mRNA transport and host shut-off (Blanchette et al., 2008). It has been suggested that the majority of early and late functions of E1B-55K are due to viral E3-ubiquitin ligase activity (Blanchette et al., 2008; Woo and Berk, 2007).

Ads have several characteristics for being an oncolytic vector (Kirn, 2001a). First of all, they are able to rapidly replicate and destroy tumor cells. Identification of the lytic functions of E1B-55K has particular importance since an E1B-deleted Ad mutant, called *dl*1520 (or ONYX-015 for commercial reasons), has been shown to be a potent oncolytic therapy vector (Bischoff et al., 1996). In theory, a virus lacking E1B-55K expression should be defective for replication in normal, p53 positive cells, but still be able to replicate in tumor cells lacking a functional p53 protein, as is the case in the majority of human tumors. The selective replication of dl1520 has been shown in different tumor cell lines and a number of clinical trials have been carried out in patients with head and neck cancer (Khuri et al., 2000; Nemunaitis et al., 2000). However, it has been shown in several different studies that tumor selectivity of *dl*1520 does not correlate with the p53 status. This virus can still replicate in several different tumor cell lines containing wt p53 (Goodrum and Ornelles, 1999; Hall et al., 1998; Harada and Berk, 1999; Rothmann et al., 1998; Turnell et al., 1999). Understanding the functions of E1B-55K in productive infection cycle is key to developing an effective oncolytic virus.

2.1.4.2 **Adenovirus DNA binding protein**

Adenovirus DNA binding protein (DBP) is a 72 kDa protein encoded by E2A transcription. DBP is detectable as early as 2 hours after infection and is continuously

synthesized throughout the infection cycle. It accumulates in the nuclei of infected cells at both early and late times (Voelkerding and Klessig, 1986). Multiple functions have been assigned to this protein, ranging from viral DNA replication (Cleat and Hay, 1989; Lindenbaum et al., 1986; Stuiver and van der Vliet, 1990; Voelkerding and Klessig, 1986) to cell transformation (Rice et al., 1987a). DBP contains at least two functionally distinct domains in its N- and C-terminus separated by a putative hinge region of hydrophilic residues (Klein et al., 1979; Linne and Philipson, 1980) The N-terminal domain of the protein is poorly conserved among different serotypes and dispensable for the functions of DBP in viral DNA replication (Cleghon and Klessig, 1986). However, this domain is required for efficient late viral gene expression and determines the host range specificity of human Ad infection. Infection of monkey cells with human Ads is abortive due to reduced late mRNA production. Particularly, in these cells the fiber mRNA shows altered splicing and diminished translation (Anderson and Klessig, 1984). Interestingly, a panel of mutant human Ad isolates that can replicate in monkey cells efficiently all have an identical mutation within the E2A gene leading to a single amino acid exchange in DBP where histidine at position 130 is replaced by a tyrosine residue (Anderson, 1981; Kruijer et al., 1981).

The C-terminal domain of the protein is highly conserved and has the ability to bind single stranded DNA and RNA (Ariga et al., 1980; Kitchingman, 1985; Tsernoglou et al., 1985). This domain is involved in the initiation of Ad DNA replication. After initiation, DBP functions in the elongation phase by increasing the processivity of the Ad DNA polymerase (Pol). DBP also functions in the regulation of early viral gene expression (Babich and Nevins, 1981b; Carter and Blanton, 1978b) and it is one of the key proteins that regulate both the early and late phase of Ad infection.

2.1.5 **Oncogenic potential of human adenoviruses**

The oncogenic potential of human Ads was first proposed by Trentin and coworkers. They showed that human Ad serotype 12 (Ad12) can induce malignant transformation in newborn hamsters (Trentin et al., 1962). This initial discovery revealing the

oncogenic potential of human Ads inspired intense research on these viruses, which continued up to the present. Today, most of the genes and their products involved in Ad transformation, as well as the differences in oncogenicity among different serotypes have been identified (Endter and Dobner, 2004). According to the frequency and time required to produce tumors in rodents, human serotypes can be subdivided into highly oncogenic, weakly oncogenic and non-oncogenic Ads (Table 2). Tumors in rodents induced by highly oncogenic subgroup A and weakly oncogenic subgroup B Ads develop at the site of injection, and depending on the route of administration vary greatly in type, including neurogenic, neuroepithelial, medulloblastic and adenocarcinomatous tumors (Graham et al., 1984). In contrast, serotypes 9 and 10 belonging to subgroup D develop estrogen-dependent mammary tumors at 100% frequency within 3 months of subcutaneous or intraperitonal injection in female Wistar-Furth rats (Ankerst and Jonsson, 1989; Javier et al., 1991). The differences in the oncogenicity among different Ad serotypes are related to the genetic background of the host animal, as well as the susceptibility of the transformed cell to the host immune system (van der Eb and Zantema, 1992; Williams et al., 1995). Despite these differential oncogenicities in animals, all tested serotypes are able to transform rodent cells in culture with similar efficiencies (McBride and Wiener, 1964).

Contrary to their oncogenic potential in animals and high transforming potential in cultured rodent cells, Ad-mediated transformation of primary human cells in culture is a very inefficient process (Hahn et al., 1999). To date, Ads could never be convincingly associated with malignant diseases in humans either (Chauvin et al., 1990; Mackey et al., 1979; Mackey et al., 1976). However, a very recent report showed the presence of Ad DNA in pediatric brain tumors (Kosulin et al., 2007). In addition, analysis of Guthrie cards of children who later developed acute lymphoblastic leukemia showed an increased frequency of detected Ad DNA (Gustafsson et al., 2007). These studies suggest a potential role for Ads in oncogenesis in humans.

Table 2. Oncogenicity of Ad serotypes in rodents.

ONCOGENICITY IN RODENTS	SUBGROUP	SEROTYPE	TUMOR TYPE
Highly oncogenic	A	12, 18, 31	undifferentiated sarcomas
	D	9, 10	fibroadenomas
Weakly oncogenic	B	3, 7, 11, 14, 16, 21, 34, 35	undifferentiated sarcomas
Non-oncogenic	C - F	**C** (1, 2, 5, 6); **D** (8, 13, 15, 17, 19, 20, 22-30, 32, 33, 36-39, 42-49, 51); **E** (4); **F** (40, 41)	none

2.1.5.1 **The Role of the E1 region in transformation**

Most Ad tumors, tumor cell lines and transformed cell lines are characterized by the persistence of chromosomally integrated viral DNA and the expression of viral specific antigens (Graham et al., 1984). Correspondingly, Ad transformation follows the classical concept of viral oncogenesis where viral genes persist within the transformed cells. Of these viral genes, the E1 region is almost invariably retained in all virus transformed cells. Likewise, in most completely transformed cell lines that were established by transfecting subgenomic viral DNA fragments, the E1 sequences are retained in an integrated form. Therefore, the E1 region is assigned to mediate the initiation of transformation and to provide functions required to maintain some of the phenotypic characteristics of the transformed cell (Endter and Dobner, 2004). As mentioned previously, E1 gene products, E1A and E1B, are necessary and sufficient for oncogenic transformation of primary cells. However, E1A proteins (12S and 13S) mediate the most critical step in cell transformation. The transforming and oncogenic properties of E1A proteins in non-permissive cells derive from their ability to deregulate normal cell growth in order to establish productive infection and modulate the interaction of the infected cell with the immune system of the host. For instance, E1A proteins stimulate entry into S phase of the cell cycle to create optimal conditions

for productive virus infection in non-proliferating human cells (Endter and Dobner, 2004).

To accomplish cell growth deregulation, E1A proteins must be able to bind to, and modulate the functions of key regulators controlling cell cycle progression and programmed cell death (Gallimore et al., 1984). The most notable example of such proteins is the retinoblastoma tumor suppressor gene product (pRb). Binding of E1A proteins to Rb family members dissociates them from the E2F family of transcription factors, resulting in the activation of cellular genes containing E2F-binding sites, and induction of cell cycle progression (Cress and Nevins, 1996). In the course of an abortive infection in non-permissive cells, these same growth deregulatory functions can lead to immortalization or transformation.

However, in the majority of E1A-immortalized cells the transformation is incomplete (Gallimore et al., 1984), and full manifestation of the transformed phenotype requires co-expression of E1B (Ruley, 1983). Studies using virus mutants carrying lesions in the E1B transcription subunit led to the hypothesis that both major E1B gene products, E1B-19 kDa and E1B-55K, are required for complete transformation (van der Eb and Zantema, 1992). Although some results suggested that E1B-19 kDa protein is not definitely needed for efficient transformation (Telling and Williams, 1993), it can be said that both E1B proteins contribute to complete cell transformation at least in part by antagonizing apoptosis and growth arrest (Debbas and White, 1993).

The Ad5 E1B-55K protein has several activities that inhibit p53 function. It binds to the amino-terminal transactivation domain of p53 (Kao et al., 1990), blocks the ability of p53 to activate transcription (Yew et al., 1994), and sequesters p53 in large cytoplasmic structures (Zantema et al., 1985a). It appears that E1B-55K functions as a transcriptional repressor that is targeted to p53-responsive promoters by binding to p53: its transforming potential correlates with its ability to act as a direct transcriptional repressor (Yew and Berk, 1992). In addition, E1B-55K's contribution to

the transformation process may involve further functions and other protein interactions. For example, E1B-55K interacts with the E1B-associated protein 5 (E1B-AP5) and nuclear body associated promyelocytic leukemia (PML) protein, both of which can individually suppress transformation of baby rat kidney (BRK) cells (Kzhyshkowska et al., 2001; Nevels et al., 1999). Modification of these cellular factors by E1 proteins is required to enhance transformation. In conclusion, E1 region is the main determinant for the oncogenic potential of Ads, and the E1A and E1B transcription units are essential for Ad-mediated oncogenic transformation.

2.2 Ubiquitination and de-ubiquitination

Ubiquitination is a post-translational modification involved in the regulation of numerous cellular functions, including cell cycle progression, signal transduction, transcription, intranuclear targeting, and viral infection (Ciechanover and Schwartz, 1998; Haglund and Dikic, 2005). The ubiquitination process involves covalent attachment of the small (76 amino acid), well-conserved ubiquitin protein to the amino group of internal lysine residues in target proteins. This modification is controlled by a three-step reaction: Activation of ubiquitin by E1 enzymes, conjugation to E2 enzymes, and attachment of ubiquitin to the target protein by E3-ubiquitin ligases that confer substrate specificity. Monomeric ubiquitin is able to modify a protein (mono-ubiquitination) and this type of modification has been shown to modulate intracellular trafficking and transcriptional regulation (Hicke, 2001; Salmena and Pandolfi, 2007). Alternatively, it can also be conjugated to preceding ubiquitin moieties to form a ubiquitin chain, a process called polyubiquitination (Haglund and Dikic, 2005; Haglund et al., 2003). A major form of polyubiquitination occurs by the attachment of ubiquitin moieties to the lysine at position 48 of the previously conjugated ubiquitin molecule, and a substrate modified by such a polyubiquitin chain is recognized by the 26S proteasome complex and subsequently degraded (Ciechanover and Schwartz, 2002; Duan et al., 2004). It has also been reported that the ubiquitin chains are conjugated to the six other lysine residues in

ubiquitin, forming atypical ubiquitin chains, and this type of ubiquitination has non-proteolytic roles (Ikeda and Dikic, 2008). Nevertheless, the regulation of selective protein degradation in the cell, which is largely mediated by polyubiquitination, is the major function of this posttranslational modification.

The conjugation of ubiquitin to target proteins is a reversible process. The removal of ubiquitins is referred as de-ubiuitination and catalyzed by cysteine protease activity of de-ubiquitinating enzymes (DUB). The DUBs comprise two groups: The ubiquitin-C-terminal hydrolyases (UCHs) and ubiquitin-specific proteases (USPs). The UCHs are small enzymes (20-30 kDa) and generally involved in cleaving ubiquitin from small processed peptides. The USPs are much larger in size (60-300 kDa) and thought to have more specific functions in the cell. De-ubiquitination and therefore USPs are central to all processes regulated by ubiquitin. Non-proteolytic functions of mono- and polyubiquitination, as well as the hydrolysis of polyubiquitin chains resulting in targeted proteins being rescued from proteasomal degradation are regulated by these enzymes (Wilkinson, 2000; Wing, 2003). The human genome encodes over 60 members of the USP family (Nijman et al., 2005). The large number of these enzymes suggests they may exert substrate specificity analogous to the E3 ligases and have discrete biological roles (Nalepa et al., 2006). Two recent examples of USPs showing substrate specificity emphasized the importance of these enzymes in the regulation of cell growth: the tumor suppressor CYLD, which is mutated in individuals with cylindromatosis (Bignell et al., 2000) and regulates NF-KB signaling (Brummelkamp et al., 2003; Kovalenko et al., 2003; Trompouki et al., 2003), and ubiquitin-specific protease 7 (Usp7) regulating the p53 pathway (Li et al., 2004; Li et al., 2002; Meulmeester et al., 2005a).

2.3 Ubiquitin-specific protease 7

The human ubiquitin-specific protease 7 (Usp7; also known as herpes-virus-associated ubiquitin specific protease, HAUSP) comprises 1102 amino acids with a molecular

weight of 135 kDa (Everett et al., 1997). It is an evolutionary conserved protein in mammals. Its mouse and rat orthologues show 98.6% amino acid identity with human Usp7 (Lee et al., 2005; Lim et al., 2004). Usp7 is structurally organized into four domains. The catalytic domain of Usp7 comprises amino acids 208-560 (Hu et al., 2002). Surrounding this domain, Usp7 contains one N- and two C-terminal protein binding regions (Holowaty et al., 2003a). N-terminal domain has attracted particular attention due to its similarity to tumor necrosis factor-associated factor (TRAF) domains that mediate protein-protein interactions (Zapata et al., 2001). Three well-known interaction partners of Usp7 have been shown to interact with this region, namely p53, Mdm2, and EBNA1 protein of Epstein-Barr virus (EBV) (Holowaty et al., 2003b; Hu et al., 2006; Sheng et al., 2006).

Usp7 was first identified by virtue of its interaction with herpes simplex virus type-1 (HSV-1) immediate early protein Icp0 (Everett et al., 1997). Icp0 is required for efficient initiation of lytic viral infection and reactivation from latency (Everett, 2000; Everett, 2004; Hagglund and Roizman, 2004). A major biological function of Icp0 is its E3-ubiquitin ligase activity. This activity leads to the degradation of cellular proteins, including the components of promyelocytic leukemia bodies (PML bodies): PML and Sp100 (Boutell and Everett, 2003; Boutell et al., 2003; Boutell et al., 2002; Hagglund et al., 2002). Similar to many E3-ubiquitin ligases, Icp0 also has auto-ubiquitination activity. It has been shown that Usp7 protects Icp0 from auto-ubiquitination and greatly increases its stability *in vivo* (Canning et al., 2004) Additionally, targeted disruption of the Usp7-Icp0 interaction results in reducing Icp0's ability to stimulate lytic replication as well as its functions in virus growth (Everett et al., 1999). However, the functional relation between these two proteins is not fully understood.

Usp7 is also targeted by another herpes virus protein, the EBNA1 protein of EBV (Holowaty et al., 2003b). EBNA1 is a DNA binding protein required for the replication and segregation of EBV DNA episomes in dividing cells. It enhances viral latency genes and therefore, distinct from Icp0, is essential for viral persistence (Reisman and

Sugden, 1986; Wilson et al., 1996). In addition, EBNA1 is believed to play a role in cellular immortalization by unknown mechanisms. Usp7 has been shown to de-ubiquitinate EBNA1 *in vitro*, although a mutation in EBNA1 eliminating the Usp7 interaction region has no effect on the viral protein's stability *in vivo*. Interestingly, EBNA1 binds to the same region of Usp7 as the tumor suppressor protein p53, but with several-fold higher affinity (Holowaty et al., 2003b). One of the potential functions of the EBNA1-Usp7 interaction could be inhibiting the interaction between Usp7 and p53.

The critical cellular functions of Usp7 started to emerge after the discovery that Usp7 specifically binds to and de-ubiquitinates both the p53 protein (Li et al., 2002) and its negative regulator Mdm2 (Cummins et al., 2004; Cummins and Vogelstein, 2004; Li et al., 2004; Meulmeester et al., 2005a). p53 is a well known tumor suppressor, promoting cell cycle arrest or apoptosis upon stress signals, including DNA damage and oncogenic conditions (Jin and Levine, 2001). The p53 levels in the cell are tightly regulated by ubiquitination and de-ubiquitination. In unstressed cells, the E3-ubiquitin ligase Mdm2 mediates the ubiquitin-dependent proteolysis of p53 and keeps the levels of p53 very low (Haupt et al., 1997a; Kubbutat et al., 1997). The expression of Mdm2 is induced by p53, thus creating an autoregulatory negative feedback loop. The importance of this regulatory pathway is highlighted by the fact that more than 50% of all human tumors contain a deletion or mutation in the p53 gene (Aylon and Oren, 2007) and approximately 10% of all human tumors with wild-type p53 overexpress Mdm2 (Juven-Gershon and Oren, 1999; Momand et al., 2000). Moreover, Mdm2 knockout mice suffer embryonic lethality in a p53 dependent manner (Jones et al., 1995).

Mdm2 induced ubiquitination of p53 can be reverted by Usp7 and ectopical expression of Usp7 results in p53 stabilization and induction of growth arrest ((Li et al., 2002). However, Usp7 also de-ubiquitinates Mdm2, and without the function of Usp7, Mdm2 is a very unstable protein due to its auto-ubiquitination activity. The

counter activities of Usp7 on p53 can be exemplified by the finding that partial reduction of Usp7 by RNA interference (RNAi) destabilizes p53, whereas nearly complete and complete ablation of Usp7 strongly stabilizes p53 due to destabilization of Mdm2 (Becker et al., 2008; Cummins et al., 2004; Cummins and Vogelstein, 2004; Li et al., 2004). The level of self and target ubiquitination activity of Mdm2 determines the efficacy of p53 ubiquitination. Thus by acting as a de-ubiquitinase for both Mdm2 and p53, Usp7 is central to the regulation of this critical pathway (Cummins et al., 2004; Cummins and Vogelstein, 2004; Li et al., 2004; Meulmeester et al., 2005a; Tang et al., 2006).

Recent structural and biochemical analyses have provided insights into this complicated regulatory pathway. It has been shown that Mdm2 and p53 can associate with the same site in Usp7 and these interactions are mutually exclusive (Hu et al., 2006; Sheng et al., 2006). In unstressed cells, Mdm2 binds to Usp7 with a higher affinity than p53, pointing to Mdm2 as the preferred substrate of Usp7. However, under stress conditions, Usp7 dissociates from Mdm2 and mainly associates with p53. This causes the self-ubiquitination and degradation of Mdm2 and at the same time stabilization of p53 (Tang et al., 2006).

Another important regulator of p53 is a protein called MdmX. This shows high structural homology to Mdm2 but lacks the E3-ubiquitin ligase activity (Marine and Jochemsen, 2004; Meulmeester et al., 2005b). MdmX can potentially inhibit p53-stimulated transcription. The importance of MdmX in p53 regulation is highlighted by the observation that deletion of the MdmX gene, like Mdm2, causes embryonic lethality in mice, which can be rescued by deletion of p53 (Finch et al., 2002; Migliorini et al., 2002; Parant et al., 2001). Overexpression of MdmX was found in approximately 30% of human tumor cell lines, correlating in most cases with the presence of wild-type p53 (Ramos et al., 2001). Interestingly, Usp7 also binds to and stabilizes MdmX by de-ubiquitination. It has been shown that impaired de-ubiquitination of MdmX by Usp7 contributes to stress-induced degradation of MdmX (Meulmeester et al., 2005a).

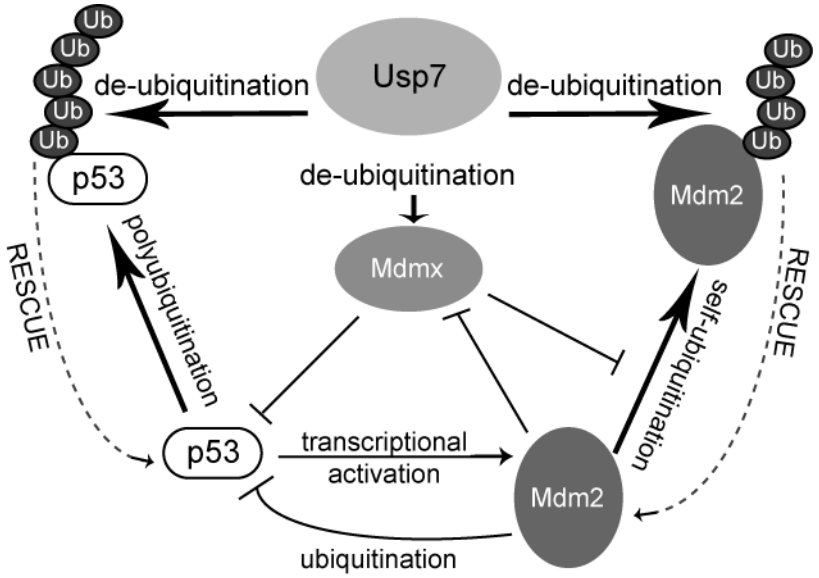

Figure 5. A model for regulating the stability of p53, Mdm2, and MdmX by Usp7. Mdm2 ubiquitinates p53, MdmX and has self-ubiquitinating activity. MdmX blocks the self-ubiquitination of Mdm2 and inhibits p53. Usp7 can de-ubiquitinate p53, Mdm2, and MdmX (Cheon and Baek, 2006).

In summary, Usp7 plays crucial roles in the regulation of cell proliferation and apoptosis by acting as a de-ubiquitinase for three key players in the p53 pathway: p53 itself, Mdm2 and MdmX. Moreover, Usp7 is targeted by the regulatory proteins of two different herpes viruses, emphasizing the importance of this protease in cellular events.

3 Materials

3.1 Cells

3.1.1 Bacteria strains

The following *E.coli* strains were used in this study.

STRAIN	CHARACTERISTICS
DH5	*sup*E44, Δ*lac*U169, (φ80d*lacZ*Δ*M15*), *hsd*R17, *rec*A1, *end*A1, *gyr*A96, *thi*-1, *rel*A1 (Hanahan, 1983)
TOP10	F-, *mcr*A, Δ(*mrr-hsd*RMS-*mcr*BC), ϕ80*lacZ*ΔM15, Δ*lac*X74, *rec*A1, *ara*D139, Δ(*ara-leu)*7697, *gal*U, *gal*K, *rps*L (Str^R), *end*A1, *nup*G (Invitrogen)
TOPP™ 3	*rif*r [F'*pro*AB *lac*IqZΔM15, Tn10 (*tet*r)] *kan*r (Hatt et al., 1992)
XL1-Blue	*rec*A1, *end*A1, *gyr*A96, *thi*1, *hsd*R17, *sup*E44, *rel*A1, lac, [F'*pro*AB, *lac*I^{q}ZΔM15, *Tn10* (Tet^r)] (Bullock, 1987)
XL2-Blue	*rec*A1, *end*A1, *gyr*A96, *thi*-1, *hsd*R17, *sup*E44, *rel*A1, lac, [F'*pro*AB, *lac*I^{q}ZΔM15, *Tn10* (Tet^r), Amy, Cam^r] (Bullock, 1987)

3.1.2 Mammalian cell lines

293 and 911 cells were used for the generation, propagation and titration of virus mutants. H1299 cells were used in transfection experiments, and general virus characterization was carried out using A549, H1299 and their knockdown derivative cells. Primary baby rat kidney cells were prepared as described in the Methods Section. HCT116 and HCT116 Usp7 -/- cells were kindly provided by Bert Vogelstein.

CELL LINE	CHARACTERISTICS
293	Ad5-transformed, human embryonic kidney cell line; the E1 region is integrated into the genome and the adenoviral E1A and E1B gene products are stably expressed (Graham et al., 1977). Helper cell line.
911	Ad5-transformed, human embryonic retinoblastoma cell line; the E1 region is integrated into the genome and the adenoviral E1A and E1B gene products are stably expressed (Fallaux et al., 1996). Helper cell line.
A549	Human lung carcinoma cell line, wild-type p53 (Giard et al., 1973; Lehman et al., 1991).
APU5	A549 derived shUsp7 expressing monoclonal cell line. This work.
APU6	A549 derived shUsp7 expressing monoclonal cell line. This work.
BRK1	Primary baby rat kidney cells, spontaneously immortalized in culture (Endter et al., 2005).
C33A	Human cervical carcinoma cell line, mutated p53 (Scheffner et al., 1991).
H1299	Human lung carcinoma cell line, p53 negative (Mitsudomi et al., 1992).
HPU2	H1299 derived shUsp7 expressing monoclonal cell line. This work.
HCT116	Human colon carcinoma cell line, wild-type p53 (Bunz et al., 1999).
HCT116 Usp7 -/-	HCT116 derived Usp7 knockout cell line (Cummins et al., 2004).
RKO	Human colon carcinoma cell line, wild-type p53 (Baker et al., 1990).
Saos-2	Human Osteosarcoma cell line, p53 negative (Chandar et al., 1992; Diller et al., 1990).
AB718	E1A/E1B-55K/pSuper-empty-vector transformed BRK cell line. This work.
AB719	E1A/E1B-55K/pSuper-empty-vector transformed BRK cell line. This work.
AB720	E1A/E1B-55K/pSuper-empty-vector transformed BRK cell line. This work.
Ashp721	E1A/pSuper-pSuper-shp53 transformed BRK cell line. This work.
Ashp722	E1A/pSuper-pSuper-shp53 transformed BRK cell line. This work.

Ashp723	E1A/pSuper-pSuper-shp53 transformed BRK cell line. This work.
ABshp724	E1A/E1B-55K/pSuper-pSuper-shp53 transformed BRK cell line. This work.
ABshp725	E1A/E1B-55K/pSuper-pSuper-shp53 transformed BRK cell line. This work.
ABshp726	E1A/E1B-55K/pSuper-pSuper-shp53 transformed BRK cell line. This work.
ABshU729	E1A/E1B-55K/pSuper-pSuper-shUsp7 transformed BRK cell line. This work.
ABshU730	E1A/E1B-55K/pSuper-pSuper-shUsp7 transformed BRK cell line. This work.

3.2 Animals

Transformation assays (4.6.2) were conducted in baby rat kidney (BRK) cells. Kidneys were obtained from 6-day-old Sprague Dawley rats (Charles River, Kißlegg).

3.3 Adenoviruses

In this work, Ad5 L4-100K virus mutants were generated and characterized. Wild-type virus (H5*dl*309 and H5*pg*4100) and other mutant viruses were propagated from virus stocks established as referred in the table below.

ADENOVIRUS	CHARACTERISTICS
Ad-GFP	GFP-expressing Ad5 virus (SC1), kindly provided by F. U. Müller.
***dl*1520**	Ad2/Ad5-chimeric virus, a stop codon at aa position 3 and a 827 bp deletion (nt 2496-3323) were inserted in E1B-55K gene (Barker and Berk, 1987).
H5*pg*4100	Wild-type Ad5 carrying a 1863 bp deletion (nt 28602-30465) in the E3 reading frame (Kindsmuller et al., 2007).
H5*pm*4102	E1B-55K mutant carrying a single aa exchange in SCM (K104R) in a H5*pg*4100 backbone (Kindsmüller, 2002).

H5*pm*4185	E1B-55K mutant carrying 2 aa exchanges in UBM (P70T/S73A) in a H5*pg*4100 backbone (This work).

3.4 Nucleic acids

3.4.1 Oligonucleotides

The following oligonucleotides were used as primers for sequencing, PCR amplification, restriction site insertion, and site-directed mutagenesis reactions. Oligonucleotides used in this study were ordered from Metabion, and numbered according to the *Filemaker Pro* data bank of the group. The target sequences of shRNAs are underlined.

#	NAME	SEQUENCE	PURPOSE
64	**E1B bp2043 fw**	5′-CGCGGGATCCATGGAGCGAAGAAACCCATC TGAGC-3′	sequencing
110	**E1B 361-389 rev**	5′-CGGTGTCTGGTCATTAAGCTAAAA-3′	PCR
635	**pcDNA3 fw**	5′-ATGTCGTACAACTCCGC-3′	sequencing
636	**pcDNA3 rev**	5′- GGCACCTTCCAGGGTCAAG -3′	sequencing
1278	**pSuper fw**	5′- GGAAGCCTTGGCTTTTG -3′	sequencing
1279	**pSuper rev**	5′- GATGACGTCAGCGTTCG -3′	sequencing
1297	**shRNA Usp7 fw**	5′-GATCCCCGGCAACCTTTCAGTTCACTTTCAAGAG AAGTGAACTGAAAGGTTGCCTTTTTGGAAA-3′	cloning
1298	**shRNA Usp7 rev**	5′-AGCTTTTCCAAAAAGGCAACCTTTCAGTTCACTTC TCTTGAAAGTGAACTGAAAGGTTGCCGGG-3′	cloning
1359	**pSG5 fw**	5′-CCTACAGCTCCTGGGCAACG-3′	sequencing
1360	**pBSSK- fw**	5′- GGTAACGCCAGGGTTTTCC-3′	sequencing
1390	**shRNA p53 M/R fw**	5′-GATCCCCGGACAGCTTTGAGGTTCGTTTCAAGAG AACGAACCTCAAAGCTGTCCTTTTTGGAAA -3′	cloning
1391	**shRNA p53M/R rev**	5′-AGCTTTTCCAAAAAGGACAGCTTTGAGGTTCGTTC	cloning

		TCTTGAAACGAACCTCAAAGCTGTCCGGG -3′	
1407	**E1B P70T/S73A fw**	5′-CCGAGAGCCGGACTGGACCCGCGGGAATGAATG-3′	mutagenesis
1408	**E1B P70T/S73A rev**	5′-CATTCATTCCCGCGGGTCCAGTCCGGCTCTCGG-3′	mutagenesis
1409	**E1B E65V/S68G fw**	5′-GCAGAGCCCATGGCCCGAGGCCGGCCTGGAC-3′	mutagenesis
1410	**E1B E65V/S68G rev**	5′-GTCCAGGCCGGCCCTCGGGGACCATGGGCTCTG C-3′	mutagenesis
1411	**E1B A13V/S16L fw**	5′- GGGTACCTGTGGATTTTGGCCATGCATCTG -3′	mutagenesis
1412	**E1B A13V/S16L rev**	5′-CAGATGCATGGCCAAGAAATCCACAGGTACCC-3′	mutagenesis
1413	**E1B A51T/S54G fw**	5′-GCAGCAGCAGCACAGGAGGAGCCAGGCGGCG G-3′	mutagenesis
1414	**E1B A51T/S54G rev**	5′-CCGCCGCCTGGCTCCTCCTGTGCTGCTGCTGC -3′	mutagenesis
1415	**Usp7 siR-r fw**	5′-CCAGTTGGCGCTCCGAAGCGACATTCCAATTTA CCGTGGAGCGCTTCAGC-3′	mutagenesis
1416	**Usp7 siR-r rev**	5′-GCTGAAGCGCTCCACGGTAAATTGGAATGTC GCTTCGGAGCGCCAACTGG-3′	mutagenesis
1592	**pSuper II fw**	5′-GGAAGATTGGTTGTGAGG-3′	sequencing

3.4.2 Vectors

The following vector plasmids were used for cloning and transfection experiments. They were numbered according to the *Filemaker Pro* data bank of the group.

#	NAME	CHARACTERISTICS	REFERENCE
101	**pGEX4T-1**	Bacterial expression vector, GST-tag	PL-Pharmacia
136	**pcDNA3**	Expression vector for mammalian cells, CMV promoter	Invitrogen
208	**pSuper.retro.puro**	Expression vector for shRNAs, H1 promoter	OligoEngine
1257	**pPG-S3**	E1-region subcloning vector	Stock of the group

3.4.3 Recombinant plasmids

The following recombinant plasmids were cloned in this work, unless stated

otherwise in the table, and numbered according to the *Filemaker Pro* data bank of the group.

#	NAME	VECTOR	INSERT	REFERENCE
129	**pGEX-E1B wt**	pGEX-2TK	Ad5 E1B-55K	Stock of the group
578	**pGEX E1B dlQ163-D496**	pGEX-4T-1	E1B (aa 1-162)	Stock of the group
1022	**pcDNA3-E1B K104R**	pcDNA3	Ad5 E1B-55K	Stock of the group
1154	**Ad5pTG-S2 (Noah)**	pTG	Ad5 genome	Stock of the group
1174	**pcDNA3-E1B V103D**	pcDNA3	Ad5 E1B-55K	Stock of the group
1199	**pGEX-Usp7-TD**	pGEX-2T	Usp7 TD	J. Zapata
1319	**pcDNA-E1B-55K**	pcDNA3	Ad5 E1B-55K	Stock of the group
1418	**pGEX -E1BZ**	pGEX-2T	E1B (aa 83-188)	Stock of the group
1496	**pcDNA-E1A 12S**	pcDNA3	E1A 12S	Stock of the group
1519	**pGEX-E1B 93R**	pGEX-2T	E1B 93R	Stock of the group
1520	**pGEX-E1B 156R**	pGEX-2T	E1B 156R	Stock of the group
1624	**pGEX-E1B 93R 1-82**	pGEX-2T	E1B (aa 1-82)	Stock of the group
1642	**pSuper-shRNA-Usp7**	pSuper.retro.puro	shUsp7	this work
1653	**pSuper-shRNA-p53**	pSuper.retro.puro	shp53	this work
1744	**His-Tag-Ub**	BSSK	Ubiquitin	S.Müller
1745	**His-sumo-1-GG**	pSG5	Sumo-1-GG	S. Müller
1813	**pGEX-Usp7-CD**	pGEX-2T	Usp7 CD	Stock of the group
1814	**pGEX-Usp7-C1**	pGEX-2T	Usp7 C1	Stock of the group
1815	**pGEX-Usp7-C2**	pGEX-2T	Usp7 C2	Stock of the group
1837	**Myc-Usp7-siR-r**	pcDNA3	Usp7 siR-r	this work
1878	**Myc-Usp7**	pcDNA3	Usp7	J. Zapata
1841	**pcDNA3-E1B P70T/S73A**	pcDNA3	Ad5 E1B-55K	this work

1842	**pcDNA3-E1B E65V/S68G**	pcDNA3	Ad5 E1B-55K	this work
1843	**pcDNA3-E1B A13V/S16L**	pcDNA3	Ad5 E1B-55K	this work
1844	**pcDNA3-E1B A51T/S54G**	pcDNA3	Ad5 E1B-55K	this work
1860	**E1-Box-E1B P70T/S73A**	pPG-S3	Ad5 E1-region	this work
1861	**E1-Box-E1B E65V/S68G**	pPG-S3	Ad5 E1-region	this work
1862	**E1-Box-E1B A13V/S16L**	pPG-S3	Ad5 E1-region	this work
1863	**E1-Box-E1B A51T/S54G**	pPG-S3	Ad5 E1-region	this work
1864	**Ad5pPG-S2-E1B P70T/S73A**	pPG-S2	Ad5 genome	this work

3.5 Antibodies

3.5.1 Primary antibodies

The following primary antibodies were used in this work:

NAME	PROPERTIES
2A6	Monoclonal mouse antibody raised against Ad5-E1B-55K protein, N-terminal (Sarnow et al., 1982b).
3D8	Monoclonal rat antibody raised against Usp7 protein, N-terminal. Stock of the group.
5E10	Monoclonal mouse antibody raised against PML protein, (Stuurman et al., 1992).
6B10	Monoclonal rat antibody raised against Ad5-L4-100K protein, N-terminal (Kzhyshkowska et al., 2004).
6E6	Monoclonal rat antibody raised against Usp7 protein, N-terminal. Stock of the group.
7C11	Monoclonal rat antibody raised against Ad5-E1B-55K protein, C-terminal (Kindsmuller et al., 2007).
α-late (L133)	Polyclonal rabbit antiserum raised against Ad5 late structural proteins

	(Kindsmuller et al., 2007).
B6-8	Monoclonal mouse antibody raised against Ad5-E2A-72K protein (Reich et al., 1983).
β-actin (AC-15)	Monoclonal mouse antibody against β-actin (Sigma).
DO-1	Monoclonal mouse antibody against p53 (Santa Cruz).
fl393	Polyclonal rabbit antibody against p53 (Santa Cruz).
M73	Monoclonal mouse antibody against E1A (Harlow et al., 1985).
Myc	Polyclonal rabbit antibody against c-Myc (A-14; Santa Cruz).
Pol	Polyclonal rabbit antibody against adenovirus DNA polymerase (Temperley and Hay, 1991).

3.5.2 Secondary antibodies

The following secondary antibodies were used for Western blot analysis:

NAME	PROPERTIES
HRP-Anti-Mouse IgG	HRP (*horseradish peroxidase*) coupled antibody raised against mouse IgGs in sheep (Amersham Life Science).
HRP-Anti-Rat IgG	HRP (*horseradish peroxidase*) coupled antibody raised against rat IgGs in goat (Amersham Life Science).
HRP-Anti-Rabbit IgG	HRP (*horseradish peroxidase*) coupled antibody raised against rabbit IgGs in donkey (Amersham Life Science).

The following secondary antibodies were used for immunofluorescence analysis:

NAME	PROPERTIES
FITC-Anti-Rat IgG	Fluorescein-isothiocyanate (FITC)-coupled antibody raised against rat IgGs in donkey; (H + L; Dianova).
FITC-Anti-Mouse IgG	Fluorescein-isothiocyanate (FITC)-coupled antibody raised against

	mouse IgGs in donkey; (H + L; Dianova) (H + L; Dianova).
FITC- Anti-Rabbit IgG	Fluorescein-isothiocyanate (FITC)-coupled antibody raised against rabbit IgGs in donkey; (H + L; Dianova) (H + L; Dianova).
Texas Red-Anti-Rat IgG	*Texas Red* (TR)-coupled antibody raised against rat IgGs in donkey; (H + L; Dianova).
Texas Red-Anti-Mouse IgG	*Texas Red* (TR)-coupled antibody raised against mouse IgGs in donkey; (H + L; Dianova).
Cy3-Anti-Mouse IgG	(Cy3)-coupled antibody raised against mouse IgGs in donkey; (H + L; Dianova).
Alexa™ 488 Anti-Mouse IgG	Alexa™ 488 antibody raised against mouse IgGs in goat (H + L; $F(ab')_2$ Fragment; Molecular Probes).

3.6 Commercial systems

The following commercial systems were purchased from the indicated companies:

NAME	COMPANY
Protein Assay	BioRad
QuikChange™ Site-Directed Mutagenesis Kit	Stratagene
SuperSignal® West Pico Chemiluminescent Substrate	Pierce
Plasmid Purification Mini, Midi und Maxi Kit	Qiagen
QIAquick Gel Extraction Kit	Qiagen
Vivapure® AdenoPack 20	Sartorius

3.7 Chemicals, reagents and equipment

The chemicals and reagents used in this study were purchased from Sigma, Merck, Biomol, AppliChem, Roche and New England Biolabs. Cell culture materials were

obtained from Falcon, Gibco BRL and Pan, other plastic materials and equipment were purchased from Falcon, Sarstedt, Whatman, Nunc, Biorad, Eppendorf GmbH, Brand, Protean, Schleicher & Schuell, Engelbrecht, Biozym, Hellma, VWR, and Greiner.

3.8 Standards and markers

Size determination of DNA fragments on agarose gels was based on a *1 kb* and *100 bp DNA ladder* (Gibco BRL), and *Precision Protein Standard* (BioRad) was used to determine the molecular weight of proteins on SDS-gels.

3.9 Software and databases

The following software and databases were used in the preparation of this work:

SOFTWARE	PURPOSE	SOURCE
Acrobat 9	Reading and writing PDF data	Adobe
Bio Edit 7.0.5.2	Sequence data processing	http://www.mbio.ncsu.edu/BioEdit/page2.html
EndNote 9.0	Reference organization	Thomson
File Maker Pro 8.0	Database of the group	FileMaker, Inc.
GeneRunner	Sequence data processing	Hastings Software Inc.
Gene Tools	Quantification of DNA and protein bands	SynGene
Illustrator CS2	Figure preparation	Adobe
Microsoft Office XP 2007	Preparation of text and tables	Microsoft
Photoshop 6.0	Image processing	Adobe
PubMed	Literature database (National Library of Medicine)	http://www.ncbi.nlm.nih.gov/PubMed
Vector NTI	Sequence alignment	Invitrogen

4 Methods

4.1 Bacteria

4.1.1 Culture and Storage

Liquid cultures of *E. coli* in sterile LB medium with appropriate antibiotics (e.g. ampicillin) were prepared by single colony inoculation method and incubated overnight at 37°C in an "incubator shaker" (New Brunswick) at 150-220 rpm. If necessary the concentration of the bacteria was determined photometrically at a wavelenght of 600 nm against the medium (1 OD_{600} = 8 x 10^8 cell/ml). After overnight incubation of single colony cultures, plate cultures were prepared on agar plates by streaking a loop-full of liquid culture, and incubated overnight at 37°C in an incubator. Plate cultures can be kept several weeks at 4°C covered with parafilm (Pechiney Plastic Packaging). Agar plates were prepared as follows: LB-agar was made by adding 15 g/l agar to LB. This medium was sterilized by autoclaving and appropriate antibiotics were added after cooling. Aliquots of LB-agar were poured onto plates and left to cool in a fume hood. From liquid cultures, glycerin cultures were also prepared for storage at - 80°C.

Glycerin Culture: Liquid cultures of single colony bacteria that were incubated overnight were centrifuged briefly at 4000 rpm for 10 min (Rotixa 120R, Hettich) at room temperature. The pellets of bacteria were then resuspended in the mixture of 0.5 ml LB medium and 0.5 ml sterile glycerol and were transferred into Cryo tubes (Nunc). Bacteria cultures can then be stored at -80°C for a few years.

LB-medium	Tryptone	10 g/l
	Yeast extract	5 g/l
	NaCl	5 g/l
	• autoclaving	

Antibiotic solutions	Ampicillin (500 x) Kanamycin (200 x) • filter sterilization • storage at –20°C	50 mg/ml in H_2O_{dd} 10 mg/ml in H_2O_{dd}

4.1.2 Transformation of E. coli

4.1.2.1 Electroporation

The production of electrocompetent *E. coli* cells was performed according to the protocol of Sharma and Schimke (Sharma and Schimke, 1996). 10 ml of an overnight culture of *E. coli* cells were incubated at 37°C. After reaching an OD of 0.5-0.9 at 600 nm, they were inoculated into 1 L of YENB medium. Afterwards, the cells were cooled for 5 min on ice and centrifuged for 10 min at 6000 rpm at 4°C (Centrikon T-124, Kontron of instrument). The bacteria pellet was washed twice by resuspending in 100 ml ice-cold dH2O and once with 20 ml of 10% glycerol. The pellet was then resuspended in a final volume of 3 ml of 10% glycerol, divided into 50 µl aliquots and frozen in liquid nitrogen. The cells were stored at -80°C. For electroporation of the ligation product, first the sample was desalted. DNA to be transformed was mixed with 1/10 volume of 3 M NaOAc and 1 volume of isopropanol. After 10 min centrifugation at 14000 rpm (Eppendorf table centrifuge 5417, Eppendorf) at room temperature, the pellet was washed with 75% EtOH, dried, and redissolved in 10 µl dH2O. The electrocompetent cells were thawed on ice; each 50 µl of the cell suspension was mixed with 1-10 µl of plasmid DNA and added to a precooled electroporation cuvette (Bio-Rad) with an electrode gap of 1 mm. Electroporation was performed in a *Gene Pulser* machine (Bio-Rad) with a voltage of 1.25 kV, a capacity of 25 µF and a bypass resistor of 200 Ω. This reached a time constant of approximately 5 ms. Alternatively, cuvettes with an electrode gap of 2 mm were used with a voltage of 2.5 kV. After the pulse, the cells were rinsed immediately with 1 ml of SOC medium,

transferred into 1.5 ml reaction tubes (Eppendorf) and incubated for 1 h at 37°C. Then, they were centrifuged, and resuspended in approximately 50 µl of the supernatant and inoculated on agar plates with LB medium containing appropriate antibiotics.

YENB	Bacto Yeast Extract	7.5 g/l
	Bacto Nutrient Broth	8 g/l
	• autoclaving	

SOC medium	Tryptone	20 g/l
	Yeast extract	5 g/l
	NaCl	10 mM
	KCl	2.5 mM
	$MgCl_2$	10 mM
	$MgSO_4$	10 mM
	Glucose	20 mM
	• autoclaving	

4.1.2.2 **Chemical transformation of *E. coli***

For this method, *Epicurian coli XL-1 Blue supercompetent* (Stratagene) strain of *E. coli* were used. 1 µl of DNA to be transformed (~1 µg/µl in concentration) was put into Eppendorf tubes and mixed with 1 µl β-mercapthoethanol (βM), which increases the efficiency of transformation. Meanwhile *E. coli* cells taken from -80°C were thawed on ice. Afterwards, 50 µl of the cell suspension was transferred into a *Falcon 2059 polypropylene* tube. The pre-made mixture of DNA and βM was added to these cells, mixed carefully and incubated for 30 min on ice. This mixture was then warmed in a pre-heated water bath at 42°C for 45 sec and transferred again to ice for 2 min. In this way plasmid DNA can enter through the pores of bacteria cell membranes that arise due to the heath shock. Afterwards, the transformed cells were mixed with 500 µl NZCYM medium, which was heated in a water bath at 42°C. These cells were then incubated at 37°C for 1 h at 150 rpm in order to recover and adapt themselves to the new phenotype. To measure the efficiency of the transformation, first 100 µl of the bacteria culture was spread on LB Amp agar plates. Then, 10 µl of the culture mixed with 90 µl of LB (10-1dilution) and 1 µl of the culture mixed with 99 µl of LB (10-2

dilution) was spread on agar plates. The rest of the cell culture was then centrifuged at 5000 rpm, supernatant was removed and the cell pellet was resuspended in the remaining supernatant and spread on an agar plate. The plates were incubated at 37°C for at least 16 h. Since the media of the plates contain ampicillin, only the transformed bacteria could grow because *XL-1 Blue* cells do not possess an Amp resistance gene.

NZCYM	NZ amine	10 g/l
	NaCl	0.5 g/l
	Yeast extract	0.2 g/l
	$MgSO_4$ x 6 H_2O	0.2 g/l
	Casamino acids	1 g/l
	• pH 7.5	
	• autoclaving	

4.2 Mammalian cells

4.2.1 Maintenance and passage of cell lines

Adhesive mammalian cells were cultured as a monolayer in polystyrene cell culture dishes (25-75-175 cm^2 flasks, 6-well or 100-mm-diameter dishes, Falcon). Dulbecco's Modified Eagle medium (DMEM; Gibco BRL) with 0.11 g/l sodium pyruvate was used as growth medium. This medium was then enriched with 10% fetal calf serum (FCS; Pan) and with 1% of a penicillin/streptomycin solution (1000 U/ml penicillin and 10 mg/ml streptomycin in 0.9% NaCl; Pan). Cultured cells were incubated at 37°C in a CO_2-incubator (Heraeus) with 5% CO_2. Depending on the cell type, in 3 to 5 days cell monolayers became very dense and required splitting in a ratio varying from 1: 3 to 1:10.

4.2.2 Splitting mammalian cells

To split the confluent cells growing on the cell culture dish, first the medium was vacuumed off, then the cells were washed with sterile phosphate buffered saline (PBS)

and afterwards, trypsin/EDTA solution (Pan) was added to the cells. After a few minutes of incubation at room temperature cells detached from the bottom of the dish. This cell suspension was transferred into a 15 or 50 ml Falcon tube containing 3-5 ml of FCS. This ensured that the protease activity of tyripsin was competitively inhibited by the protein content of the FCS serum and cellular proteins were protected from further destruction. This cell suspension was centrifuged at 1500 rpm for 3-5 min at 20°C (Hettich Rotixa 50RS, Heraeus Multifuge 3S-R). After the supernatant was removed, the cell pellet was resuspended in DMEM in a volume required to achieve desired dilution and transferred to cell culture dishes (1 ml cell suspension/dish) containing defined volume of DMEM with FCS and Pen/Strep. The cells prepared for transfection or infection were counted before seeding. The dishes were incubated at 37°C in an incubator (Heraus).

To count, the cell pellets were resuspended in 1 ml DMEM. 50 µl of this cell suspension was mixed with 50 µl Trypan-blue in a 1.5 ml eppendorf tube. One drop of this mixture was applied to *Neubauer* cell counting slide. The cells in 4 areas of 16 square quadrates were counted and the total number of the suspension was determined by the formula below:

$$\text{Cell number/ml} = \text{Counted cells} \times 2(\text{dilution factor}) \times 10^4$$

PBS (pH 7.0 – 7.7)	NaCl	140 mM
	KCl	3 mM
	Na_2HPO_4	4 mM
	KH_2PO_4	1.5 mM
	• autoclaving	

Trypan blue solution	Trypan blue	0.15%
	NaCl	0.85%

4.2.3 Storage of mammalian cells

Mammalian cells can be stored in liquid nitrogen or at -80°C for a long time. For the storage, subconfluent cells were trypsinized (4.2.2), and the pellets were resuspended in 1 ml FCS (Pan) supplemented with 10% DMSO (Sigma) and then transferred into *CryoTubes*™ (Nunc). Cells were slowly cooled down with the help of "*Mr. Frosty*" (Zefa Laborservice) and either transferred to liquid nitrogen storage tanks or stored at -80°C. To reculture the frozen cells, the cryo tube was rapidly thawed at 37°C and the cells were immediately seeded in an appropriate cell culture dish (Falcon) containing pre-warmed growth medium. When cells were attached to the bottom of the culture dish, DMSO-containing medium was exchanged with fresh 10% FCS-containing growth medium and further cultured as described in the previous sections.

4.2.4 Transfection of mammalian cells

4.2.4.1 Calcium phosphate method

For the transfection of mammalian cells with viral DNA fragments, the calcium phosphate method was used (Graham and van der Eb, 1973b). First, the cells to be transfected were seeded onto 6-well dishes 6-12 h before transfection. The desired viral DNA fragments cloned into pcDNA3 plasmids were prepared by plasmid DNA isolation and purification techniques and their concentrations were determined as described in Sections 4.4.1 and 4.4.2. One to five µg of these DNAs were dissolved in double distilled water. 30 µl of $CaCl_2$ solution and $_{dd}H_2O$ up to a final volume of 300 µl were added to these DNAs. These mixtures were transferred into polystyrene reaction tubes (Falcon). While vortexing the tubes at very low speed, 300 µl of 2 x BBS solution were added drop by drop to let calcium phosphate crystals form. Tubes were incubated for 20 min at room temperature to let the crystals encapsulate the DNA molecules. Meanwhile, 6-well dishes prepared previously were checked since cells need to occupy 40-60% of one well. After 20 min, 600 µl from the mixtures were taken up by sterile micro pipettes and added onto the cells drop by drop. After 16 h of

incubation, the media of the cells were changed and they were further incubated for least 24 h after transfection.

2 x BBS (*BES buffered saline*)	BES NaCl Na_2HPO_4 • pH 7.02 exact • filter sterilized	50 mM 280 mM 1.5 mM

2.5 M $CaCl_2$	$CaCl_2$ • filter sterilized	2.5 M

4.2.4.2 **Polyethyleneimine (PEI) method**

H1299 (2.5 x 10^6) or HEK-293 cells (5 x 10^6) seeded in 100 mm dishes were transfected with 10 µg of plasmid DNA by the polyethylenimine (PEI, 25 kDa, linear-Polysciences) transfection method. PEI was dissolved in H_2O_{dd} to give a concentration of 1 mg/ml. The solution was neutralized (pH 7.2) with 0.1N HCl, filter sterilized (0.2 µm), aliquoted and stored at -80°C. The working solution is stable at 4°C for 1 - 2 months. For transfection, 50 µg of PEI was added to the DNA dissolved in 600 µl of DMEM and kept at RT for 10 min. The DNA-PEI mixture was added to the cells seeded in DMEM without FCS and antibiotics. Six hours post transfection medium was replaced with normal growth medium. Transfected cells were harvested 24 or 48 h post transfection as described in Section 4.2.5.

4.2.4.3 **Polysome Method**

To reach maximal transfection efficiency, mammalian cells were transfected with plasmid or linearized bacmid DNA using *Lipofectamine™2000* reagent (Invitrogen). In this method, cationic lipid vesicles or liposomes interact with negatively charged DNA molecules. These lipid-DNA complexes fuse with cell membranes and mediate the internalization of DNA molecules. Adherent cells were seeded 6-12 h before

transfection in appropriate culture dishes (6-well or dish, Falcon) to reach a confluency of 70-90% at the time of transfection. Cells were washed once with PBS before adding DMEM without FCS or antibiotics. DNA-liposome complexes, prepared according to the manufacturer's instructions, were added to the cells. This transfection medium was changed with 10% FCS containing growth medium 6-12 h post transfection. Cells were harvested 24-72 h after transfection as described in Section 4.2.5.

4.2.5 Harvesting mammalian cells

Transfected or infected adherent mammalian cells were harvested using cell scrapers (Sarstedt). Collected cells were transferred into 15 or 50 ml Falcon tubes and centrifuged at 2000 rpm for 3 min at RT (Multifuge 3 S-R, Heraeus). After removing the supernatant, the cell pellet was washed once with PBS and stored at –80°C for subsequent experiments.

4.2.6 Transformation of rodent cells by adenovirus oncogenes

Baby rat kidneys were incubated with 1 mg/ml dispase-collagenase (Boehringer Mannheim) at 37°C for 4 h, and single cells were seeded in DMEM supplemented with 10% FCS on 100 mm-diameter tissue culture dishes (Falcon). Then $3x10^6$ primary baby rat kidney cells were transfected with the indicated amount of each plasmid by either calcium phosphate coprecipitation (4.2.4.1) or the PEI method (4.2.4.2). To avoid effects of promoter competition, all DNA combinations were adjusted to the same amount of cytomegalovirus promoter with pCMV/neo vector. Additionally, when calcium phosphate coprecipitation was used as transfection method, all combinations were brought to 20 µg of DNA per dish by the addition of salmon sperm DNA. Three days after transfection cells were trypsinized and seeded on three 100 mm-diameter dishes in DMEM supplemented with 10% FCS. They were fed with fresh medium every 4 days. Four to five weeks after transfection foci were stained with crystal violet

and scored. To establish permanent cell lines single foci or pools of foci were isolated and expanded (4.2.7).

Crystal violet	Crystal violet	1g/l
	Methanol	25% (v/v)

4.2.7 Establishing transformed cell lines

Single transformed foci were isolated and established as cell lines in this work. First, the growth media were removed and the cells were washed once with PBS. To isolate single foci, glass cloning cylinders (5 mm diameter) were placed circling single colonies. The cells within the cylinders were trypsinized with 100 µl of trypsin/EDTA solution. When the cells were detached from the dish, they were collected as described in 4.2.2, and seeded onto the wells of a 24-well plate (Falcon) containing DMEM with 10% FCS. These cells were grown for several weeks and expanded to obtain monoclonal cell lines.

4.2.8 Establishing stable knockdown cell lines

To establish stable monoclonal knockdown cell lines from A549 and H1299, these cells were seeded onto 6-well dishes and transfected with pSuper-shUsp7 by the polysome method (4.2.4.3). One day after transfection, fresh media containing 3 µg/ml of puromycin (Sigma) was added to the transfected cells. Three days later, the cells were split (4.2.2) in a ratio of 1:30, and seeded onto two 150 mm-diameter tissue culture dishes (Falcon). Fresh media containing puromycin were added to the cells every 3-4 days to select the stably transfected ones. Three weeks after splitting, foci were chosen to establish monoclonal cell lines and expanded as described in 4.2.7. Puromycin was always included in the growth medium of these cells.

4.3 Adenovirus

4.3.1 Generating virus from DNA

To generate mutant viruses, first the viral genome was released from the recombinant bacmid by *Pac*I digestion. This linearized DNA was precipitated with $^1/_{10}$ vol 3 M NaOAc and 1 vol of isopropanol and washed with 75% ethanol. Five micrograms of purified viral DNA were used to transfect $3x10^5$ complementing K16 cells seeded in a 10 mm dish (Falcon) by the calcium phosphate procedure (Graham and van der Eb, 1973a). The transfection medium was changed to normal growth medium 16 h post transfection. After 5 days, cells were harvested (4.2.5), centrifuged at 2000 rpm for 5 min (Multifuge 3 S-R, Heraeus) and the cell pellet was resuspended in 1 ml of DMEM. Viruses were released from these cells by three cycles of freezing in liquid nitrogen and thawing at 37°C in a water bath. Virus particles released into the medium were separated from the cell debris by centrifugation at 4500 rpm for 5 min (Multifuge 3 S-R, Heraeus). The virus-containing supernatant was used to infect 1 x 10^6 K16 cells seeded onto a 60 mm dish and infectious viral particles were collected 3-5 days after infection by freezing/thawing as described above. This re-infection procedure was repeated 2 to 5 times until a cytopathic effect was observed in 90% of the cells. The preliminary virus solution obtained was used to yield a high-titer virus stock after confirming the inserted mutations by DNA sequencing and testing the integrity and identity of the viral genome by *HindIII* digestion.

4.3.2 Propagation and storage of high-titer virus stocks

In order to establish a high titer virus stock, several 150 mm dishes were infected with the virus obtained as described in 4.3.1. After 3-5 days of incubation, cells were harvested and centrifuged at 2000 rpm for 5 min (Multifuge 3 S-R, Heraeus). The virus-containing cell pellet was washed once with PBS and resuspended in DMEM without FCS and antibiotics. After releasing the viral particles from the cells by freezing/thawing as described above (4.3.1), virus-containing supernatant was mixed

with 87% glycerol (sterile, 10% final concentration) for preservation at -80°C.

4.3.3 Titration of virus stocks

The titer of the virus stocks was determined in terms of fluorescent forming units (FFU) by immunofluorescence staining of the infected cells with an antibody (B6-8) against the E2A-72K DNA binding protein (DBP) of adenovirus. To do this, $3x10^5$ K16 cells were seeded in the wells of a 6-well dish (Falcon) and infected with 1 ml of virus dilution (10^{-2} to 10^{-6} in infection medium) 12 to 24 h after seeding. After incubation at 37°C in an incubator (Heraeus) with gentle shaking every 15 min for efficient and homogenous virus adsorption, infection medium was replaced with 2 ml of 10% FCS-containing growth medium per well. Infected cells were fixed 20 h p.i. with 1 ml of ice-cold methanol and further incubated at -20°C for 15 min. After removing the alcohol, 6 wells were air-dried at RT and washed once with TBS-BG buffer before immunostaining. Cells were incubated with 2 ml of TBS-BG for 30 min at RT. Primary antibody B6-8 was diluted in TBS-BG (1:10) and 1 ml of antibody dilution was added to each well after removal of TBS-BG. Cells were incubated with the primary antibody for 2 h at RT or overnight at 4°C with gentle agitation. After removing the primary antibody solution, cells were washed 3 times with 1 ml of TBS-BG for 5 min. For the fluorescence reaction, FITC-coupled secondary mouse antibody was diluted 1:100 in TBS-BG and 1 ml of this dilution was added to each well. This step was carried out in the dark to prevent bleaching of the fluorescent signal. The cells were incubated with the secondary antibody for 2 h at RT or overnight at 4°C with gentle agitation. Infected cells were counted using a fluorescence microscope after washing the samples 3 times with TBS-BG. The total infectious particle number of a virus stock was calculated according to the counted infected cell number and virus dilutions.

TBS-BG	Tris/HCl, pH 7.6	20 mM
	NaCl	137 mM
	HCl	3 mM
	$MgCl_2$	1.5 mM
	Tween 20	0.05%
	Sodium azide	0.05%
	Glycine	5 mg/ml
	BSA	5 mg/ml

4.3.4 Determination of the cell-specific titer

The infectivities of H1299, HPU2, A549, APU5, and APU6 cells were determined by infecting each cell line with Ad-GFP at 0.1, 0.5, and 1 FFU per cell. At 20 h p.i., GFP positive cells were counted using a fluorescent microscope (Leica) and cell-specific titers were calculated.

4.3.5 Infection with adenovirus

Mammalian cells were seeded in appropriate dishes 6-16 h before infection, resulting in a confluency of 60-80%. Growth medium was removed and cells were washed once with PBS. According to the size of the dish, virus dilutions (1-50 FFU/cell) were prepared in an appropriate volume of DMEM without antibiotics and FCS. Cells were incubated with this infection medium 1 – 2 h at 37°C. During incubation, the dish was gently shaken every 15 min to achieve efficient and homogenous adsorption of virus particles. Finally, infection medium was replaced with DMEM containing 10% FCS and 1% penicillin/streptomycin. Infected cells were harvested or fixed according to the experiment at indicated time points after infection.

4.3.6 Determination of virus yield

To determine the progeny virion production efficiency of an adenovirus stock, $1x10^6$ HeLa or A549, $5x10^5$ H1299, or $2.5x10^5$ HepaRG cells were seeded into the wells of a 6-well plate, infected with adenovirus (1-10 FFU/cell) as described in 4.3.4. The infected cells were harvested 24, 48, or 72 h post infection using a cell scraper (Sarstedt).

Collected cells were transferred into a 15 ml reaction tube (Falcon) and centrifuged at 2000 rpm for 5 min (Multifuge 3 S-R, Heraeus). After removing the supernatant, the cell pellet was washed once with PBS and resuspended in 1 ml of DMEM without antibiotics or FCS. To release the virus particles from the cells, the cell suspension was subjected to 3 sequential freeze and thaw cycles as described in 4.3.1, and further centrifuged at 4500 rpm for 10 min (Multifuge 3 S-R, Heraeus). Supernatant containing the released virus particles was transferred into a 1.5 ml reaction tube (Eppendorf) and stored at 4°C. To determine the particle number in this virus solution titration was carried out as described in 4.3.3, and the particle number produced per cell was calculated.

4.4 DNA techniques

4.4.1 Preparation of plasmid DNA from *E. coli*

In this study, plasmid isolation kits (Qiagen, Stratagene) of different sizes (mini-midi-maxi) were used to prepare plasmid DNA from *E. coli*. In order to purify DNA from bacterial culture, 100 ml of inoculated culture was incubated overnight at 37°C in shaker incubator (New Brunswick). 50 ml Falcon tubes were used to centrifuge the cells at 4000 rpm for 10 min at 20°C (Rotixa 120R, Hettich). After centrifugation, supernatants were removed and pellets were combined in one Falcon after resuspending them in 4 ml of P1 (resuspension buffer) buffer. 4 ml of P2 (lysis buffer) buffer was then added to the resuspended culture, mixed carefully and incubated in a water bath at 37°C for 5 min to lyse the cells completely. Afterwards, 4 ml of ice-cold P3 buffer was added to the lysate, mixed carefully and kept on ice for 2-3 min. To clear the lysate, the mixture was centrifuged at 4000 rpm for 30 min at 4°C. Meanwhile maxi or midi columns were prepared and treated with 2.5 ml QBT (equilibration buffer). After centrifugation, the supernatants between two pellets were applied to the columns, waited until the liquid drains out. Then, the columns were washed

immediately without letting the surface get dry, with 5 ml QC (wash buffer) and allowed to drain out. This step was repeated two more times. In order to detach the plasmid DNA from the filters, 15 ml Falcon tubes were put under the columns and 5 ml of QF (elution buffer) was poured on the filters, waiting until the DNA in QF gathered in the tube. After drainage, 0.8 volume of isopropanol was added to the DNA solution and centrifuged (Hettich Rotixa 50RS, Heraeus Multifuge 3S-R) at 4000 rpm for 30 min at 4°C to precipitate the DNA. After centrifugation, isopropanol was removed, 600 µl of 70% ethanol was added to the DNA precipitate and the final mixture was centrifuged again at 4000 rpm for 15 min at 4°C. After centrifugation ethanol was removed and the DNA pellet was dried by vacuumed centrifuge. Pellets were afterwards dissolved in 50-100 µl of 10 mM Tris solutions. The concentrations of these DNA solutions and their purity were then determined. The DNA preparations were kept at 4°C.

P1	Tris/HCl, pH 8.0	50 mM
	EDTA	10 mM
	RNAse A	100 µg/ml
	• storage at 4°C	

P2	NaOH	200 mM
	SDS	1% (w/v)

P3	Ammonium acetate	7.5 M
	• storage at 4°C	

QC	NaCl	1 M
	MOPS	50 mM
	Isopropanol	15% (v/v)
	$_{dd}H_20$	

QBT	NaCl	750 mM
	MOPS	50 mM
	Isopropanol	15% (v/v)
	Triton X-100	0.15% (v/v)

QF	NaCl	125 mM
	Tris	50 mM
	Isopropanol	15% (v/v)
	$_{dd}H_20$	

4.4.2 Determination of DNA concentrations

The concentration of the prepared DNA was determined using UV absorption spectrophotometers (Uvikon Spektralfotometer 930, Kontron and SmartSpecTM 3000 Spectrophotometer, Bio-Rad) at 260 nm wavelength. The DNA sample was diluted 20 times in dH2O and transferred into the quartz cuvette (1 cm thick). The cuvettes were put into a UV-spectrophotometer scanning wavelengths from 230 nm to 300 nm. Double stranded DNA gives maximum absorption at 260 nm and 1 absorption unit, OD (stands for optical density) shows a DNA concentration of 50 µg/ml (Sambrook, 1989).

$$\text{DNA } \mu g/\mu l = OD \times 50 \times 20/1000$$

By this method, the purity of the DNA preparation can also be determined. The OD at 260 nm/OD at 280 nm ratio of a DNA solution is higher than 1.8 when the DNA solution is pure.

4.4.3 Agarose gel electrophoresis

The investigation of DNA samples by agarose gel electrophoresis is based on the relative speeds of motion of the DNA molecules in an electrical field as a function of their fragment length. To prepare an agarose gel, an appropriate quantity (0.6-1%) of Agarose (Seakem® LE agarose, FMC Bioproducts) was dissolved in 1 x TBE buffer by boiling the mixture in a microwave oven for 5 min (Moulinex) and then mixing with 50 ng/ml of ethidium bromide solution, which interchelates with DNA and makes it visible under UV light. The cooled down agarose gel solution was then poured into a

gel tray carrying a comb of appropriate size. When the gel was completely set, 1 x TBE buffer was added and the comb was removed to form the wells. The DNA samples were loaded into the wells of the solidified agarose gel with 1/6 volume of loading buffer. DNA size markers *(Gibco BRL)* were also loaded. Separation of the fragments took place by running the gel with a voltage of 5-10 V/cm for several hours depending on the length of the gel tray and the size of the DNA used. Analytical gels were visualized on a UV transilluminator (Bachofer) at a wavelength of 312 nm and documented with a gel documentation system (*gel print 2000i*, MWG Biotech). Preparative gels (gels that are prepared if it is necessary to isolate DNA from the gel) were detected with UV light of longer wavelength (365 nm) to help protect the DNA, and appropriate DNA bands were cut out.

5 x TBE	Tris	0.45 M
	Boric acid	0.45 M
	EDTA	10 mM
	• with acetic acid pH 7.8	

6x loading buffer	Bromphenol blue	0.25% (w/v)
	Xylene cyanol	0.25% (w/v)
	Glycerol	50% (v/v)
	50 x TAE	2% (v/v)

Ethidium bromide solution	Ethidium bromide	10 mg/ml
	• storage at 4°C, light protection	

4.4.4 Isolation of DNA fragments from agarose gels

The isolation of DNA fragments from agarose gels was performed using the *Qiagen gel extraction kit* (Qiagen). First, the DNA bands were cut out by a scalpel (Feather) under UV light (365 nm) and placed into 1.5 ml Eppendorf tubes. Then, the procedure of the manufacturer was followed. The concentration of the isolated DNA was measured after preparation.

4.4.5 Polymerase chain reaction (PCR)

4.4.5.1 Standard PCR protocol

The polymerase nuclear chain reaction (polymerase chain reaction = PCR; Saiki et al., 1988) is a procedure for amplifying defined nucleic acid sequences *in vitro*, where the specificity of the reaction is guaranteed by the primer oligonucleotides used. For a 50 µl standard reaction, 0.01-1 µg of DNA and 0.2 µM of the desired oligonucleotides (forward and reverse primers), 1 µl dATP, dTTP, dCTP and dGTP, 5 µl 10 x PCR buffer and 0.5 µl *Taq* DNA polymerase (5 U/µl; Roche) were mixed. This mixture was incubated in thin-walled 0.2 ml reaction containers (Biozym) in a Thermocycler (GeneAmpTM PCR system 9700, Perkin-Elmer) and processed successively as follows: denaturation at 95°C, hybridization (annealing) at 55-70°C and polymerization at 68-72°C. Following 20-30 cycles and after the final round the reaction was kept at 4°C. After PCR amplification 5 µl of amplified DNA was analyzed by agarose gel electrophoresis and examination under UV light to determine the fragment size and yield.

4.4.5.2 Site-Directed mutagenesis by PCR

In this study, all mutations were introduced using a *QuickChange™ Site-Directed Mutagenesis Kit* (Stratagene) as described by the manufacturer. By this method it is possible and easy to mutate one or more defined bases on a desired DNA fragment. First, a primer oligonucleotide with a length of 25-45 bases was designed as follows: the Tm value of this oligonucleotide must be higher than 78°C, its GC content must be at least 40% of its sequence, the altered base/bases must be located approximately in the middle and the oligonucleotide should start and end up with a G or C base. In this study, designed primers were supplied by Metabion and they were diluted in 10 mM Tris solution to a final concentration of 125 ng/µl.

DNA fragments to be mutated were amplified by PCR using primers containing the desired mutations. Therefore, mutations were inserted during the DNA amplification.

PCR mixtures were prepared in a 0.2 ml PCR tube (Biozym) with 5µl of 10x reaction buffer, 1 µl of forward and reverse primers, 1 µl dNTPmix (deoxynucleotide triphosphates; dATP, dGTP, dCTP, dTTP; supplied within the kit) and the DNA fragment to be mutated. The reaction tube was filled with dH2O up to a final volume of 50 µl. Finally 1 µl of *pFU Turbo DNA Polimerase* was added. The contents were mixed by gentle shaking and spun down by a desk-top centrifuge (Eppendorf desk-top centrifuge, 5417) and placed in a thermocycler *(GeneAmp™PCR System 9700,* Perkin-Elmer*)*. The PCR was programmed for 15-18 cycles (denaturation at 95°C, hybridization at 55°C and polymerization at 72°C). Amplified DNA products were then investigated by agarose gel electrophoresis to confirm if the PCR was successful. Then, in order to digest the non-mutated template DNA, a DPN-I restriction digest was performed. DPN-I is a restriction enzyme digesting only methylated DNA. Therefore, it can only digest the methylated template DNA isolated from an organism, but not the DNA amplified by PCR *in vitro*. 50 µl of PCR product and 1 µl of DPN-I was mixed, and the reaction took place at 37°C for at least 2 h of incubation. Resulting mutant plasmids were then transferred into bacteria by heath shock transformation or electroporation as described in 4.1.2.

4.4.6 Cloning of DNA fragments

4.4.6.1 Enzymatic restriction of DNA

Restriction enzymes used in this study and their appropriate 10 x reaction buffers were supplied by New England Biolabs, Boehringer Mannheim and Roche and used in accordance with the data of the manufacturer. For analytic digestion usually 0.5-1 µg of DNA and 3-10 U of restriction enzyme were used, if not indicated otherwise, the mixture was incubated at 37°C for 1 h. For preparative restriction digest, 5-20 µg of DNA and 50 U of enzyme were used and incubated at 37°C for at least 2 h. PCR products were purified and concentrated by isopropanol precipitation to remove interfering oligonucleotides and dNTPs before restriction digest and subsequent

cloning. When necessary, the restricted fragments were seperated by agarose gel electrophoresis (4.4.3) and isolated by gel extraction (4.4.4).

4.4.6.2 **Oligonucleotide annealing**

The DNA oligonucleotides for hairpin RNA expression were dissolved in sterile, nuclease-free H_2O to a concentration of 3 mg/ml. The annealing reaction was assembled by mixing 1 µl of each oligo (forward + reverse) with 48 µl of annealing buffer (OligoEngine). The mixture was incubated at 90°C for 4 min, and then at 70°C for 10 minutes. The annealed oligos were slowly cooled to 10°C (e.g.. step-cooled to 37°C for 15-20 min, then to 10°C or RT). The annealed oligo inserts were either used immediately in a ligation reaction, or cooled further to 4°C. For longer storage, they were kept at -20°C.

4.4.6.3 **Ligation and transformation**

After restriction digests, linearized vector DNAs were directly reacted with 1 U of alkaline phosphatase (SAP, shrimp alkaline phosphatase, Boehringer Mannheim) for 30 min at 37°C and dephosphorylated in order to prevent religation of the vector itself. DNA fragments were purified by isopropanol precipitation as explained in Section 4.4.1 and their concentrations were measured. A standard ligation mixture was prepared with 100 ng of vector DNA, 100-500 ng of insert DNA, 2 µl of 10 x ligation buffer and 1 U of T4-DNA ligase (Boehringer Mannheim). For the covalent binding of phosphodiester bridges, the mixture was incubated overnight at 13°C. Afterwards, ligated plasmid DNAs were transformed into *E. coli* (4.1.2).

4.4.6.4 **DNA Sequencing**

To check whether the cloned DNA had the desired mutation and no other mutations in the reading frame, the sequence of the original DNA was compared to the mutated DNA sequence by BLAST software of NCBI (www.ncbi.nih.gov/blast, 2004). Mutated DNAs were checked both by agarose gel electrophoresis and also by sequencing. In

this study, DNA sequencing was outsourced to Geneart. DNA that was mutated, produced in *E. coli,* and purified was put in a PCR mixture with appropriate primers and DNA sequencing was performed by an automated DNA sequencing device. 1 µg of recombinant DNA, 10 pmol of primer (primer on the reading frame) and dH2O up to a final volume of 8 µl were mixed in 0.2 PCR tubes (Biozym). These procedures were performed by the company.

4.5 Protein techniques

4.5.1 Preparation of total cell lysates

Harvested mammalian cell pellets were resuspended directly in an appropriate quantity of pre-cooled RIPA or RIPA-*light* buffer and incubated for 30-60 min on ice. In order to obtain a complete cell extraction, the cell lysates were treated with ultrasound. Then, the protein extracts were transferred into 1.5 ml reaction tubes (Eppendorf) and centrifuged at 12,000 rpm for 10 min at 4°C (Eppendorf centrifuge 5417R) to separate insoluble cell portions. Afterwards, supernatants were transferred into new reaction tubes (Eppendorf) for further experiments. Before using these extracts for the following experiments their protein concentrations were determined.

RIPA lysis buffer (high stringency)	Tris/HCl, pH 8.0	50 mM
	NaCl	150 mM
	EDTA	5 mM
	Nonidet P40	1% (v/v)
	SDS	0.1% (w/v)
	Sodium desoxycholate	0.5% (w/v)

RIPA-*light* (middle stringency)	Tris/HCl, pH 8.0	50 mM
	NaCl	150 mM
	EDTA	5 mM
	Nonidet P40	1% (v/v)
	SDS	0.1% (w/v)
	Triton X-100	0.1% (v/v)

4.5.2 Quantitative determination of protein concentrations

The concentration of soluble proteins in a sample was determined using the *Bio-Rad Protein Assay*. The assay is based on the protein quantification procedure of Bradford (Bradford, 1976) and measures the increase in the absorption at 595 nm using a spectrophotometer (Bio-Rad) after the proteins in the sample bind to the chromogene substrate of the system. Different dilutions of calibration protein, bovine serum albumin (BSA; Sigma), varying from 1 to 20 µg were mixed with 200 µl coloring reagent. The mixture was filled with dH2O up to a final volume of 1 ml in polystyrene cuvettes (Sarstedt). Then, samples were prepared by mixing 1 µl of sample plus 200 µl of coloring reagent plus 800 µl of dH2O in cuvettes and incubated for 5-30 min at room temperature. Subsequently, the absorptions were determined spectrophotometrically at 595 nm against blank solution (800 µl dH2O plus 200 µl coloring reagent). According to the calibration curve obtained from different dilutions of BSA, the protein concentrations of the samples were calculated.

4.5.3 SDS-polyacrylamide gel electrophoresis (SDS-PAGE)

SDS-PAGE is used for seperating proteins electophoretically according to their molecular weights in the presence of denaturating SDS detergent. Negatively charged SDS molecules compensate for positive charges of denatured proteins and all the proteins in the gel move towards the anode under the voltage applied. The seperation of proteins according to their molecular weights takes place in the pores of the polyacrylamide gel, since the differential velocities of the proteins are determined only by their size. The quality of protein isolation by this method was increased by Laemmli (Laemmli, 1970) using an intermittent buffer system that first concentrates proteins in a lower percentage collecting or stacking gel and lets proteins start migration together before separation. Then, the isolation takes place in separating gel. The compositions of the gel solutions used in this study are given below (Harlow and Lane, 1988). The gel equipment was used according to the manufacturer (Biometra). Protein samples were mixed with Laemmli sample buffer (Sambrook, 1989) before

loading on the gel and denaturated in a thermal block (Eppendorf thermal mixer comfort) by incubating for 5 min at 95°C. Electrophoresis took place by applying 20 mA/gel volume (ml) in TGS buffer and continued until the bromphenol blue band reached the end of the gel. Following SDS polyacrylamid gel electrophoresis, isolated proteins were detected by either Coomassie blue staining or by immunoblotting.

30% Acrylamide-Stock solution	Acrylamide	37.5% (w/v)
	N, N'Methylenbisacrylamide	1% (w/v)

Stacking gel (5%)	Acrylamide stock solution	17% (v/v)
	Tris/HCl, pH 6.8	120 mM
	SDS	0.1% (w/v)
	APS	0.1% (w/v)
	TEMED	0.1% (v/v)

Seperating gel (10%)	Acrylamide stock solution	38% (v/v)
	Tris/HCl, pH 8.8	250 mM
	SDS	0.1% (w/v)
	APS	0.1% (w/v)
	TEMED	0.1% (v/v)

TGS Buffer	Tris	25 mM
	Glycine	200 mM
	SDS	0.1% (w/v)

Laemmli sample buffer	Tris/HCl, pH 6.8	100 mM
	SDS	4% (w/v)
	DTT	200 mM
	Bromphenol blue	0.2% (w/v)
	Glycerol	20%

4.5.4 Coomassie blue staining of the SDS gel

To detect the proteins on the polyacrylamid gel after electrophoresis colloidal Coomassie System Deep Blue (Ener-Gene) with a sensitivity of around 100 ng was applied according to the instructions of the manufacturer. For documentation, gels

were dried afterwards on Whatman filters in a vacuum dryer (Drystar, H. Hoelzel) for 2 h at 70°C and sealed into plastic foil.

4.5.5 **Western blots**

Western blots are carried out to transfer the proteins from polyacrylamid gels onto nitrocellulose membranes. This immobilizes electrophoretically isolated proteins on nitrocellulose membranes (Protran, Schleicher & Schuell), as required for immunological investigations. The transfer took place using a *Trans Blotâ Electrophoretic Transfer Cell* (Bio-Rad) in Towbin buffers with an current of 400 mA for 80 min. The instructions of the manufacturer about handling the equipment were followed. Subsequently, the proteins transferred onto membranes were stained reversibly by *Ponceau S* (Sigma) to visualize the protein and marker bands. Then, the membranes were washed with water before immune staining.

Before incubating the nitrocellulose membranes with specific antibodies, free binding areas of the membranes were saturated by incubating them in 5% milk powder in PBS for at least 1h at room temperature or overnight at 4°C. Afterwards, the membranes were washed twice with PBS containing 0.1% Tween 20 (PBS/Tween) and once with PBS alone for 5 min each. Subsequently, membranes were incubated with primary antibodies diluted in suitable concentrations with PBS plus 1% milk powder solution for 1 h at room temperature on a middle speed shaker. After binding of the primary antibodies the membranes were washed again two times with PBS/Tween and once with PBS alone and incubated with horseradish peroxidase (HRP) coupled secondary antibodies (anti-rat, or anti-rabbit; Amersham Biosciences) diluted 1 : 5000 in PBS plus 1% milk powder for 1 h at room temperature on a shaker. After three further washing steps with PBS/Tween, nitrocellulose membranes were treated with chemiluminescent substrates for the HRP reaction and color formation. For this specific purpose a commercial kit, *Super Signal West Pico Chemiluminiscent Substrates* (Pierce), was used. This procedure was based on the enhanced chemiluminiscence formation with the participation of HRP and represents a highly sensitive protein

detection system. In this system, cyclic Diacylhydrazide Luminol coupled to the anti-immunglobulin antibody is oxidized by peroxidase under alkaline conditions, which leads to a maximum light emission at 428 nm. Chemical amplifiers such as phenol increase the light intensity approximately 1000-fold and extend the period of emission. In this way, a maximum intensity is obtained 5-20 min after using the chemicals, followed by a reduction of the emission with a half-life of 1 h. For this process, two detection solutions supplied with the kit were mixed in a 1:1 ratio just before use and the mixture was applied to the membranes after the last washing step with PBS/Tween in a quantity of approximately 0.125 ml/cm². After 5 min of incubation, nitrocellulose filters were dripped off briefly and packed in stretch-film. The autoradiographic detection of the signals was performed by the *ChemiDoc System* (Bio-Rad) under exposure lasting 20 sec to 20 min.

PBS/Tween	Tween 20 • in PBS	0.05% (v/v)
***Towbin* buffer**	Tris/HCl, pH 8.3 Glycine SDS Methanol	25 mM 200 mM 0.05% (w/v) 20% (v/v)
Ponceau S	Ponceau S Trichloroacetic acid Sulfosalicylic acid	0.2% (w/v) 3% (w/v) 3% (w/v)

4.5.6 **Immunoprecipitation**

Cell lysates were prepared as described (5.6.1) using appropriate volumes of ice-cold immunoprecipitation (IP) buffer RIPA-*light*, or NP-40 supplemented with protease inhibitors. Protein concentrations of individual samples were determined (4.6.2) and lysate volumes containing equal amounts of protein (250 µg-2 mg) were precleared by addition of Protein G- or A-sepharose (Sigma-Aldrich) for 1 hour at 4°C with rotation (GFL, Gesellschaft für Labortechnik). Simultaneously, antibodies were coupled with

Protein G- or A-sepharose. After centrifugation at 6000 rpm for 5 min (Eppendorf 5417), antibody-coupled beads were added to the cleared lysates and antigen-antibody complexes were left to form overnight at 4°C. The following day, Protein G-/A-sepharose–immune complexes were spun down and washed five times in ice-cold IP buffer before the addition of 10 µl of Laemmli sample buffer to elute the proteins. Samples were boiled for 5 min and spun down in preparation for SDS-PAGE and Western blotting.

NP-40 (low stringency)	Tris/HCl, pH 8.0	50 mM
	NaCl	150 mM
	EDTA	5 mM
	Nonidet P-40	0.15% (v/v)
	Protease Inhibitor Mix *Complete EDTA-free* ; Roche	1 tablet per 50 ml

4.5.7 Immunofluorescence staining

4.5.7.1 Methanol fixation

Sterile glass coverslips (VWR) were placed into 6-well dishes before the mammalian cells were seeded and the culture dishes were incubated as explained before (4.2.2) for at least 6 h or overnight. When the cells reached the desired density they were transfected (4.2.4) or infected (4.3.5). After 24-48 h the culture media was removed and the cells were washed in PBS. Then, pre-cooled methanol was added onto the cells and they were incubated for 20 min at -20°C. Subsequently, methanol was removed and the cover glasses were air dried at room temperature. The cells fixed this way were either stored at -20°C for a few weeks or used immediately for immunostaining.

4.5.7.2 Indirect immunofluorescence staining

After fixation, the cells on glass coverslips were washed with PBS for 5 min on a shaker and incubated in 5% milk powder dissolved in PBS/Tween for 1 h at room temperature to eliminate nonspecific reactions with antibodies. Afterwards, they were washed 3 times for 5 min with PBS/Tween and appropriate dilutions of primary antibodies were applied on coverslips (30 µl per coverslip) and they were incubated

for 1 h at room temperature in a dark and damp chamber in order to prevent drying up of the antibody solution. After incubation, they were washed 3 times with PBS/Tween and then secondary fluorescent-marked antibodies were applied (FITC – anti-rat or anti-rabbit, Texas Red – anti-rat or anti–rabbit; Dianova) diluted 100 times in PBS plus 5% milk powder. These secondary antibody solutions also contained 0.5 µg/ml of DAPI (4', 6-Diamidine-2'-phenylindol Dihydrochloride; which stains DNA by forming chromatin complexes). After an hour, unbound secondary antibodies were removed by washing 3 times with PBS/Tween. Then, coverslips were rinsed slightly and were fixed on slides with 10 µl of *Glow Mounting medium* (Ener-Gene) per coverslip. These preparates were stored in dark at 4°C for several weeks. Further analysis of the immunostained cell preparates were performed using an immunofluorescent microscope (Leica) with a digital image processing system. The images were cropped and decoded by Photoshop CS2 (Adobe Systems) and assembled with Illustrator CS2 (Adobe Systems).

4.5.8 GST pull-down assays from cell lysates

4.5.8.1 GST-protein expression

In this study, expression of recombinant proteins in *E. coli* was accomplished by fusing the target proteins with Glutathione-S-Transferase (GST) from *Schistosoma japonicum* (Smith et al., 1986). The GST portion of the fusion protein, so called "GST-tag", allows the foreign polypeptides to be purified rapidly under non-denaturating conditions from crude cellular lysates. pGEX plasmids (Amersham Biosciences) provide a multiple cloning site for fusing a gene of interest to the C-terminal of GST. GST is a 26 kDa enzyme that binds reversibly and with high affinity to glutathione-containing affinity matrices such as glutathione-coupled sepharose beads. Therefore, the system allows the rapid purification of the target protein by affinity chromatography. Once purified, the protein of interest can also be cleaved from GST, since the pGEX vectors provide a proteolytic cleavage site, such as thrombin, between GST and the target protein (Frangioni et al., 1992). In this study, one of the basic pGEX

plasmid vectors, pGEX-2TK (Amersham Biosciences) was used. The kinase site that is present in the vector allows the detection of the expressed protein by direct labeling of the fusion products *in vitro* by phosphorylation. Another feature of this pGEX plasmid is that the expression of the fusion protein is under the control of the *lac* promoter. This promoter is controlled by the *lac* operator, which binds the *lacIq* gene product (*lac* repressor) during normal bacterial growth, blocking transcription of the target gene. Toxic effects of the recombinant gene products that lead to reduced cell growth and instability of the expression vector can be prevented by this expression control.

The pGEX-2TK (Amersham Biosciences) plasmid possesses the *trp-lac*-hybrid promoter called *tac*, which is likewise controlled by the *lac* repressor. By chemical induction with the lactose analogue isopropylthio-β-D-galactoside (IPTG) the interaction of the *lac* repressor with its target sequence can be prevented, thus inducing expression of the plasmid-encoded genes. Expression of the target protein was started by inoculating 10 ml of LB medium containing appropriate antibiotics with the recombinant *E. coli* strain. The culture was grown overnight at 37°C with shaking at 220 rpm in an incubator-shaker (New Brunswick). 2 ml of this overnight culture was then transferred into 100 ml of fresh, pre-warmed medium and grown until the OD600 of the culture reached 0.6. A 1 ml sample was taken from the culture at this step to check whether "leaky" expression took place before induction. For inducing protein expression, 1 mM IPTG was added to the culture and incubation continued for 4 h at 37°C. Alternatively, 0.1 mM IPTG for induction and 30°C growth temperature after induction were used to avoid the formation of insoluble inclusion bodies (Smith, 1998). Another sample of 1 ml was taken from the 4 h induced culture to monitor the level of expression after induction. Afterwards, the bacterial culture was harvested by centrifugation (6000 rpm, 10 min, 4°C; Centrikon T-124) and the pellet was washed with STE buffer. If necessary, the cells were stored in PBS containing protease inhibitor (*complete*™, *EDTAfree*, Boehringer Mannheim) at -80°C. The samples taken before and after induction was centrifuged and the pelleted cells

were resuspended in 50 µl of SDS-PAGE sample buffer and stored at -20°C until SDS-PAGE analysis.

STE buffer	Tris/HCl, pH 8.0	10 mM
	NaCl	150 mM
	EDTA	1 mM

4.5.8.2 **GST-protein purification**

Bacterial expression cultures prepared as described in the previous section were thawed on ice. Then, the cells were lyzed by the addition of 1 mg of lysozyme (Sigma), 100 µl of DNAse I (1 mg/ml; Sigma), 130 µl $MgCl_2$ and 13 µl $MnCl_2$ (both 1M) per 10 ml of cell suspension. The suspension was incubated for 10 min on ice. Afterwards, in order to obtain a complete cell extract, the suspension was sonicated three times with ultrasound (1 min, output 40, 0.5 impulse/sec; Branson Sonifier 450) on ice. After sonication, appropriate amounts of 5 M NaCl (to a final concentration of 0.5 M) and 20% Triton X-100 (to a final concentration of 1%) were added to the lysate.

To precipitate insoluble cell parts, the lysate was centrifuged at 15,000 rpm for 30 min at 4°C (Centrikon T-124, Kontron Instruments) and the supernatant was transferred to a fresh 15 ml falcon tube. The pellet was directly resuspended in SDS loading buffer or in 1 ml of PBS or 1 ml of 0.25% Tween 20, 0.1 mM EGTA buffer. A 1 ml sample was also taken from the supernatant. These samples were kept at -20°C to be analyzed by SDS-PAGE in order to determine whether the protein of interest was in the soluble or insoluble portion of the lysate. GST fusion proteins were purified from the lysate under nondenaturating conditions by GST affinity chromatography using glutathione immobilized to a matrix such as Sepharose. Batch purification using Glutathione Sepharose 4B (Amersham Biosciences) was performed. First, Glutathione Sepharose 4B beads supplied as 75% slurry were prepared to give a 50% slurry in PBS according to the instructions of the supplier. 1 ml of the 50% slurry of Glutathione Sepharose 4B (0.5 bed volume) was added to the supernatant obtained from a 100 ml culture lysate. The mixture was incubated for 1 h at 4°C in an overhead incubator (GFL, Society for

Laboratory Technology). Afterwards, the mixture was centrifuged at 500 g for 5 min at 4°C (Rotixa 120R, Hettich) and the pellet was washed three times with 5 ml of PBS containing protease inhibitors (*complete*TM Edta-free, Boehringer Mannheim). A 1 ml sample was taken from both the first flow-through containing the non-bound proteins and the supernatant of each washing step for SDS-PAGE analysis. After the last washing step the proteins were either eluted from Glutathione Sepharose 4B or resuspended and kept in 500 µl of PBS for GST pull-down assays. Elution of the fusion proteins was achieved by adding 750 µl of elution buffer to the pellet and incubating for 10 min in an overhead incubator. The elution step was repeated three times and a sample of 75 µl was taken from each eluate to detect the purified proteins by SDS-PAGE analysis. Alternatively, the protein of interest without the GST-tag was eluted from Glutathione Sepharose 4B by thrombin cleavage. For this purpose, 40 µl of thrombin (1 unit/µl, Amersham Biosciences) was mixed with 460 µl of PBS and loaded onto the pellet of 0.5 bed volume of fusion protein bound Glutathione Sepharose 4B after the last washing step. The mixture was incubated at room temperature for 16 h. After incubation, the suspension was centrifuged and the supernatant containing the eluted protein and thrombin was transferred into a new tube. The pellet was also resuspended in 500 µl of PBS. 50 µl of sample was taken from both the eluate and Glutathione Sepharose for SDS-PAGE analysis.

4.5.8.3 **GST pull-down assays**

GST pull-down is a technique used to analyze reciprocal protein-protein effects *in vitro*. First, the quantities of the fusion proteins bound to Glutathione Sepharose 4B were obtained by analyzing the stained SDS-PAGE with *QuantityOne software* (Bio-Rad). Afterwards, equal amount of proteins were centrifuged (7000 rpm, 5 min, 4°C; Eppendorf table-top centrifuge, Eppendorf) and washed with NETN-40 buffer. Then, the pellet was resuspended in 300 µl of PBS buffer with a defined quantity of cell lysate. This mixture was then incubated for 2 h at 4°C on a turning rotor (GFL, society for laboratory technology). The proteins bound to the Glutathione Sepharose were subsequently precipitated by centrifugation (6500 rpm, 5 min, 4°C; Bio joint fresco,

Heraeus of instrument), six times washed with PBS or RIPA-*light* buffer, centrifuged and boiled in 25 µl of SDS sample buffer as explained in 4.5.3. The protein samples were then analyzed by SDS-PAGE and Western blotting.

4.5.9 Purification of his-tagged sumo/ubiquitin conjugates

H1299 cells were transfected either with His-sumo-1 or His-ubiquitin plasmids (Muller et al., 2000) by the PEI method (4.2.4.2). 6 h post transfection, these cells were either mock or virus infected (4.3.4). 36 h post transfection, cells were washed once with PBS and harvested (4.2.5). Histidine purification was carried out as previously described (Xirodimas et al., 2001). First, the cell pellets were lysed in 6 ml of 6 M guanidium-HCI. 75 µl of Ni2+-NTA-agarose beads (Qiagen) were then added to each lysate and the samples were rotated at RT for 4 h. The beads were sequentially washed with wash buffers WB1, WB2, WB3, and WB4 for 5 min at RT. After the last wash, his-tagged sumoylated proteins were eluted by incubating the beads in elution buffer at RT for 20 min. The eluates were analyzed by SDS-PAGE (4.6.3) and Western blotting (4.6.4).

6 M guanidinium-HCl		
	Guanidium-HCl	6 M
	Na_2HPO_4/NaH_2PO_4	0.1 M
	Tris/HCl, pH 8.0	10 mM
	Imidazole	5 mM
	β-mercaptoethanol (freshly added)	10 mM

WB1		
	Guanidium-HCl	6 M
	Na_2HPO_4/NaH_2PO_4	0.1 M
	Tris/HCl, pH 8.0	10 mM
	β-mercaptoethanol (freshly added)	10 mM

WB2		
	Urea	8 M
	Na_2HPO_4/NaH_2PO_4	0.1 M
	Tris/HCl, pH 8.0	10 mM
	β-mercaptoethanol (freshly added)	10 mM

WB3		
	Urea	8 M
	Na_2HPO_4/NaH_2PO_4	0.1 M
	Tris/HCl, pH 6.3	10 mM
	β-mercaptoethanol (freshly added)	10 mM

WB4		
	Urea	8 M
	Na_2HPO_4/NaH_2PO_4	0.1 M
	Tris/HCl, pH 6.3	10 mM
	Triton X-100	0.1% (v/v)
	β-mercaptoethanol (freshly added)	10 mM

Elution buffer		
	Imidazole	200 mM
	Tris/HCl, pH 6.7	150 mM
	Glycerol	30% (v/v)
	SDS	5% (w/v)
	β-mercaptoethanol (freshly added)	720 mM

5 RESULTS

5.1 Usp7 as a novel interaction partner of adenovirus E1B-55K protein

5.1.1 Usp7 interacts with adenovirus E1B-55K protein

E1B-55K plays key regulatory roles during adenovirus infection (Dobner and Kzhyshkowska, 2001). To gain insights into the functions of this protein, cellular interaction partners of E1B-55K have been previously profiled by a yeast two-hybrid system in our group. In those experiments, using the N-terminal region of adenovirus type 5 (Ad5) E1B-55K protein as the bait identified several positive clones encoding Usp7, suggesting a potential direct interaction between these proteins. The critical role of Usp7 in the p53 pathway (Brooks and Gu, 2004) and data identifying Usp7 as a target of the regulatory proteins from two different DNA viruses (Herpes simplex type-1 Icp0 and Epstein-Barr virus EBNA1)(Everett et al., 1997; Holowaty et al., 2003b) prompted the detailed analysis of the potential interaction between Usp7 and E1B-55K in this work.

First, to verify this interaction in virus infected cells, immunoprecipitation (IP) reactions were performed in both directions (Fig. 6). Both E1B-55K and Usp7 have been previously shown to interact strongly with p53 (Li et al., 2002) and to exclude the potential contribution of p53 in the interaction between these proteins, the experiments were conducted in p53 negative H1299 cells (Mitsudomi et al., 1992). Extracts from mock and H5*pg*4100 (used as a wild-type adenovirus type 5 in this work) infected H1299 cells were incubated with either rat monoclonal antibody (mab) 3D8 raised against Usp7 in our group, or anti-E1B mab 2A6 (Sarnow et al., 1982b). Western blots of immunoprecipitates probed with appropriate antibodies showed the presence of Usp7 - E1B-55K complexes in virus infected cells. Thus, Usp7

was identified as a novel interaction partner of E1B-55K *in vivo*.

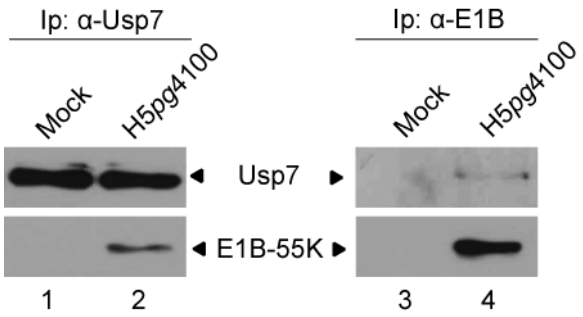

Figure 6. Usp7 interacts with E1B-55K in virus infected cells. H1299 cells were mock infected or infected with wt adenovirus type 5 (H5*pg*4100). 48 hours after infection total cell extracts were prepared and subjected to immunoprecipitation (Ip) reactions with a rat mab 3D8 raised against Usp7 (α-Usp7) or anti-Ad5 E1B-55K antibody 2A6 (α-E1B). The immunocomplexes were separated by SDS-PAGE and Usp7 was visualized by immunoblotting using 3D8 in both IP reactions. E1B-55K was detected with either 2A6 antibody in the IP with Usp7, or a rat mab 7C11 in the IP with E1B-55K.

5.1.2 Usp7 stabilizes the E1B-55K protein

Usp7 belongs to the class of de-ubiquitinating enzymes containing a cysteine residue in its active site (Brooks and Gu, 2004; Everett et al., 1999; Hu et al., 2002) and regulates the stability of several proteins, including cellular p53, Mdm2 and viral Icp0, by blocking their proteasomal degradation through de-ubiquitination (Brooks and Gu, 2004; Everett et al., 1999). Therefore, to investigate whether Usp7 has such an effect on E1B-55K stability, activity of Usp7 was inhibited in infected cells using the general cysteine-protease inhibitor E64, and E1B-55K steady state levels were analyzed in the presence and absence of this inhibitor by immunoblotting. Surprisingly, treating the H5*pg*4100 infected cells with E64 resulted in significant reductions in wild-type (wt) E1B-55K levels compared to untreated cells (Fig. 7A). Levels of a non-related adenovirus late-phase protein, L4-100K, remained unaffected upon E64 treatment, verifying that the observed effect was specific to E1B-55K and not due to a general negative effect of the inhibitor on virus infection. To test whether this effect can be attributed to Usp7 functions, RNA interference (RNAi) experiments were employed. Cells were transfected with short hairpin RNAs (shRNAs) against Usp7 and then infected with H5*pg*4100. Consistent with the data above, shRNA-

mediated reduction of Usp7 resulted in a decrease in E1B-55K steady-state levels (Fig. 7B). More importantly, treating these cells with the 26S proteasome inhibitor Mg132 returned E1B-55K levels back to normal, suggesting that E1B-55K is more prone to proteasomal degradation in the absence of Usp7. These results indicated that Usp7 stabilizes E1B-55K protein in infected cells by preventing its proteasomal degradation.

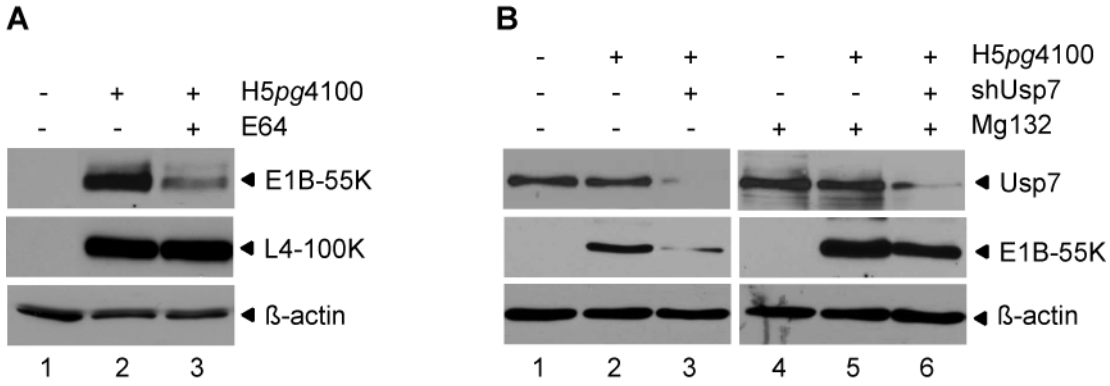

Figure 7. Stabilization of E1B-55K by Usp7. (A) H1299 cells were infected with H5*pg*4100 or left uninfected and 24 hours after infection, cysteine protease inhibitor E64 (10 μM) was added to the cells as indicated. Total cell extracts were prepared 6 hours after treatment and subjected to immunoblotting. E1B-55K was detected with 2A6 and L4-100K was detected as a negative control with 6B10 antibody. β-actin was analyzed as a loading control. **(B)** H1299 cells were transfected with plasmids expressing short hairpin RNAs against Usp7 (shUsp7) as indicated. 24 hours after transfection, the cells were infected with H5*pg*4100 or left uninfected and further incubated for 24 hours. Proteasome inhibitor Mg132 (10 μM) was added to the cells 6 hours prior to harvesting as indicated. Total cell extracts were analyzed by immunoblotting with 3D8 and 2A6. β-actin was analyzed as a loading control.

5.1.3 Usp7 binds to the N-terminal region of E1B-55K

To further analyze the interaction between these two proteins, the minimal region of E1B-55K required for Usp7 binding was identified by GST pull-down experiments. As summarized in Figure 8A, GST fusion proteins including the full-length form, a series of truncation segments and alternative splicing variants of E1B-55K protein were generated to evaluate their interaction with cellular Usp7. Among these products, purification of full-length E1B-55K protein was inefficient due to its poor stability when expressed in bacteria. Still, the combination of full-length protein and its bacterial degradation products could precipitate Usp7 (Fig. 8B, lane 3). In contrast,

no binding was observed with GST alone indicating that Usp7 binds to E1B-55K specifically. Besides the full-length protein, all the fusion products containing the first 79 residues of E1B-55K precipitated Usp7 regardless of their C-terminal extensions. Consistently, the residues between 83 and 188 were shown to be dispensable for this interaction. Taken together, these data demonstrated that the N-terminal 79 amino acid region of E1B-55K is necessary and sufficient for binding to Usp7 *in vitro*.

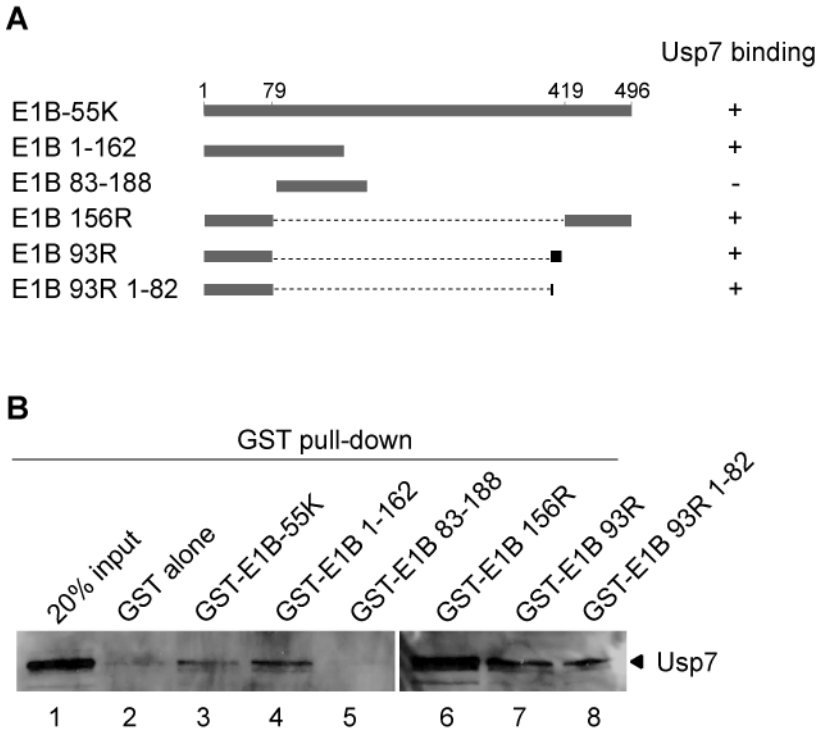

Figure 8. Mapping the Usp7 binding region of E1B-55K by GST pull-down experiments. **(A)** Schematic representation of E1B-55K splice-variants (E1B 156R, and 93R) and segments (E1B 83-188, 93R 1-82, and 1-162) fused to GST and summary of their binding to Usp7. The unique C-terminus of E1B 93R due to using a different reading frame is illustrated as a black box. Numbers refer to amino acid residues of wt E1B-55K protein from Ad5. **(B)** GST fusion proteins were expressed in bacteria and purified as described in the Methods section. Similar amounts of fusion products immobilized to Glutathione-sepharose beads were incubated with the extracts of H1299 cells. GST alone served as a negative control. Twenty percent of the input and the precipitated proteins were subjected to immunoblotting using anti-Usp7 antibody 3D8.

5.1.4 E1B-55K contains a highly conserved Usp7 binding motif in its N-terminus

Previous investigations in our group identified the first 215 amino acid residues of Usp7 as being responsible for binding to E1B-55K in GST pull-down experiments. These N-terminal residues correspond to a so-called TRAF-like domain (TD) in Usp7, which was previously reported to mediate the interactions with p53, Mdm2, and EBNA1 (Holowaty et al., 2003a; Hu et al., 2006; Hu et al., 2002; Sheng et al., 2006). Moreover, it has been shown that all these three proteins bind to the same substrate recognition site in Usp7 (Hu et al., 2006; Sheng et al., 2006) via their four-residue binding motif with a consensus sequence of ø/E-G-ø/G-S (Hu et al,2006) or P/A-X-X-S (Sheng et al, 2006)(Fig. 9). Although these two motifs suggested simultaneously by two different groups differ in their composition, the significance of the last serine and the consistent hydrophobicity of the first residue were emphasized by both reports. Since the first 79 residue in E1B-55K were found to be sufficient for Usp7 binding in the experiments described above (Fig. 8), possible interaction motifs were screened within this sequence. As can be seen in Figure 9B, four separate amino acid patches showing similarities to the suggested consensus sequences were identified. Three of these sequences containing residues 13-16 (AGFS), 51-54 (AGGS), and 70-73 (PGPS) were found to match perfectly to both motifs. The fourth one (residues 65-68; EPES) did not fit well with the suggested consensus sequences, however it resembled to that of EBNA1 (EGPS) with E at the first, and S at the last position.

To reveal whether one of these motifs acts as an Usp7 binding signal, amino acid substitutions were introduced as summarized in Figure 9B. First, steady-state levels of wt and mutant E1B-55K proteins were determined from cells transfected with the constructs expressing these proteins using immunoblotting (Fig. 9C). Two of the mutant proteins, E65V/S68G and A51T/S54G accumulated E1B-55K levels comparable to the wt protein. However, the P70T/S73A mutant exhibited significantly reduced protein steady-state levels compared to wt E1B-55K. The A13V/S16L mutation produced an unstable protein and for unknown reasons this protein was observed to migrate faster than the others in SDS-PAGE.

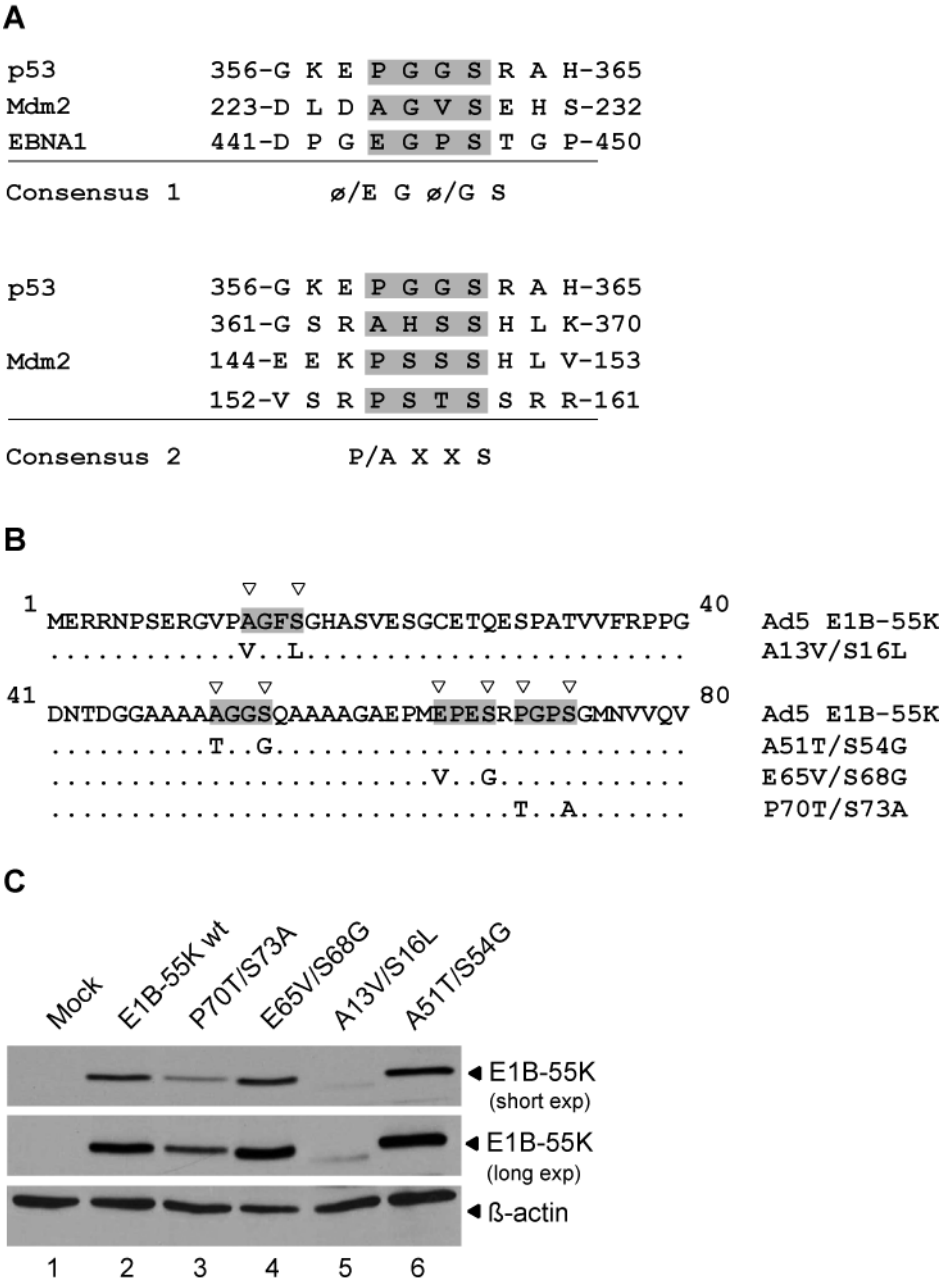

Figure 9. Putative Usp7 binding motifs within the N-terminal region of E1B-55K and their mutagenesis. (A) The alignment of p53, Mdm2, and EBNA1 sequences identified to be responsible for binding to Usp7 TD. The four-residue sequences mediating the interaction with Usp7 are indicated by gray boxes. The consensus (Ø/E)G(Ø/G)S motif, where Ø stands for a hydrophobic residue, was suggested in Hu et al, 2006 (Consensus 1) and (P/A)XXS, where X stands for any amino acid, was suggested in Sheng et al, 2006 (Consensus 2). **(B)** Mutagenesis of potential residues mediating the binding of E1B-55K to Usp7. Amino acid sequence of the N-terminus of Ad5 E1B-55K protein is shown. Tetrapeptides that could be a potential binding site for Usp7 are marked by gray boxes. The amino acids at position one and four in each putative binding motif, suggested to be critical for mediating specific interactions with Usp7, are marked by triangles. These amino acids were exchanged as indicated in the rows below the sequence. Generated mutant proteins were named according to the amino acid substitutions (right) **(C)** Steady-state levels of wt and mutant E1B-55K

proteins. H1299 cells were transfected with plasmids encoding the wt and the mutant E1B-55K proteins. Total cell extracts were prepared and subjected to immunoblotting using anti-E1B-55K antibody 2A6. Shorter (short exp) and longer (long exp) exposures of the X-ray film are shown. β-actin served as a loading control.

Next, the binding of these mutants to Usp7 was investigated by IP experiments. While performing these assays, the reduced stability of P70T/S73A and A13V/S16L mutants was considered and the E1B-55K protein levels in total cell extracts were equilibrated as described in the legend to Figure 10. Following confirmation of equivalent levels of Usp7 in each sample by immunoblotting (Fig. 10, lower lane), these extracts were probed with anti-E1B antibody 2A6 and the immunoprecipitates were analyzed by Western blotting with E1B- and Usp7-specific antibodies. Analysis of the immunoprecipitates with a rat mab against E1B-55K showed the presence of comparable amounts of 55K product in each reaction, with the exception of the A13V/S16L mutant, which was slightly less than the wt. Still, the A13V/S16L mutant precipitated Usp7 as efficient as wild-type. The binding of E65V/S68G and A51T/S54G mutants to Usp7 was also found to be similar to the wt protein. However, it was observed that the interaction between E1B-55K and Usp7 was significantly impaired, if not fully abolished, only when P70T/S73A substitutions were inserted (lane 3). Thus, these experiments indicated that the PGPS motif located between residues 70 and 73 in E1B-55K serves as a Usp7 binding motif (UBM).

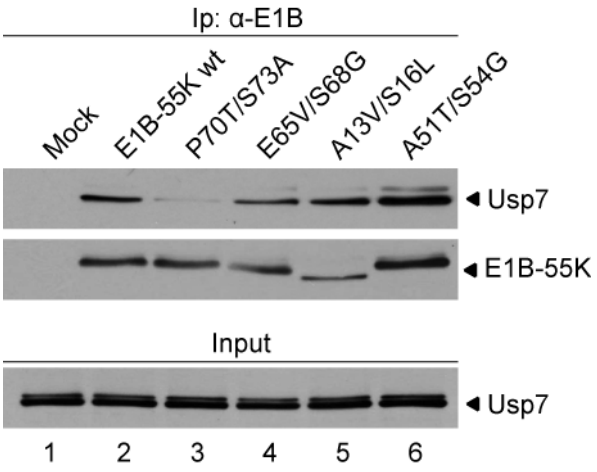

Figure 10. Binding of the E1B-55K mutants to Usp7. H1299 cells were mock transfected or transfected with plasmids encoding wt and mutant E1B-55K proteins as indicated and total cell extracts were prepared. E1B-55K levels were equilibrated by using 1.5 times more extract

from the P70T/S73A mutant and 2.5 times more from the A13V/S16L mutant. Total protein amount per sample was then equalized by adding appropriate amounts of mock extract to the rest of the samples. The extracts prepared in this way were subjected to Ip with 2A6 antibody (α-E1B). Precipitated proteins were resolved by SDS-10% PAGE and visualized by immunoblotting using anti-E1B-55K antibody (7C11) and anti-Usp7 antibody (3D8). To show the input levels of Usp7, 10% of the extracts used in IPs were subjected to immunoblotting and visualized by 3D8.

To determine whether the identified UBM is conserved, amino acid sequences of large E1B products from eighteen different human adenovirus serotypes were aligned using Vector NTI software. Interestingly, alignment data showed the conservation of the complete four-residue UBM, PGPS, in sixteen human serotypes (Fig. 11A). The other three putative motifs were not conserved (data not shown). The notable similarity of the PGPS motif in E1B-55K to the EGPS motif in EBNA1, and the complete conservation of these four residues when present in E1B sequences suggests the importance of this motif for the functionality of large E1B proteins.

Previous investigations have identified several important motifs and domains in the E1B-55K amino acid sequence that contribute to the multiple functions of this protein. While investigating the conservation of UBM, it was noted with interest that all of these reported motifs and domains are well conserved among different adenovirus serotypes. Some of these conserved regions are presented in Figure 11B. Interestingly, the N-terminus of E1B-55K exhibits the highest sequence diversity. In this most variable part, three regions were observed to be strikingly well conserved. Two of these regions have previously been identified as being the CRM1-dependent nuclear export signal (NES) mediating the nucleocytoplasmic shuttling of E1B-55K (Krätzer et al., 2000), and the Sumo1 conjugation motif (SCM)(Endter et al., 2001). Here, UBM is presented as the third and most conserved motif in the N-terminus of E1B-55K.

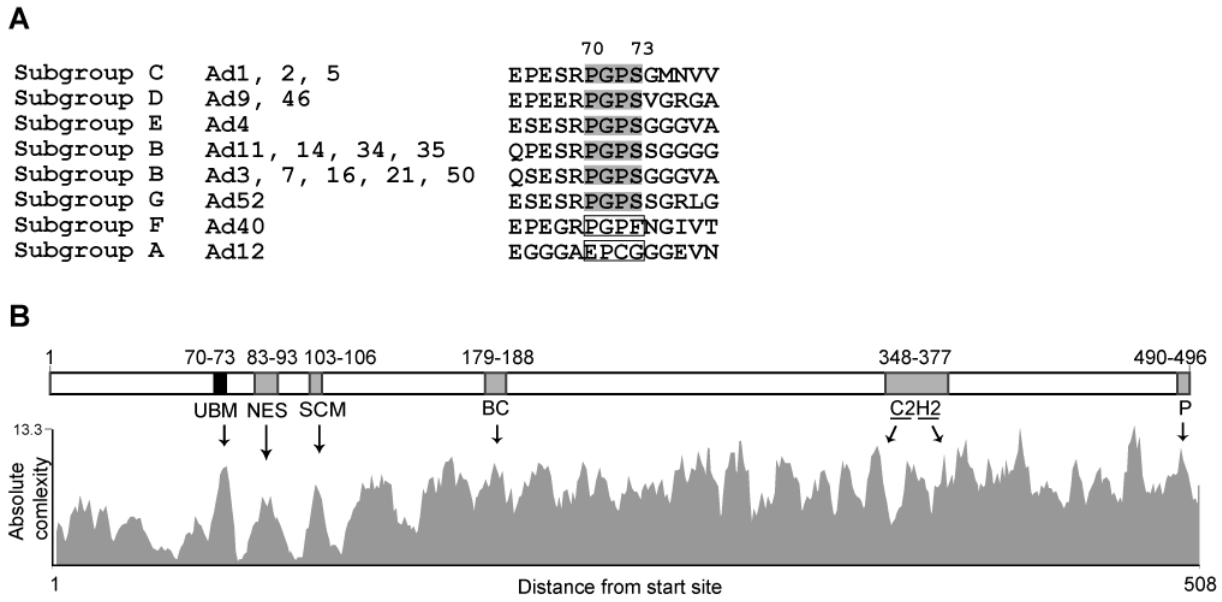

Figure 11. Conservation of Usp7 binding motif in large E1B products of different adenovirus serotypes. (A) Alignment of Usp7 binding sites in large E1B products from 18 different human serotypes belonging to all seven human subgroups (A-G). Serotypes presented in the same row contain identical residues for the shown sequence. Numbers above the sequences refer to the amino acid positions in Ad5. The consensus Usp7 binding motif (UBM) is marked by gray boxes. Empty boxes show the lack of the motif in the aligned region. **(B)** Diagram and absolute complexity profile of Ad5 E1B-55K protein. The leucine-rich nuclear export signal (NES)(Krätzer et al., 2000), the Sumo1 conjugation motif (SCM)(Endter et al., 2001), the putative elongin B- and C- binding motif (BC)(Blanchette et al., 2004), the predicted zinc finger (C2H2)(Gonzalez and Flint, 2002) and the region containing phosphorylated residues (P)(Teodoro and Branton, 1997) are indicated in gray boxes, whereas UBM is shown in black. To show the conservation of these motifs and domains, absolute complexity (*y*-axis) of the aligned E1B sequences was calculated by Vector NTI in terms of average pair-wise alignment scores. Higher values in the *y*-axis show higher sequence conservation. The *x*-axis indicates the distance from the start site. The peaks corresponding to particular E1B motifs are marked with arrows.

5.1.5 Generation and characterization of the virus mutant H5*pm*4185

In the experiments described above, the interaction between Usp7 and E1B-55K was verified and shown to be responsible for the stabilization of E1B-55K. In addition, the interaction was mapped to two highly conserved residues in the N-terminal region of the 55K protein, allowing the construction of a minimally mutated version of E1B-55K in the viral context, which would be Usp7 binding deficient. In this context, to assess the functional significance of this interaction in adenovirus infection, we generated the virus mutant H5*pm*4185 carrying the P70T/S73A substitutions in E1B-55K using a cloning strategy established in our group (Groitl and Dobner, 2007) as

described in the Methods section.

5.1.5.1 **Usp7 binding and the stability of E1B-55K in H5*pm*4185 infection**

After propagating the mutant virus, we first tested the effect of the amino acid substitutions on the stability of the 55K protein. The steady-state levels of E1B-55K were determined by immunoblot analysis of total cell extracts from H1299 cells infected with wt H5*pg*4100 and mutant H5*pm*4185 viruses. As shown in Figure 12A, at 24 h p.i., compared to wt infection, H5*pm*4185 accumulated significantly lower levels of E1B-55K protein in H1299 cells. Furthermore, treating the cells with proteasome inhibitor Mg132 rescued the mutant protein levels back to wt, indicating that the mutant E1B-55K is subjected to increased proteasomal degradation. To note, infecting cells with viruses or Mg132 treatment had no profound effect on the steady-state levels of Usp7.

Subsequently, IP reactions were performed to confirm the defective Usp7 binding of the mutant protein expressed by H5*pm*4185. Extracts containing equilibrated levels of E1B-55K proteins from wt and mutant virus infected cells were incubated with 3D8 antibody and immunoprecipitates were analyzed for the presence of E1B-55K – Usp7 complexes using 2A6 antibody (Fig. 12B). The input levels of E1B-55K proteins were analyzed and confirmed to be equal by immunoblotting (lower panel, lanes 2 and 3). The results of the IP confirmed the defect of the P70T/S73A mutant in binding to Usp7. Notably, the mutant protein could still precipitate small amounts of Usp7, which was detected in longer exposures of the immunoblot. Nevertheless, the effect of the mutation on Usp7 binding and the stability of E1B-55K was found to be consistent in the tested cell line.

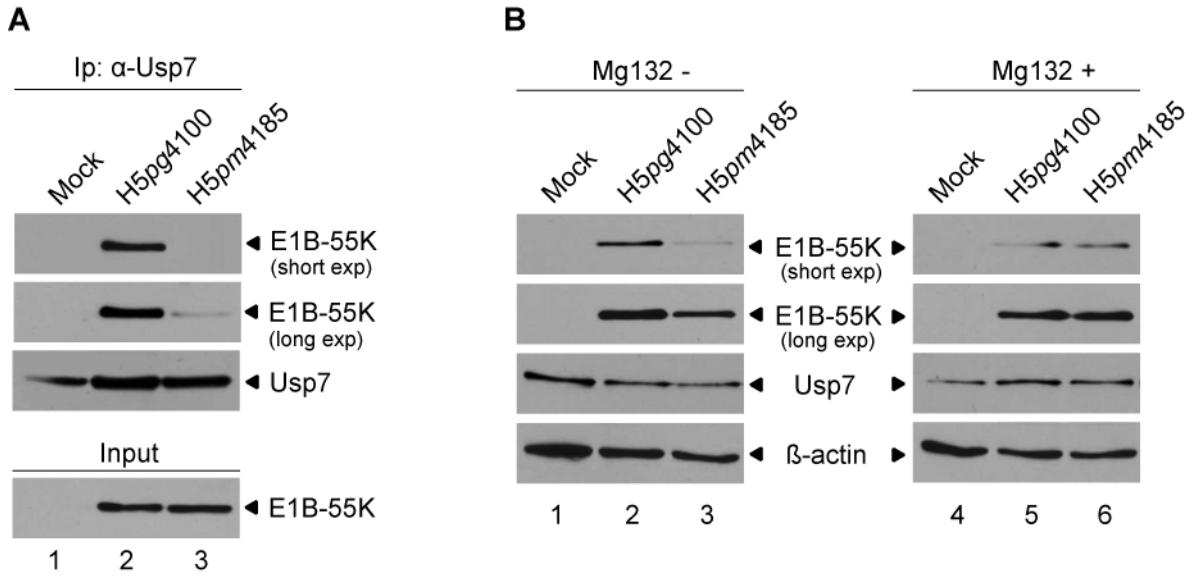

Figure 12. Effect of the inserted mutations on Usp7 binding and the stability of E1B-55K in virus infected cells. (A) H1299 cells were mock infected or infected with wt H5*pg*4100 and H5*pm*4185 expressing the E1B-55K UBM mutant. Twenty-four hours after infection total cell extracts were prepared and subjected to immunoprecipitation (Ip) reactions with 3D8 antibody against Usp7 (α-Usp7). To equilibrate the E1B-55K levels, 1.5 times more extract from H5*pm*4185 infected extracts were used. Total protein amount per sample was then leveled by adding appropriate amounts of mock extract to the rest of the samples. The immunocomplexes were separated by SDS-PAGE and visualized by immunoblotting using 3D8 and 2A6. The E1B-55K input was shown by immunoblotting the 10% of the extracts using 2A6 antibody. **(B)** H1299 cells were infected as described in the panel A. Proteasome inhibitor Mg132 (10 μM) was added to the cells 6 hours prior to harvesting as indicated. Total cell extracts were analyzed by immunoblotting with 3D8 and 2A6. β-actin was analyzed as loading control. Shorter (short exp) and longer (long exp) exposures of the X-ray film are shown.

5.1.5.2 Effect of the inserted mutations on the sumoylation and subcellular localization of E1B-55K

Generation of a mutant virus H5*pm*4185 which is defective in Usp7 binding enabled a thorough analysis of the functions of E1B-55K with respect to its interaction with Usp7 during virus infection. First, two of the important characteristics of the 55K protein were investigated during H5*pm*4185 infection: Sumoylation and nucleocytoplasmic shuttling. E1B-55K protein actively shuttles between the nuclear and cytoplasmic compartments. Its nuclear export is mediated via the cellular export receptor Crm-1 and requires a leucine-rich nuclear export signal (Fig. 11). It has also been shown that E1B-55K is covalently modified by the small ubiquitin-related

modifier protein 1 (Sumo1) and interestingly nuclear targeting and export of E1B-55K is regulated by sumoylation (Kindsmuller et al., 2007). It is noteworthy that the Usp7 recognition site of E1B-55K is in close proximity to NES and SCM. Therefore, it is a reasonable question whether Usp7 interaction has a further effect on sumoylation and/or the subcellular localization of E1B-55K. In addition, previous investigations in our group suggested that Usp7 is relocalized to adenovirus replication centers during infection. This observation was further analyzed using H5*pm*4185 virus as a tool to study the specific function of E1B-55K in this process.

Accordingly, the consequence of the Usp7 binding defect for E1B-55K sumoylation was investigated first. In adenovirus infected cells only a minor proportion of the 55K protein is Sumo1 conjugated and this form can hardly be detected by Western blots (Endter et al., 2001; Kindsmuller et al., 2007). Hence, the experiments were conducted in both transiently transfected and virus infected cells where a histidine-tagged version of Sumo1 protein (His-Sumo1) is overexpressed. In these experiments, His-Sumo1 transfected cells were either co-transfected with the plasmids encoding wt E1B-55K, P70T/S73A, and two sumoylation-deficient mutants of E1B protein (K104R and V103D)(Endter et al., 2001) or infected with H5*pg*4100, H5*pm*4185, and a virus expressing the sumoylation-deficient mutant of E1B-55K (K104R) H5*pm*4102 (Kindsmuller et al., 2007). Subsequently, Sumo1 conjugated 55K proteins were purified and analyzed by immunoblotting. In both transfected and virus infected cells, sumolyated forms of wt and P70T/S73 mutant could be detected and the lack of this E1B form in the sumoylation-deficient mutants showed the specificity of the assay (Fig. 13A). As expected, only a small amount of Sumo1 conjugated E1B-55K was detected in the infection experiments. At first sight, it can be considered that the mutant E1B-55K protein expressed by H5*pm*4185 is less sumoylated than the wild-type. However, due to its reduced stability, the input levels of the mutant protein were also less and when this difference is considered, it can be concluded that mutating the Usp7 binding motif has no significant effect on Sumo1 conjugation of the 55K protein in infection. Similarly, in the transfected cells no obvious difference was detected between the sumoylation levels of the wt and the P70T/S73A mutant (Fig. 13B).

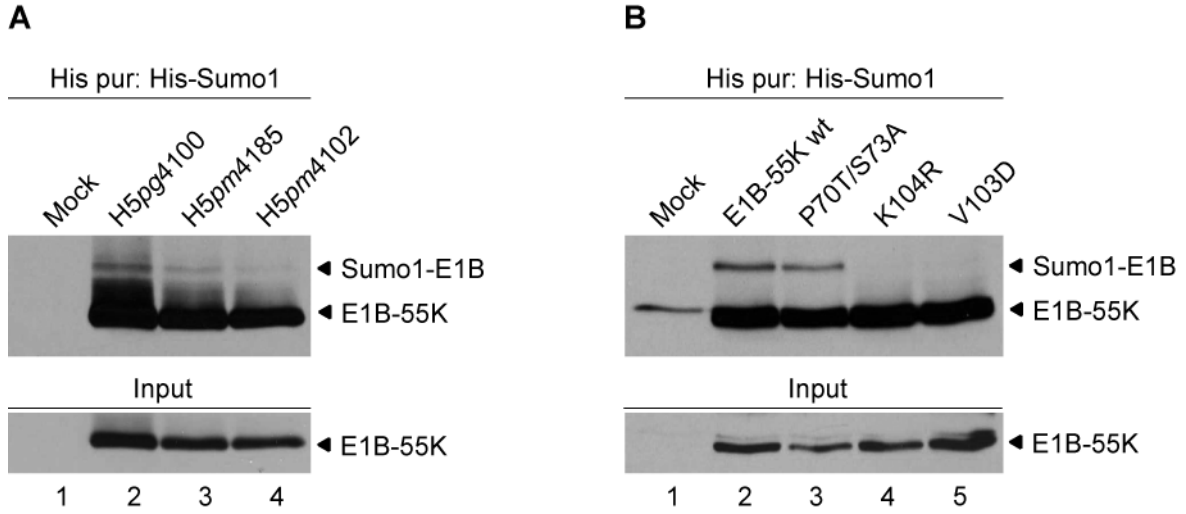

Figure 13. The effect of P70T/S73A mutation on the sumoylation of E1B-55K protein. (A) H1299 cells were transfected with a plasmid encoding a histidine-tagged Sumo1 (His-Sumo1) and 24 hours after transfection cells were infected with H5*pg*4100, H5*pm*4185, and H5*pm*4102 (producing a sumoylation deficient E1B-55K, K104R) viruses and further incubated for 24 h, **(B)** or co-transfected with His-Sumo-1 plasmid and plasmids encoding wt E1B-55K, P70T/S73A mutant and the sumoylation-deficient mutants K104R and V103D. An aliquot of the cells were used to prepare total cell extracts. The cells were lysed by the addition of 6 M guanidine hydrochloride and ubiquitinated proteins were purified by Ni^{2+} - agarose beads as described in the Methods section. The eluted proteins were separated by SDS-PAGE and E1B proteins were visualized by immunoblotting using 2A6 antibody.

To investigate whether the interaction between these proteins has an influence on the CRM1-dependent nuclear export of E1B-55K, their steady-state localizations in H5*pg*4100 and H5*pm*4185 virus infections were determined by immunofluorescence analysis in the absence or presence of a specific CRM1 inhibitor Leptomycin B (LMB). Consistent with previous reports, in infected cells, the wt E1B-55K protein demonstrated a diffuse cytoplasmic staining with dot-like structures close to the nucleus and a nuclear distribution that was mostly diffuse (Fig. 14A, panel h)(Gonzalez and Flint, 2002; Ornelles and Shenk, 1991). The inactivation of CRM1 by LMB resulted in the retention of E1B-55K in large dot-like aggregates in the nucleus (panel k). In both cases, the mutant protein showed an intracellular distribution indistinguishable from the wild-type (panel n and q). The accumulation of this protein in nuclear aggregates upon treatment with LMB indicated that the protein can enter and exit the nucleus under normal circumstances. Thus, it can be concluded that mutating the UBM also does not affect the NES of E1B-55K.

On the other hand, the subcellular localization of Usp7 was completely altered upon adenovirus infection. In mock-infected cells, Usp7 exhibited a diffuse nuclear staining with a few dot-like accumulations in the nucleus, which is consistent with previous reports (panel a)(Everett et al., 1999; Everett et al., 1997), and this localization was not disturbed by LMB treatment (panel d). However, in both H5*pg*4100 and H5*pm*4185 infection, Usp7 was found to be concentrated almost exclusively in large nuclear bodies resembling adenovirus replication centers. Interestingly, treating the cells with LMB resulted in nearly perfect co-localization of E1B-55K and Usp7 in these nuclear bodies. These results suggest two conclusions: First, the relocalization of Usp7 upon adenovirus infection is independent of its interaction with E1B-55K, and second, the interaction between these two proteins occurs mostly in these nuclear structures during adenovirus infection.

To further test whether the observed relocalization of Usp7 in nuclear bodies is due to its interaction with E1B-55K and to confirm whether these bodies are viral replication centers, the steady-state localization of Usp7 and adenovirus single-stranded DNA binding protein (DBP; marker for replication centers) were investigated (Fig. 14B). The cells were infected with wt H5*pg*4100 as a positive control, H5*pm*4185, and *dl*1520 (virus lacking all E1B functions)(Barker and Berk, 1987) as a negative control. Interestingly, in all three virus infections, Usp7 was found to be relocalized to adenovirus replication centers, confirming that this redistribution is independent of E1B-55K. Nevertheless, the possibility of an enhancing effect of an E1B-55K-Usp7 interaction on this process should not be excluded.

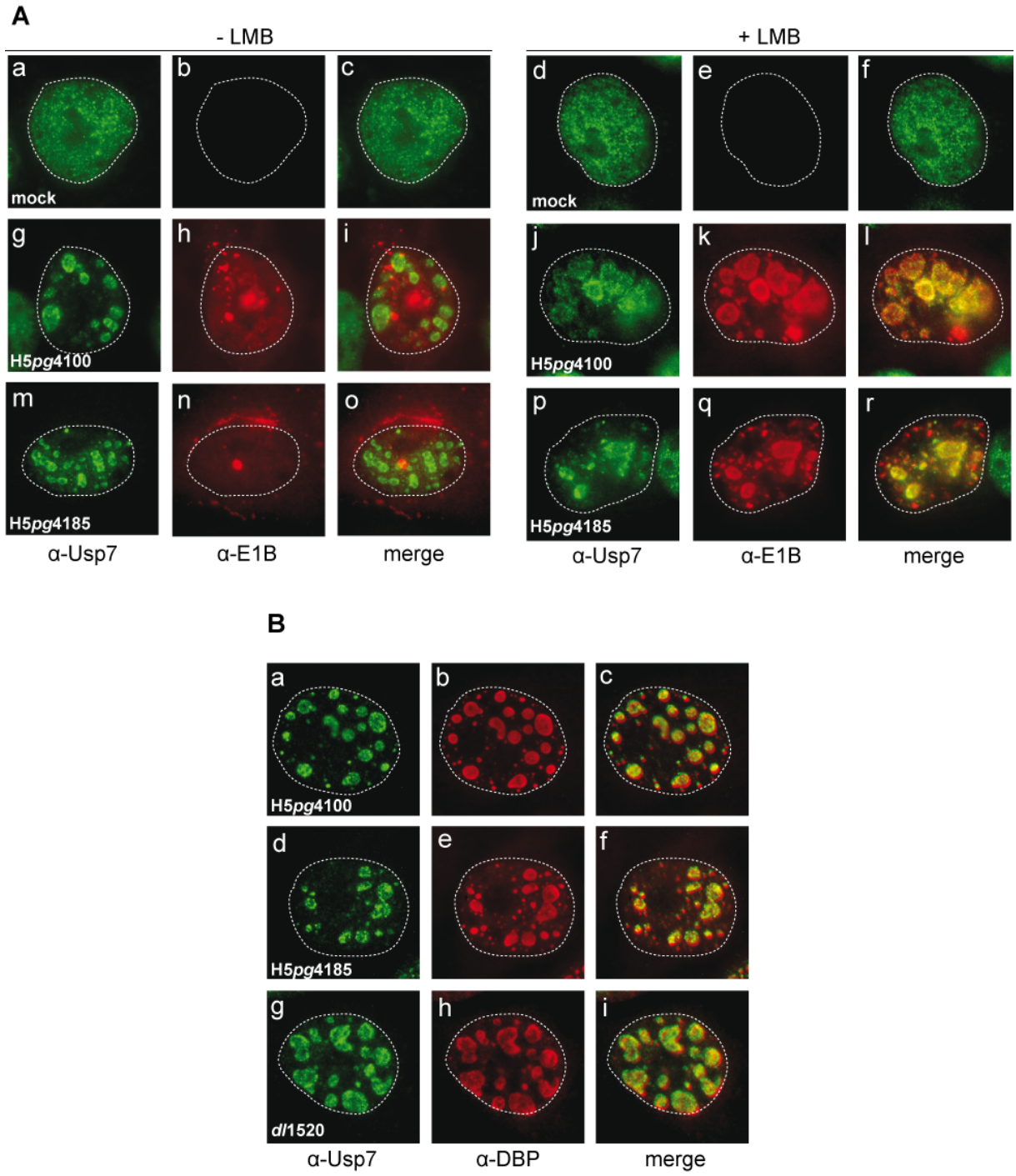

Figure 14. Subcellular localization of E1B-55K and Usp7 in virus infected cells. (A) H1299 cells were infected with H5*pg*4100 and H5*pm*4185 viruses at a multiplicity of 20 ffu per cell or remained uninfected. CRM1 inhibitor LMB (10 nM) was added to the cells 3 hours prior to fixation as indicated. 24 hours after infection, the cells were fixed and Usp7 was labeled by 3D8 (α-Usp7) and E1B-55K by 2A6 (α-E1B) antibodies. These proteins were then visualized by FITC- and Texas Red-conjugated secondary antibodies respectively. Representative Usp7 (green, panels a, d, g, j, m and p) and E1B-55K (red, panels b, e , h, k, n, and q) staining and the overlay of these patterns (merge, panels c, f, i, l, o, and r) are shown. **(B)** Usp7 localization in viral replication centers. Cells were infected with H5*pg*4100, H5*pm*4185, and *dl*1520 and fixed at 24 hours after infection. Usp7 was labeled with 3D8 (α-Usp7) and viral replication centers were marked with anti-E2A-72K antibody B6-8 (α-DBP). The proteins were

visualized by FITC- and Texas Red-conjugated secondary antibodies, respectively. Anti-Usp7 (green, panels a, d and g) and anti-DBP (red, panels b, e and h) staining patterns, and their overlay (merge, panels c, f and i) are shown. In all panels, nuclei are shown by dotted lines.

5.1.5.3 **Effect of the inserted mutations on virus replication**

To further characterize the effect of the P70T/S73A mutation on virus infection, the H5*pm*4185 virus was tested in a time course experiment to compare the expression of early and late viral gene products to that of the wt virus. One of the critical functions of E1B-55K is targeting the tumor suppressor p53 for proteasomal degradation during virus infection (Berk, 2005). To be able to analyze this event in H5*pm*4185 infections, in addition to p53 negative H1299 cells (Mitsudomi et al, 1992), the experiments were also conducted in A549 cells expressing wt p53 (Lehman et al., 1991). These two cell types were infected with H5*pg*4100 and H5*pm*4185 viruses at a moi of 20 ffu/cell and cells were harvested at different time points (Fig. 15A). Analysis of these extracts for E1B-55K expression confirmed once more the defect of the mutant virus in maintaining E1B-55K levels in H1299 cells. In contrast, single-stranded DNA binding protein (DBP) expressed by the early region 2A (E2A) accumulated to levels comparable to wt. E1B-55K is known to be involved in the efficient transport and translation of late viral mRNAs (Dobner and Kzhyshkowska, 2001). Indeed, a clear delay in the expression of the late gene product L4-100K was observed, showing that the late phase of the infection is affected mainly in H1299 cells. However, interestingly, H5*pm*4185 behaved like wild-type in A549 cells. In this cell line, the steady-state levels of the mutant 55K protein were comparable to wt and similarly no difference was observed in either DBP or L4-100K levels.

In infected cells p53 is targeted for ubiquitination by E1B-55K (Querido et al., 2001), whereas Usp7 acts as a de-ubiquitinase for the tumor suppressor under stress conditions (Ronai, 2006; Tang et al., 2006). The opposite activities of these two proteins on p53 raised the question of whether Usp7 interaction is necessary for the efficient degradation of p53 by the adenoviral protein. An intriguing possibility is that Usp7 is targeted for proteasomal degredation by the 55K protein together with p53. To test these possibilities, the steady-state concentrations of these cellular

proteins were determined by immunoblotting. As shown in Figure 15B, p53 protein levels gradually decreased in both virus infections at an equal rate, suggesting that the binding of E1B-55K to Usp7 is not a prerequisite for p53 degradation in A549 cells. On the other hand, a surprising difference was observed between the wt and mutant virus regarding the Usp7 expression pattern. Contrary to expectations, during infection of both H1299 and A549 cells with wt virus, Usp7 protein was observed to accumulate slightly over time. This increase in Usp7 levels seems to be an effect induced by E1B-55K since in H5*pm*4185 infection, this accumulation reverted to a slight reduction in Usp7, which could be observed better in A549 cells. Although the reason for this phenotype remained unclear, these observations suggest the possibility that Usp7 and E1B-55K activities are reciprocal and the induction of Usp7 levels may be critical for the biological functions of E1B-55K.

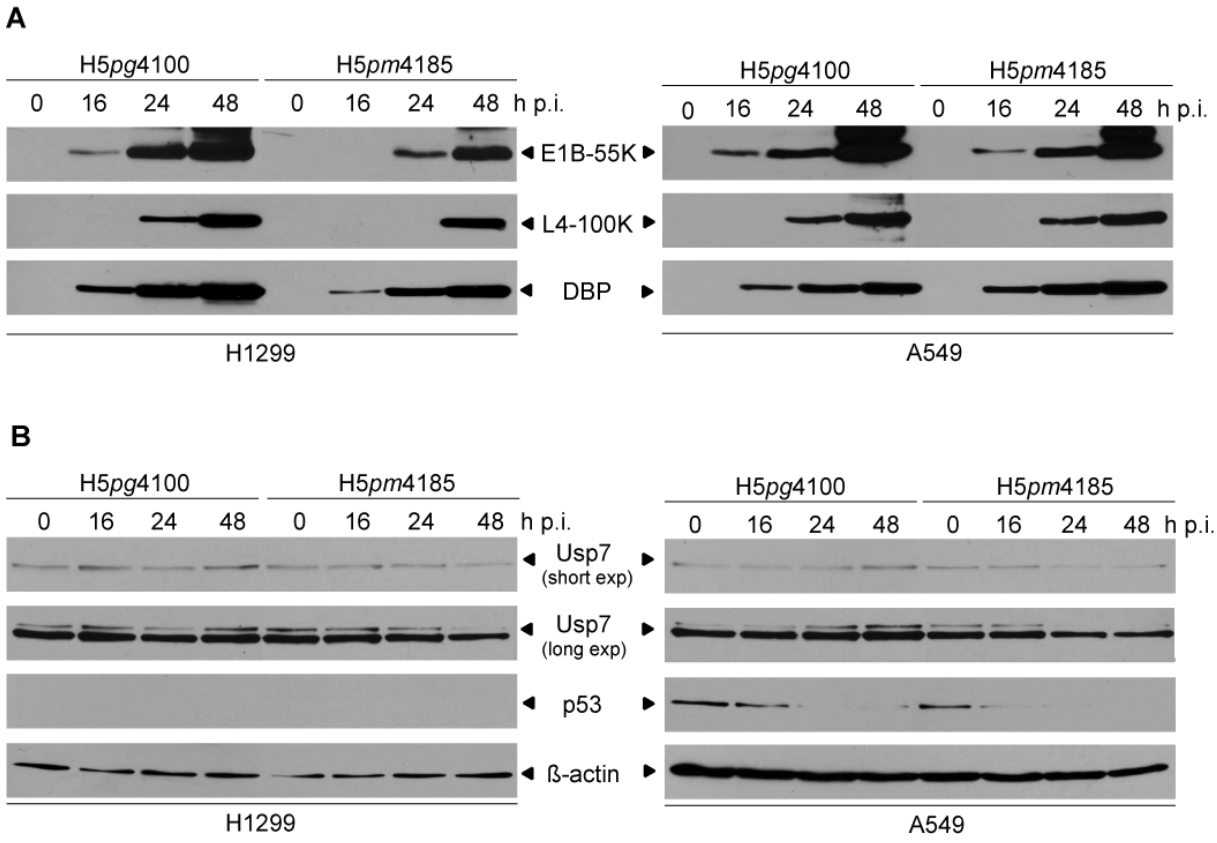

Figure 15. Steady-state levels of selected viral and cellular proteins in virus infected cells. H1299 and A549 cells were infected with H5*pg*4100 and H5*pm*4185 viruses at a multiplicity of 20 ffu per cell. Total cell extracts were prepared at indicated times post-infection (p.i.) and subjected to immunoblotting. **(A)** E1B-55K was detected with 2A6, late viral protein L4-100K was detected by a rat mab 6B10 (Kzhyshkowska et al., 2004). **(B)** The cellular proteins Usp7

and p53 were detected with 3D8 and mouse mab DO1, respectively. Shorter (short exp) and longer (long exp) exposures of the X-ray film are shown. β-actin was analyzed as a loading control.

The effect of this mutation on virus growth was investigated by one-step growth curve experiments conducted in both tumor cell lines and the results were compared to those of H5*pg*4100 and *dl*1520 infections, which served as positive and negative controls, respectively (Fig. 16). Correlating with the immunoblot data, A549 cells produced similar amounts of progeny for wt and H5*pm*4185 viruses, with a slight reduction observed for the latter. In contrast, virus production of H5*pm*4185 was found to be impaired in H1299 cells with levels comparably low to E1B-deleted virus, which implied the biological significance of the Usp7 interaction for adenovirus infection in this line. Moreover, the requirement for the E1B-55K – Usp7 interaction in adenovirus infection was found to be cell type dependent and may involve p53 activity.

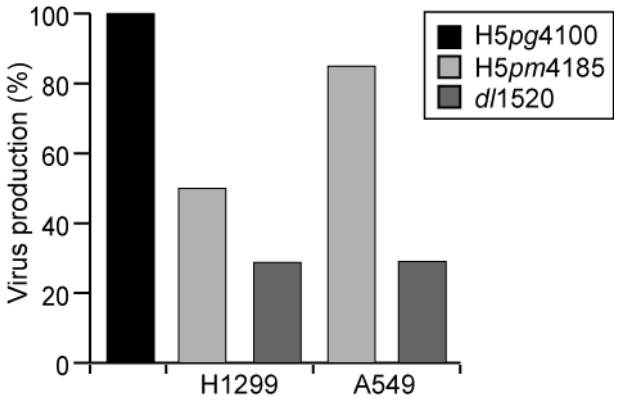

Figure 16. The effect of P70T/S73A mutation in E1B-55K on progeny virion production. H1299 and A549 cells were infected with wt H5*pg*4100, H5*pm*4185, and E1B-deleted *dl*1520 viruses at a multiplicity of 20 ffu per cell. Viral particles were harvested at 24 and 48 hours post infection (h p.i.) and infectious virus particles were determined by quantitative DBP staining on 293 cells. Virus production is represented as a percentage of production compared to wt. The results represent the averages from two independent experiments.

5.2 Usp7 is required for efficient adenovirus infection

In this work, the physical interaction between E1B-55K and Usp7 was found to be critical for maintaining normal E1B-55K protein levels for efficient virus production

in H1299 cells. In contrast, in A549 cells this interaction was found to be dispensable for the functions of the adenoviral protein. Moreover, E1B-55K independent relocalization of Usp7 to viral replication centers raised the possibility that Usp7 has functions other than stabilizing E1B-55K during adenovirus infection. To gain a better understanding of the interaction between Usp7 and E1B-55K, and to ascertain how Usp7 contributes to adenovirus infection, stable Usp7 knockdown (Usp7kd) cell lines were generated using RNAi technology and adenovirus infection was characterized in these lines.

5.2.1 Generation of stable Usp7 knockdown cell lines

For the generation of Usp7kd cell clones the lung carcinoma cell lines H1299 and A549 were chosen in particular due to the difference in their genetic background concerning p53. Regarding the role of Usp7 in the p53 pathway, these cells would provide an additional tool to understand the Usp7 functions in adenovirus infection.
To stably knock down Usp7 expression, A549 and H1299 cells were transfected with pSuper-shUsp7 plasmid containing a puromycin resistance marker, so stable clones could be selected by growing the cells in the presence of puromycin. For each cell line, more than 20 clones were screened for Usp7 expression by immunoblotting. Figure 17 shows the results from six different monoclonal cell lines derived from each parental cell line. As shown, several clones derived from H1299 cells exhibited reduced levels of Usp7. Especially in HPU1 and HPU2 (panel A, lanes 2 and 3) Usp7 levels were reduced to nearly background levels, providing optimum conditions for further experiments. On the other hand, although several puromycin resistant clones were isolated from the stable transfection of A549 cells, only one of them (APU6; panel B, lane 7) exerted a significant reduction in Usp7 expression, indicating that these cells cannot tolerate reduced Usp7 levels, probably due to the presence of wt p53.

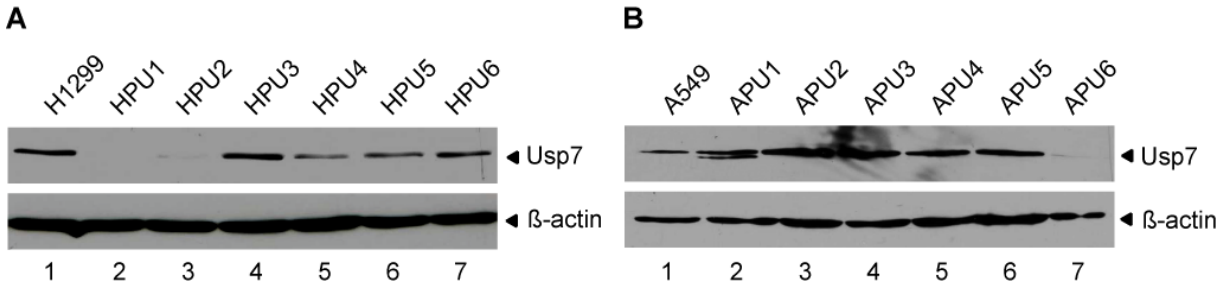

Figure 17. Generation of stable Usp7 knockdown monoclonal cell lines with p53-positive and p53-negative backgrounds. (A) A549 cells and **(B)** H1299 cells were transfected with pSuper-shUsp7 vector containing a puromycin selection marker. After an incubation period of four weeks under selective pressure (puromycin, 3 µg/ml), stable puromycin-resistant clones (A549-pSuper-shUsp7; APU or H1299-pSuper-shUsp7; HPU) were selected and established as permanent cell lines. Usp7 protein levels in these clones were determined from total cell extracts by immunoblotting using 3D8 antibody.

To ascertain whether the inserted Usp7 shRNAs affected properties that could influence virus infection, growth rate and infectivity of the generated lines were determined. Figure 18A shows the growth rates of HPU2, APU5 and APU6 and their parental H1299 and A549 lines. Being the only clone that could be established from the A549 line, APU6 cells were found to grow much slower than its parental cells. However, another cell line derived from A549, APU5, with comparably slow growth to APU6 cells presents normal Usp7 levels. To exclude the possible influence of slower growth, this line was used as an additional control while characterizing virus infection in these cells. On the other hand, HPU2 cells were found to grow as efficient as the parental H1299 cells, as expected.

To test whether the generated lines can be as efficiently infected as their parental lines, the indicated cells were infected with an adenovirus variant expressing green fluorescent protein (Ad-GFP) and the infectivity of the cells were determined by quantitative analysis of GFP positive cells in each line. As shown in Figure 18B, these newly generated cell lines were found to be equally infected by adenovirus. Collectively, these data showed that HPU2, APU5, and APU6 cell lines can be used to investigate the role of USP7 in adenovirus replication.

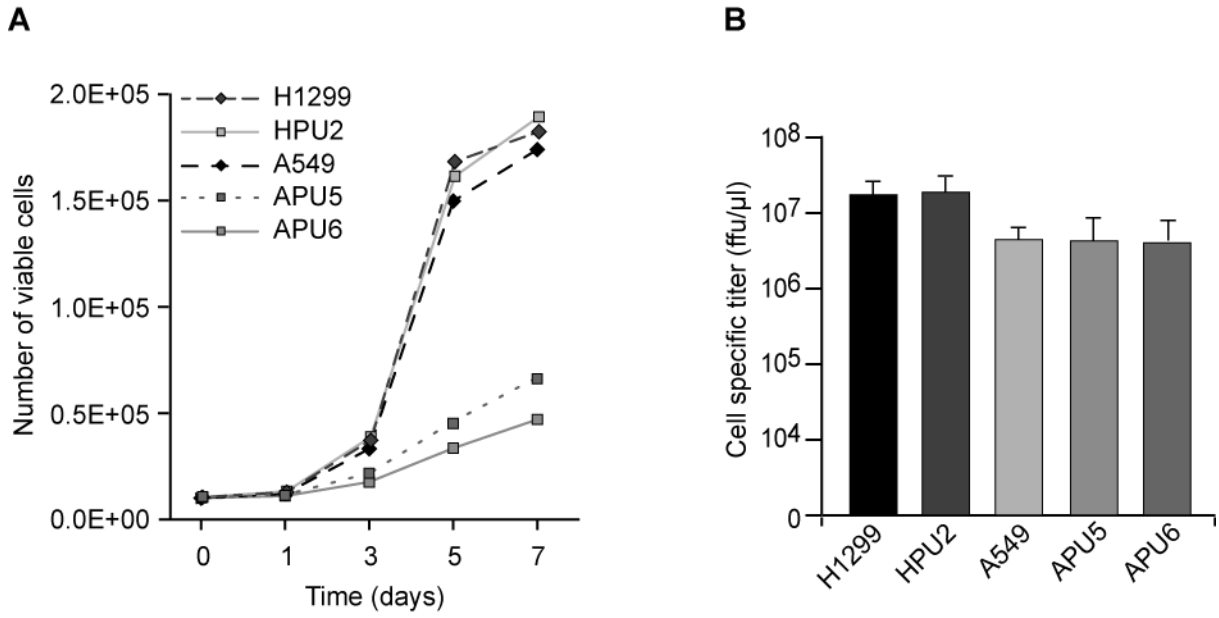

Figure 18. Growth characteristics and infectivity of the selected cell lines. (A) Growth rate of parental A549 and H1299 cells and isolated APU5, APU6 and HPU2 lines. A total of 1X 10^5 cells were plated on six-well dishes in culture medium, and viable cells were counted every day. The mean number of viable cells for duplicate dishes is shown. **(B)** Indicated cell lines were infected with a variant of adenovirus expressing GFP (Ad-GFP). Sixteen hours post infection, GFP positive cells were scored and the cell specific titer of Ad-GFP was determined. The results represent the averages from three independent experiments. Error bars indicate the standard error of the mean.

5.2.2 Characterization of H5*pg*4100 infection in Usp7 knockdown cells

To evaluate the influence of Usp7 on adenovirus infection, the generated Usp7kd cells were infected with wt H5*pg*4100 virus and the synthesis of early and late viral proteins as well as the production of progeny virions were compared to those of the Usp7 positive parental cell lines in the time course of infection. In these experiments, APU5 cells were also tested as a control due to the reasons described above. Since similar results were obtained from both A549 and APU5 cells, the results of APU5 cells were represented.

5.2.2.1 Synthesis of early viral proteins

First, the persistence of Usp7 knockdown throughout the infection was verified by determining Usp7 levels by immunoblotting. As can be seen in Figure 19, Usp7 was detected to accumulate slightly in both H1299 and APU5 cells as the infection

proceeds. As anticipated, the rate of this accumulation was higher in the Usp7kd cells, since it has been proposed that adenovirus interferes with the siRNA processing machinery (Andersson et al., 2005). Nevertheless, at 48 hours post infection, the level of Usp7 in the knockdown cells was still markedly lower than in the Usp7 positive (Usp7+) cells. Thus, both cell lines proved to be suitable for the analysis of adenovirus infection even at late time points.

Next, the effect of Usp7 depletion on the synthesis of the early viral proteins E1A, E1B-55K and DBP was assayed by immunoblotting (Fig. 19). Surprisingly, being the first gene products expressed, E1A proteins showed a defect in accumulating protein levels in HPU2 and APU6 cells compared to the Usp7+ counterparts. Nonetheless, the normal increasing-and-decreasing expression pattern of E1A proteins, which can be better observed in the 13S splice-variant (slower migrating form), was maintained in both knockdown cell lines. Similarly, DBP levels were also detected to be lower in these cells than in the Usp7+ APU5 and H1299 cells. Consequently, when the expression pattern of E1B-55K was investigated a significant defect was observed not only in the expression time, but also in the amounts of this protein. This reduction in E1B-55K levels correlates with the similar defect observed for H5*pm*4185 virus and can be assigned to the stabilizing effect of Usp7 on this protein. Taken together, these results suggest Usp7 plays a role in promoting the early protein expression in adenovirus infection in a general way.

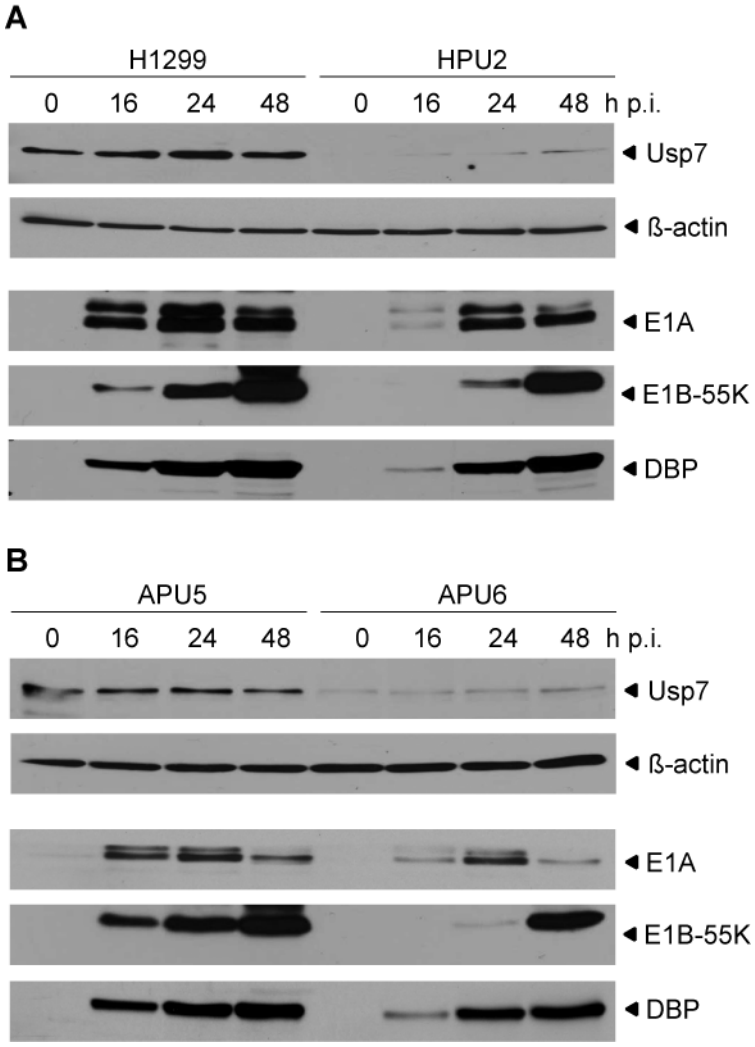

Figure 19. Synthesis of early viral proteins in Usp7 knockdown cells infected with wt adenovirus H5*pg*4100. (A) H1299 and HPU2 cells were infected with H5*pg*4100 virus at a multiplicity of 20 ffu per cell. Total cell extracts were prepared at indicated hours post-infection (h p.i.) and subjected to immunoblotting by M73, 2A6 and B6-8 antibodies detecting the early viral proteins E1A, E1B-55K and DBP, respectively. Usp7 levels were detected with 3D8 antibody to confirm the effect of RNAi and β-actin was analyzed as a loading control. **(B)** The experiments were conducted in APU5 and APU6 cells as described in panel A.

5.2.2.2 **Synthesis of late viral proteins**

Subsequent to the early viral proteins, the expression of the late structural proteins was investigated in the knockdown cells. As expected, the observed inefficient synthesis of the early viral proteins resulted in a delay in the accumulation of late structural proteins in both HPU2 and APU6 cells compared to the Usp7+ counterparts during H5*pg*4100 infection. As shown in Figure 20, late structural

protein synthesis was either delayed in Usp7kd lines (e.g. pIV in HPU2, or pII and minor capsid proteins in APU6), or these proteins did not accumulate to the parental cell line levels (e.g. pIII in both knockdown lines).

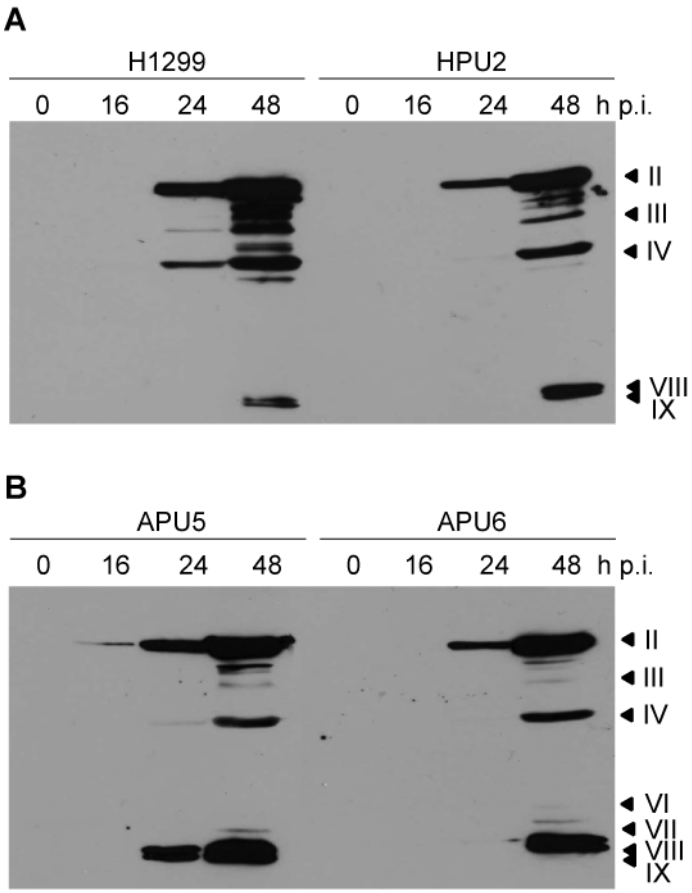

Figure 20. Synthesis of late viral proteins in Usp7 knockdown cells infected with wt adenovirus H5*pg*4100. (A) H1299 and HPU2 cells were infected with H5*pg*4100 virus at a multiplicity of 20 ffu per cell. Total cell extracts were prepared at indicated times post-infection (h p.i.) and subjected to immunoblotting by the anti-Ad5 rabbit polyclonal serum L133. Bands corresponding to viral late proteins hexon (II), penton (III), fiber (IV) and minor capsid proteins (VI, VII, VIII, IX) are indicated on the right. **(B)** The experiments were conducted in APU5 and APU6 cells as described in panel A.

5.2.2.3 **Virus growth**

To further test the effect of Usp7 knockdown on the production of infectious virus particles, virus growth was determined in the control and the test cell lines. The cells were infected at low (2 moi) and high (20 moi) multiplicity of infection and harvested at indicated time points (Fig. 21). At low moi, a defect more than 10-fold was

observed in both Usp7kd cell lines at a 24 h time point. Increasing the moi partially recovered virus production activity at 24 and 48 h post infection. However, even at a high moi and at the late time point of 48 h p.i. the defect in virus production was still significant in both Usp7kd cells, implicating the biological significance of Usp7 for efficient adenovirus infection. Altogether, the comparable early and late phase defects observed in both Usp7 knockdown lines further suggests that the role of Usp7 in adenovirus infection is independent of the p53 status and the growth rate of the host cell.

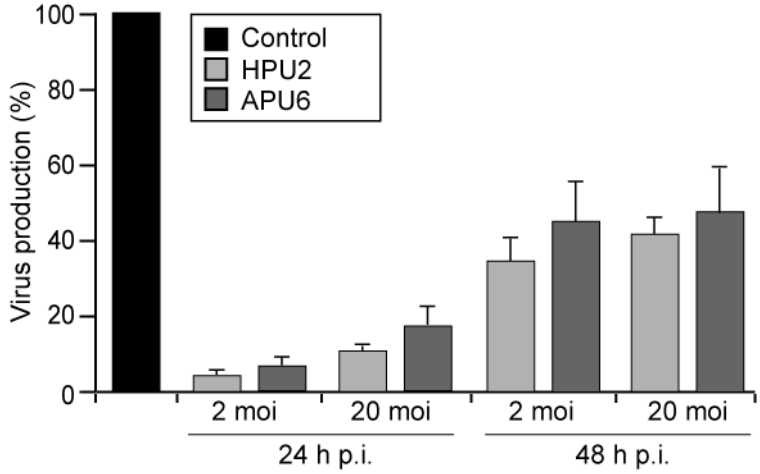

Figure 21. Production of progeny virions in Usp7 knockdown cells infected with wt adenovirus H5*pg*4100. Usp7 knockdown cell lines HPU2 and APU6, and their corresponding control cell lines H1299 and APU5 were infected with H5*pg*4100 virus at a multiplicity of 2 and 20 ffu per cell as indicated. Viral particles were harvested at 24 and 48 hours post infection (h p.i.) and infectious virus particles produced were determined by quantitative DBP staining on 293 cells. Virus production is represented as a percentage of virus production in the respective control APU5 or H1299 cells. The results represent the averages from three independent experiments. Error bars indicate the standard error of the mean.

5.2.3 Characterization of *dl*1520 infection in Usp7 knockdown cells

5.2.3.1 Synthesis of early and late viral proteins

The inefficient expression of early and late phase proteins followed by defective production of progeny virions was consistently observed with wt virus infection in the Usp7kd cell lines regardless of the p53 status, or the growth rate of the cells. To

ascertain the contribution of E1B-55K to this phenotype, the time course experiments were conducted in APU5 and APU6 cells, as described above, with a virus lacking all E1B-55K functions (*dl*1520)(Barker and Berk, 1987). The immunoblot analysis of the infected cells confirmed the lack of E1B-55K expression (Fig. 22). Further detection of early and late viral proteins by the immunoblot showed defective accumulation of E1A, DBP, and the late structural proteins in Usp7kd cells. The defect was similar to the one observed for wt infection, which was surprising since this finding implies that in the absence of a Usp7 – E1B-55K interaction, knockdown of the former still has an influence on virus infection.

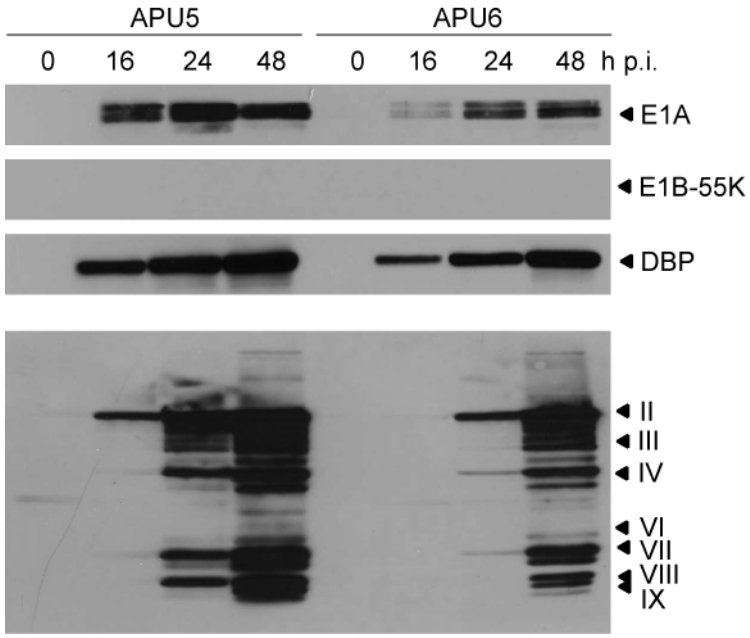

Figure 22. Synthesis of early and late viral proteins in Usp7 knockdown cells infected with E1B-deleted adenovirus *dl*1520. APU5 and APU6 cells were infected with *dl*1520 virus at a multiplicity of 20 ffu per cell. Total cell extracts were prepared at indicated times post-infection (p.i.) and subjected to immunoblotting by M73, 2A6 and B6-8 antibodies detecting the early viral proteins E1A, E1B-55K and DBP, respectively, and the anti-Ad5 rabbit polyclonal serum L133 detecting the late structural proteins of adenovirus. Bands corresponding to late viral proteins hexon (II), penton (III), fiber (IV) and minor capsid proteins (VI, VII, VIII, IX) are indicated on the right.

5.2.3.2 **Virus growth**

To quantify the extent of the defect of *dl*1520 virus in Usp7kd cells, virus growth was determined in APU5 and APU6 lines. The cells were infected with *dl*1520 at low (2)

and high (20) moi and harvested at two different time points. As shown in Figure 23, low moi infection at the 24 h time point resulted in production of ~15-fold less infectious virus particles in Usp7kd cells compared to Usp7+ cells. At the longer incubation period (48 h) and/or higher moi the defect in virus production partially recovered but still remained significant. Unexpectedly, the difference observed in virus particle production in *dl*1520 infection between APU5 and APU6 cells was bigger than that observed in wt virus infection at each time point and moi in the same cells. These results suggest that Usp7 plays a critical role in adenovirus infection via E1B-55K dependent and independent pathways, and further confirms the previously observed reciprocal activities between these two proteins in promoting adenovirus infection.

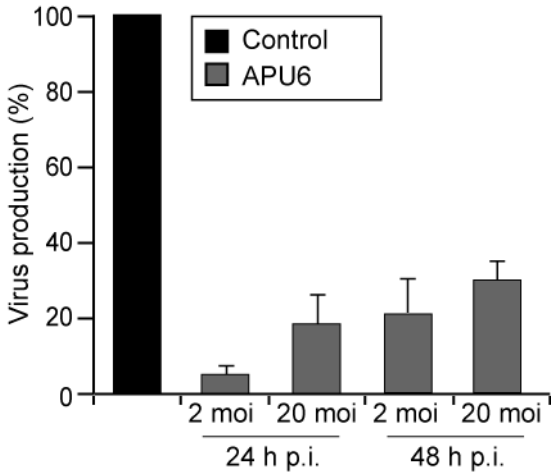

Figure 23. Production of progeny virions in Usp7 knockdown cells infected with E1B-deleted adenovirus *dl*1520. Usp7 knockdown cell line APU6, and its corresponding control cell line APU5 were infected with *dl*1520 virus at a multiplicity of 2 and 20 ffu per cell as indicated. Viral particles were harvested at 24 and 48 hours post infection (h p.i.) and infectious virus particles produced were determined by quantitative DBP staining on 293 cells. Virus production is represented as a percentage of virus production in the control APU5 cells. The results represent the averages from three independent experiments. Error bars indicate the standard error of the mean.

5.2.4 Analysis of the relation between Usp7 levels and adenovirus replication efficiency

5.2.4.1 Ectopical Usp7 expression rescues the RNAi effect

The results showing the significant contribution of Usp7 to adenovirus replication regardless of the p53 status, and the growth rate of the cells were striking. In addition, the negative effect of Usp7 depletion was persistent even in the absence of E1B-55K, which was unexpected. To assign these defects to specific functions of Usp7, this protease was ectopically expressed in HPU2 cells. To achieve successful expression of Usp7 in these cells that stably express short hairpin RNAs against Usp7, a Myc-tagged Usp7 expression plasmid with silent mutations in the siRNA target region of the Usp7 gene was generated by site-directed mutagenesis (Fig. 24A). Indeed, gradually increasing the Usp7 levels resulted in an obvious increase in E1B-55K and DBP levels (panel B), and an enhanced virus replication (panel C). The rescue of the RNAi effect by expressing Usp7 verified that the defects observed in Usp7kd cells were primarily due to the functions of Usp7, and not secondary effects such as inactivation of a non-specific gene during insertion of the shRNA construct or the potential induction of an anti-viral response due to shRNA overexpression in the knockdown lines (panel C). Additionally, these results are critical since they support a correlation between the level of Usp7 and the efficiency of adenovirus infection.

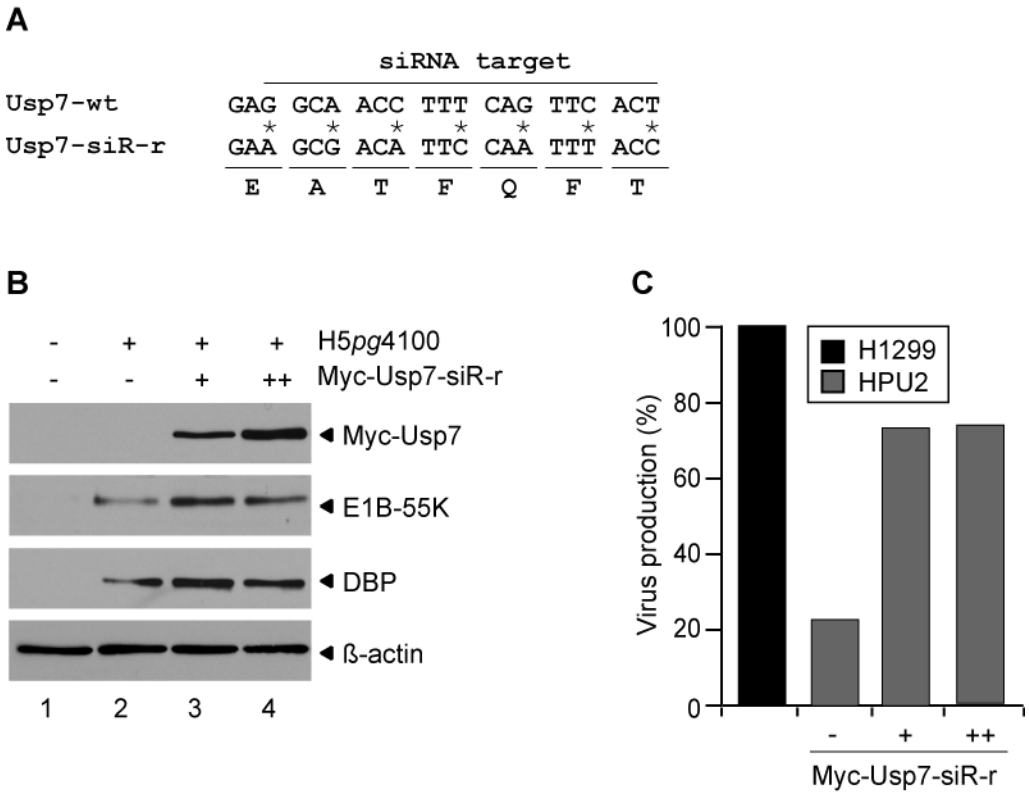

Figure 24. Effect of ectopical expression of Usp7 in Usp7 knockdown cells on early viral protein expression and virus growth. (A) Generation of an siRNA-resistant plasmid construct for expression of Usp7 in knockdown cells. Silent mutations were introduced into the siRNA target region of the Usp7 gene in a plasmid encoding a Myc-tagged Usp7. The nucleotide sequence of the relevant region in the wt Usp7 gene and the siRNA-resistant mutant (Usp7-siR-r) is shown. The nineteen nucleotide siRNA target sequence is indicated by a bar above. The positions of the nucleotide exchanges are marked by an asterisk. Amino acids encoded by this region are shown in the bottom line. **(B)** A total of 5 X 10^5 HPU2 cells were transiently transfected with 1 µg (+) and 2 µg (++) of the siRNA-resistant construct of Usp7 (Myc-Usp7-siR-r) described in panel A or transfected with empty vector (-). 24 hours after transfection, cells were infected with H5*pg*4100 virus or left uninfected as indicated and further incubated for 24 h. Total cell extracts were prepared and subjected to immunoblotting by 2A6 and B6-8 antibodies detecting the early viral proteins E1B-55K and DBP, respectively. Myc-tagged Usp7 expressed by the plasmid construct was detected by anti-Myc antibody. β-actin was analyzed as a loading control. **(C)** HPU2 cells were transfected with Myc-Usp7-siR-r plasmid and infected with H5*pg*4100 as described in panel B. Viral particles were harvested at 24 hours post infection (h p.i.) and infectious virus particles produced were determined by quantitative DBP staining on 293 cells. Virus production is represented as a percentage of virus production in the control H1299 cells. The results represent the averages of two independent experiments.

5.2.4.2 **Virus growth in Usp7 knockout cells**

To further verify the dependence of efficient adenovirus infection on Usp7 levels, growth of wt virus was assayed in a cell line where the Usp7 gene was

homozygously disrupted (Usp7 -/-)(Cummins et al., 2004) and compared to growth in the parental HCT116 line (Figure 25). In these experiments, ~120-fold more infectious virus particles were produced by the HCT116 cells than the Usp7 -/- cells at 48 h p.i and the difference was not resolved even at 72 h p.i. (~70 fold). These results further and strongly support the finding that Usp7 is required for efficient adenovirus infection.

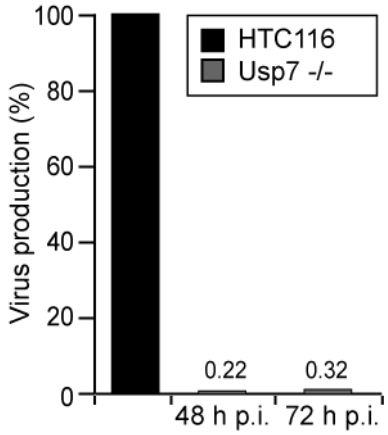

Figure 25. Production of progeny virions in Usp7 double-knockout cells during H5*pg*4100 infection. Control HCT116 and HCT116 Usp7 double-knockout cells (Usp7 -/-)(Cummins et al., 2004) were infected with H5*pg*4100 virus at a multiplicity of 20 ffu per cell. Viral particles were harvested at 48 and 72 hours post infection (h p.i.) and infectious virus particles produced were determined by quantitative DBP staining on 293 cells. Virus production is represented as a percentage of virus production in the control HCT116 cells and indicated by the numbers above the bars. The results represent the averages of two independent experiments.

5.2.4.3 Rational relationship between Usp7 levels and adenovirus replication efficiency

It is known that adenovirus replicates efficiently in some tumor cell types but not in others for reasons not yet fully understood (Berk, 2005). Identification of the factors pioneering this discrepancy in replication is particularly important since adenovirus is one of the most potent oncolytic viruses. Interestingly, the results obtained from the Usp7kd and Usp7 -/- cells in this work point to a correlation between Usp7 levels and the efficiency of adenovirus replication. To test this hypothesis further, a panel of

different tumor cell lines with different adenovirus production efficiencies was examined by immunoblotting to determine their Usp7 protein levels (Fig. 26A). Notably, compared to their β-actin levels, the tested tumor cell lines exhibited diverse Usp7 protein concentrations. More importantly, the level of Usp7 in these lines correlated perfectly with the virus yield data. RKO and Saos-2 cells with lower Usp7 protein levels also produce less virus in both wt Ad5 and *dl*1520 infections than 293, C33A and A549 cells containing higher levels of this protease.

To further clarify whether the low Usp7 levels can be a reason for such inefficient adenovirus replication in RKO and Saos-2 cells, Usp7 was ectopically expressed in these cells by transient transfection and afterwards infected with wt virus. Since transfection of Saos-2 cells was very inefficient, results could only be obtained with RKO cells. As shown in Figure 26B, expression of increasing amounts of Myc-Usp7 in RKO cells resulted in substantially increased steady-state levels of E1B-55K and DBP. These results again support the idea that there is a rational relationship between Usp7 levels and replication efficiency of adenovirus.

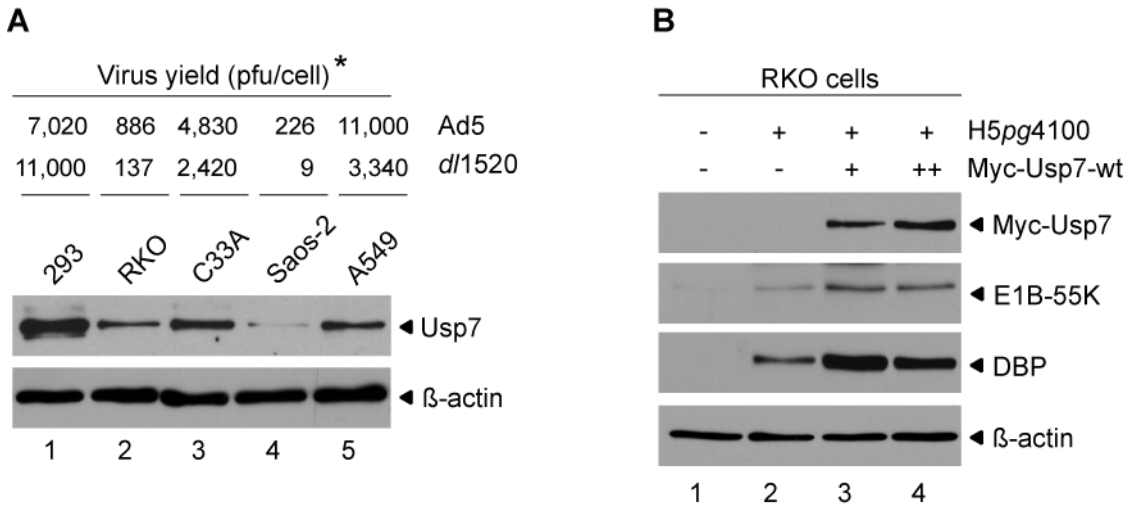

Figure 26. Expression levels of Usp7 in different tumor cell lines and effect of Usp7 expression in the efficient synthesis of early viral proteins. (A) Total cell extracts were prepared from 293, RKO, C33A, Saos-2 and A549 cells and subjected to immunoblotting by 3D8 antibody. β-actin was analyzed as a loading control. Virus yield for the given cell line upon Ad5 and *dl*1520 infection is indicated as plaque forming unit (pfu) above. (* The values are obtained from ref) **(B)** RKO cells were transfected with plasmid encoding Myc-tagged Usp7 (Myc-Usp7-wt). 24 hours after transfection, cells were infected with H5*pg*4100 virus or left uninfected as indicated and further incubated for 24 h. Total cell extracts were prepared

and subjected to immunoblotting by 2A6 and B6-8 antibodies detecting the early viral proteins E1B-55K and DBP, respectively. Myc-tagged Usp7 expressed by the plasmid construct was detected by anti-Myc antibody. β-actin was analyzed as a loading control.

5.2.5 Investigating the role of Usp7 in the early phase of the adenovirus infection

5.2.5.1 Analysis of replication center formation in Usp7 knockdown cells

The data above showed that Usp7 is a factor required for efficient adenovirus replication, and the underlying mechanism seems to be more related to the functions of Usp7 that do not involve p53 and E1B-55K interactions. Since Usp7 is detected in viral replication centers, a reasonable question was whether Usp7 plays a role in the efficient formation of replication centers. To investigate the potential contribution of Usp7 in replication center formation, H1299 and HPU2 cells were infected with wt H5*pg*4100 virus and fixed at different time points. The initial formation of replication centers and localization of Usp7 into these structures were analyzed by indirect immunofluorescence. As shown in Figure 27, Usp7 exhibited diffuse staining in mock-infected cells, and as expected, the amount of this protein was significantly less in HPU2 cells (A and B, panel a). The infection of both cell lines caused accumulation of Usp7 in dot-like structures starting as early as 6 h p.i. (panel b). At this time point, DBP could be readily detected as diffuse staining in the nucleus of both cell lines (panel g). However, the amount of DBP fluorescence was brighter in H1299 cells than in HPU2 cells (panel g), showing that Usp7 operates very early in adenovirus infection.

As the infection proceeds, together with DBP, Usp7 starts to accumulate in more dot-like structures in the nucleus, referred to as virus replication centers, and this accumulation was visible at 8 h p.i. in H1299 cells. At 16 h p.i., the diffuse nuclear staining of both DBP and Usp7 was almost completely converted into a dominant staining in replication centers. In HPU2 cells the process of relocalization of Usp7 and DBP into the replication centers was similar, however, it was significantly delayed

(~4 h) compared to H1299 cells. The first dot-like structures containing the DBP and Usp7 proteins were detectable at 12 h p.i. in these cells and when the number and volume of these structures are considered, it can be concluded that the formation of replication centers is inefficient in Usp7kd cells.

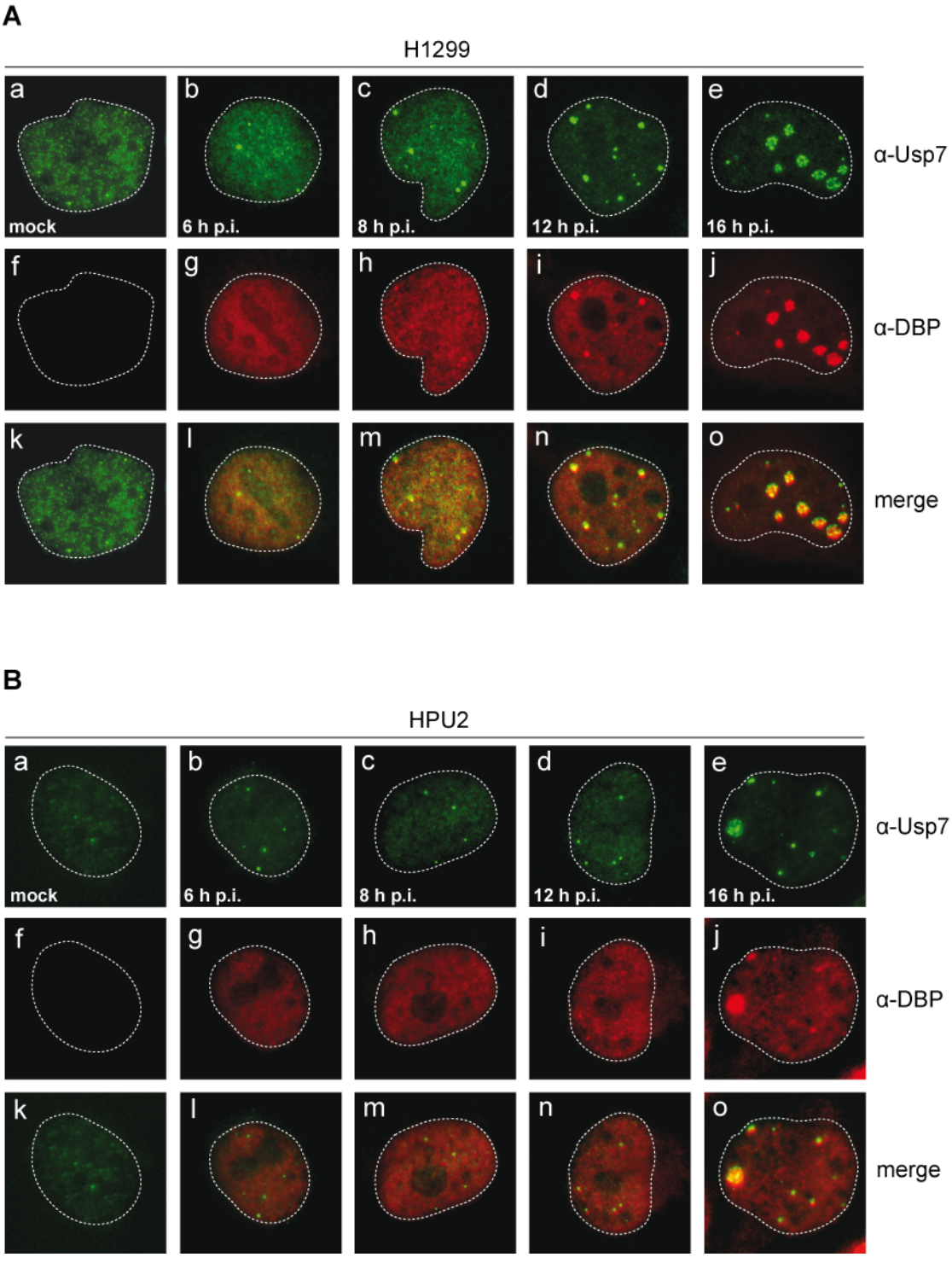

Figure 27. Immunofluorescence analysis of adenovirus replication formation in Usp7

knockdown cells. (A) H1299 cells and **(B)** HPU2 cells were infected with H5*pg*4100 virus at a multiplicity of 20 ffu/ cell or remained uninfected (mock). The cells were fixed at indicated time points and Usp7 was labeled with 3D8 (α-Usp7) and viral replication centers were marked with anti-E2A-72K antibody B6-8 (α-DBP). The proteins were visualized by FITC- and Texas Red-conjugated secondary antibodies, respectively. Anti-Usp7 (green, panels a – e) and anti-DBP (red, panels f – j) staining patterns, and their overlay (merge, panels k – o) are shown. In all panels, nuclei are shown by dotted lines.

5.2.5.2 **Co-localization of Usp7-containing PML bodies with replication centers**

Promyelocytic leukemia nuclear bodies (PML bodies; also known as ND10) are small nuclear structures that contain several proteins involved in pathways related to gene expression, protein post-translational modification, DNA repair and virus infection (Ching et al., 2005; Ishov and Maul, 1996a). It has been shown that adenovirus genomes associate with specific PML bodies during the early stages of infection and viral replication centers form adjacent to these structures (Ishov and Maul, 1996b). Usp7 is a component of PML bodies and in the cells a minority of the nuclear Usp7 co-localizes with a subset of these bodies (Everett et al., 1997). Therefore, an intriguing question is whether the same Usp7 containing population of PML bodies is targeted by adenovirus for forming adjacent replication centers.

To test this, we first confirmed the presence of Usp7 in PML bodies in adenovirus infected and uninfected cells and analyzed the co-localization of DBP and Usp7 within the PML bodies by immunofluorescence. Consistent with previous reports, in uninfected cells, Usp7 was identified in only a small population of PML bodies (Fig. 28A, panels a – c). Adenovirus infection was observed to induce the accumulation of Usp7 in the specific PML bodies shortly after infection (6 h p.i.; panels d – f). Interestingly, triple-labeling of cells with antibodies against PML, Usp7 and DBP detected the initial formation of replication centers (marked by DBP) next to PML bodies containing Usp7 (Figure 28B, panels a – d). Later in the infection (12 h p.i.), PML bodies were found to be disrupted and formed elongated track-like structures, whereas DBP and Usp7 continued to accumulate in the dot-like structures to form large nuclear aggregates (panels e – h). Collectively, the data presented in this section led to the speculation that Usp7 plays a role in the initial formation of adenovirus

replication centers.

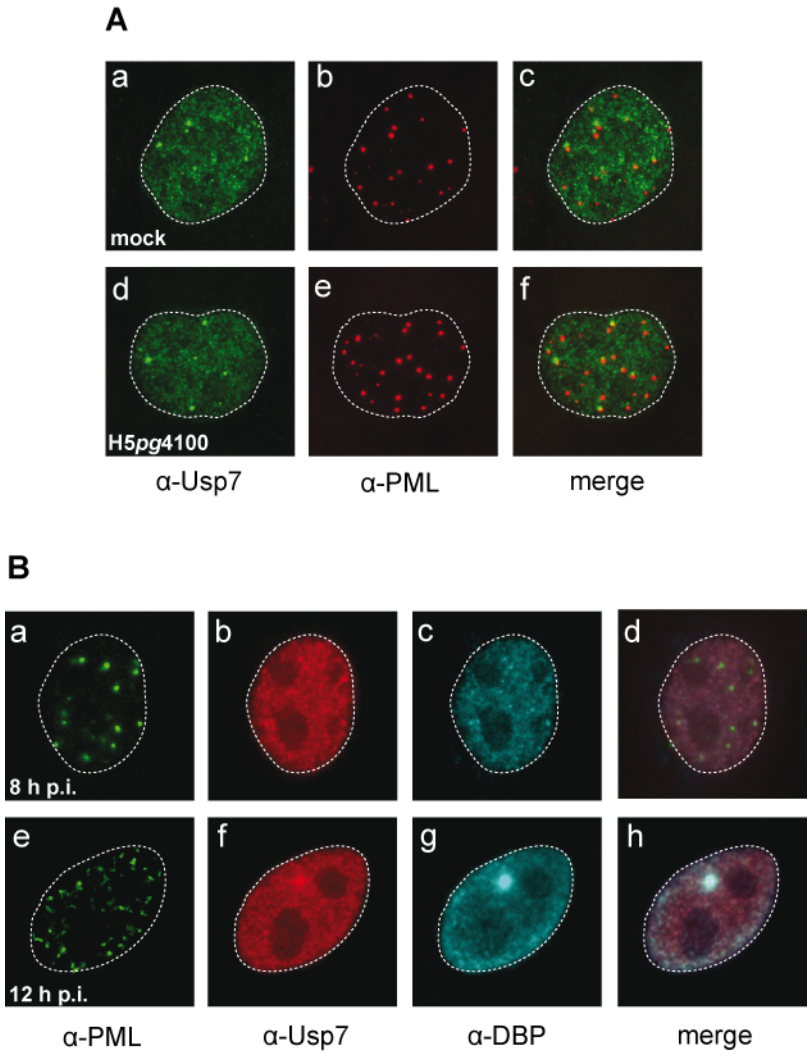

Figure 28. Co-localization of Usp7 and DBP in PML bodies. (A) H1299 cells were infected with H5*pg*4100 virus at a multiplicity of 20 ffu/cell or remained uninfected (mock). The cells were fixed at 8 hours post infection and Usp7 was labeled with 3D8 (α-Usp7) and PML bodies were marked with 5E10 antibody detecting the PML protein (α-PML). The proteins were visualized by FITC- and Texas Red-conjugated secondary antibodies, respectively. Anti-Usp7 (green, panels a and d) and anti-PML (red, panels b and e) staining patterns, and their overlay (merge, panels c and f) are shown. **(B)** H1299 cells were infected with H5*pg*4100 virus at a multiplicity of 20 ffu per cell. The cells were fixed at indicated times post infection (p.i.) and triple-labeled with 3D8 (α-Usp7), 5E10 (α-PML) and B6-8 (α-DBP) antibodies. The proteins were visualized by Texas Red, FITC and CY3-conjugated secondary antibodies, respectively. Anti-PML (green, panels a and e), anti-Usp7 (red, panels b and e) and anti-DBP (blue, panels c and g) staining patterns, and their overlay (merge, panels d and h) are shown. In all panels, nuclei are shown by dotted lines.

5.2.6 Identification of Usp7 as a novel interaction partner of adenovirus DBP

5.2.6.1 Usp7 interacts with adenovirus DBP

The observations connecting the functions of Usp7 to the initial formation of adenovirus replication centers may explain how Usp7 affects the adenovirus infection starting from the very early stages. However, it was necessary to identify the viral factor(s) required for the relocalization of Usp7 into the replication centers. In this context, the potential interaction of Usp7 with two of the major adenovirus replication centers components, DBP and adenovirus DNA polymerase (Pol), was tested by *in vitro* binding experiments.

Here, GST-Usp7 constructs corresponding to different regions of Usp7 were generated and GST pull-down experiments were carried out on H5*pg*4100 infected H1299 cell extracts (summarized in Fig. 29A). The precipitates were then analyzed for the presence of Pol, DBP and E1B-55K, which served as a positive control. Consistent with previous findings in our group, the specific interaction between E1B-55K and the N-terminal segment of Usp7, called the TRAF-like domain (TD; residues 1-215) was identified (Fig. 29B). Interestingly, the same domain of Usp7 also precipitated DBP strongly, whereas none of the GST constructs interacted with Pol, indicating that DBP specifically interacted with the N-terminal TD of Usp7. The interaction between these proteins was also verified by IP experiments in both directions (Fig. 29C). As a result, after E1B-55K, DBP was identified as another novel interaction partner of Usp7.

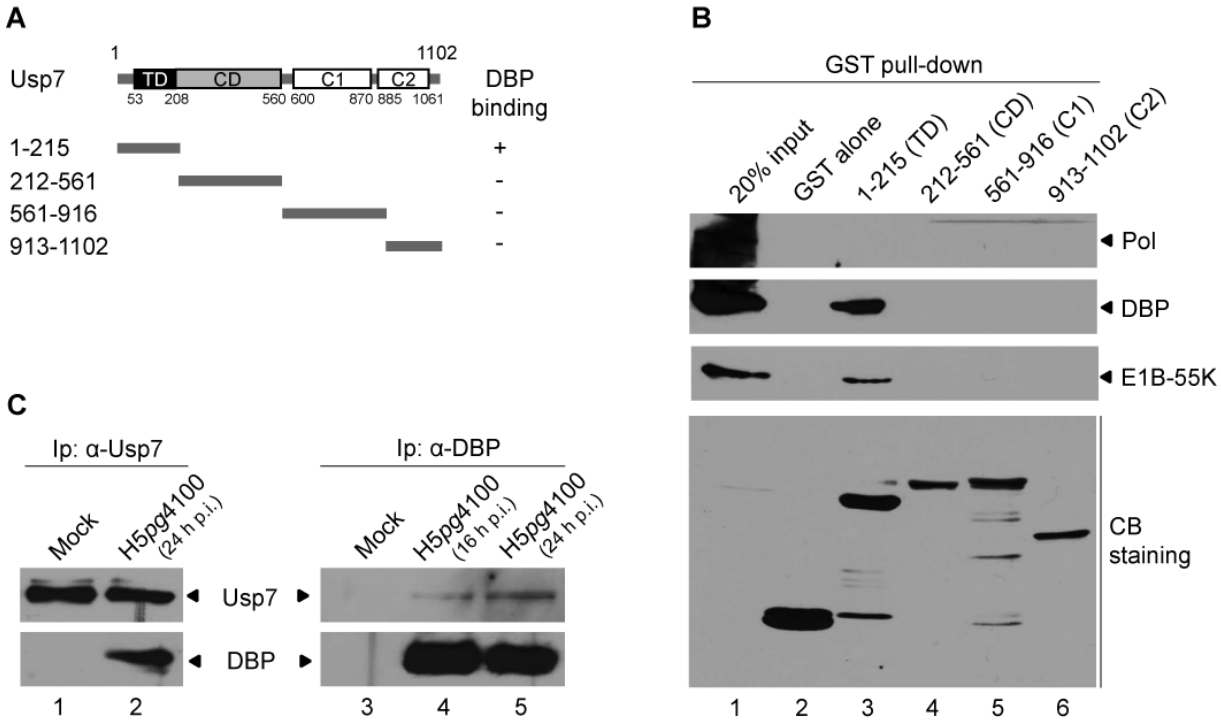

Figure 29. Usp7 inteacts with adenovirus DBP in virus infected cells. (A) Segments corresponding to the four structural domains of Usp7 (Holowaty and Frappier, 2004), namely N-terminal TRAF-like domain (TD; 1-215), catalytic domain (CD; 212-561) and two C-terminal domains (C1 and C2; 561-916 and 913-1102), and summary of the binding assay are shown. Numbers refer to amino acid residues in Usp7. **(B)** Similar amounts of GST-fused Usp7 segments were incubated with Ad5 infected H1299 cell extracts prepared 48 hours post infection. GST alone was used as a negative control. 20 percent of the input and precipitated proteins were separated by SDS-PAGE and analyzed by 2A6, anti-adenovirus DNA Polymerase (Pol) and B6-8 antibodies. Relevant GST fusion proteins were visualized by Coomassie blue (CB) staining. **(C)** The extracts described in panel B were subjected to immunoprecipitation (Ip) reactions with anti-Usp7 antibody 3D8 (α-Usp7) or anti-DBP antibody B6-8 (α-DBP). The immunocomplexes were separated by SDS-PAGE and visualized by immunoblotting using 3D8 and B6-8 antibodies.

5.2.6.2 **DBP is sufficient to relocalize Usp7 to replication centers**

After detecting the interaction between DBP and Usp7, the possible role of DBP in the relocalization of Usp7 to the viral replication centers was investigated. To reveal whether DBP alone is sufficient for redistributing Usp7, H1299 cells were transfected with a plasmid encoding adenovirus DBP and the localization of Usp7 and DBP were analyzed by dual-label immunofluorescence in these cells (Fig. 30). Interestingly, the transfected DBP showed a distribution in the cells similar to its localization in virus infection. Around 65% of the transfected cells (number of cells examined, n > 50)

exhibited a diffuse nuclear distribution of DBP with a few dot-like structures resembling the early (time < 8 h p.i.) localization of this protein in the infected cells. In the remaining 35% of the cells, DBP was observed to form large ring-shaped bodies and a number of small dots in the nucleus. This distribution was similar to the distribution of DBP in large replication centers in the late phase of infection. However, in infected cells, staining of large replication centers show punctuated distribution of DBP inside these bodies, most probably due to the presence of adenovirus DNA and other viral components. Interestingly, in both distributions described above, the steady-state localization of Usp7 is altered just as it is in virus infection. Transfection of DBP alone induced the accumulation of Usp7 in dot-like structures or large nuclear bodies formed by DBP. These results indicate that DBP alone is sufficient to alter the localization of Usp7 into the DBP-induced structures, and suggest that DBP is the protein responsible for the translocation of Usp7 into adenovirus viral replication centers.

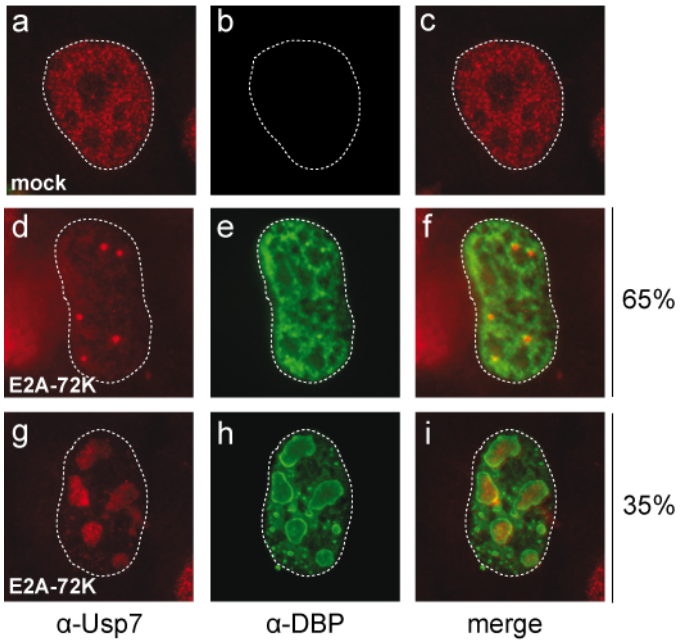

Figure 30. Co-localization of Usp7 with DBP in plasmid transfected cells. (A) H1299 cells were mock transfected or transfected with a plasmid encoding adenovirus DBP (E2A-72K). 48 hours after transfection, the cells were fixed and Usp7 was labeled with 3D8 (α-Usp7) and DBP was labeled with B6-8 antibody (α-DBP). The proteins were visualized by Texas Red- and FITC-conjugated secondary antibodies, respectively. Anti-Usp7 (red, panels a, d, and g) and anti-DBP (green, panels b, e, and h) staining patterns, and their overlay (merge, panels c,

f and i) are shown. The percentage of two different staining patterns observed for DBP is indicated. In all panels, nuclei are shown by dotted lines.

5.2.6.3 **Usp7 de-ubiquitinates and stabilizes DBP**

Identification of DBP as a binding partner of Usp7 raised the possibility that this protease regulates the stability of DBP. To test this, we first determined the half-life of DBP in Usp7+ and Usp7kd cells during adenovirus infection. H1299 and HPU2 cells were infected with adenovirus and cells were treated with a protein synthesis inhibitor, Cycloheximide (Chx). Subsequently, the levels of Usp7 and DBP were analyzed in these cells by immunoblotting. The E1A protein was also detected as a negative control. As shown in Figure 31A, the half-life of E1A was similar in both H1299 and HPU2 cell lines. Usp7 was found to be a very stable protein, since 8 hours of Chx treatment only resulted in a minor decrease in protein levels. Similarly, in H1299 cells DBP levels remained nearly constant. However, in cells with reduced Usp7 levels, a significant decrease in the half-life of DBP was observed. Thus it can be concluded that DBP is stabilized by Usp7.

To investigate whether the stabilization of DBP is due to specific de-ubiquitination of this protein by Usp7, the ubiquitination status of DBP was examined by an *in vivo* system described in ref. In these experiments, a histidine-tagged version of ubiquitin (His-Ub) was transiently expressed in H1299 and HPU2 cells. The cells were then infected with adenovirus, which allowed the subsequent purification of ubiquitin conjugated forms of the adenoviral proteins. Additionally, four hours prior to lysis, the cells were incubated with the proteasome inhibitor Mg132 to block the degradation of poly-ubiquitinated proteins. Analysis of the extracts prepared from these cells gave the first hint that DBP is subjected to increased proteasomal degradation in Usp7kd cells. As can be seen in Figure 31B, the reduced levels of DBP in Usp7kd cells (lane 2) were rescued by the addition of Mg132 (lane 4), whereas no significant effect was observed for Usp7.

Afterwards, the remaining cells were lysed under denaturing conditions (6 M

guanidine-HCl) to prevent de-ubiquitination of the proteins and non-covalent protein interactions, and His-Ub modified proteins were purified as described in the Methods section. The purified proteins were then subjected to immunoblotting to detect the ubiquitinated forms of DBP. As shown in Figure 31C, a ladder of slower migrating forms of DBP was observed only when the cells were transfected with His-Ub, which showed that these are the ubiquitin conjugates of DBP. Interestingly, in H1299 cells, only a single DBP form migrating at ~250 kDa could be detected in the short X-ray film exposure (marked with an empty triangle). This may correspond to a poly-ubiquitin chain conjugated to a specific lysine residue in DBP. In Usp7 depleted cells, this form was enhanced but more significantly, several ubiquitinated forms of DBP migrating at different molecular weights were detected. Three of these forms, which could be distinguished as separate bands (lane 4, marked by arrowheads), were almost exclusively observed in HPU2 cells and perhaps they represent specific ubiquitinated forms of DBP that are targeted by Usp7 under physiological conditions. In the longer film exposure, this substantial difference in the ubiquitination pattern of DBP between H1299 and HPU2 cells is more obvious. Taken together, these data not only strongly suggest that DBP is de-ubiquitinated by Usp7, but also highlight that some specific lysine residues in DBP are preferentially de-ubiquitinated by Usp7.

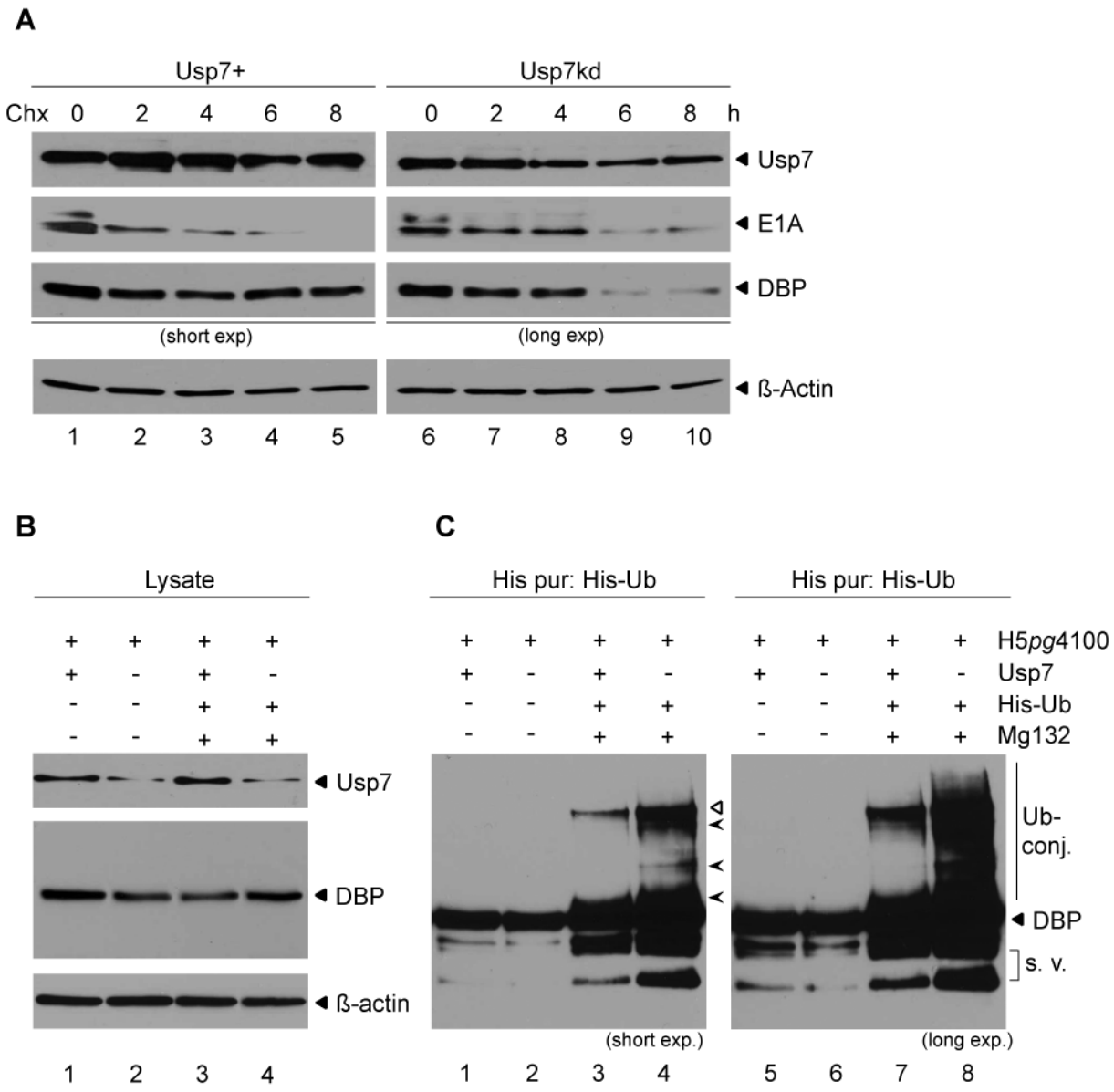

Figure 31. Usp7 is required for the de-ubiquitination and maintenance of DBP protein levels in virus infection. (A) H1299 and HPU2 cells were infected with H5*pg*4100 virus. 24 hours after infection, cells were treated with cycloheximide (Chx; 50 µg/µl). The cells were harvested at different time points after treatment as indicated. Total cell extracts were prepared and subjected to immunoblotting by 3D8 antibody detecting Usp7, M73 antibody detecting E1A, and B6-8 antibody detecting DBP. β-actin was analyzed as a loading control. **(B)** H1299 and HPU2 cells (indicated by a plus and minus sign in Usp7 panel) were transfected with a plasmid encoding for a histidine-tagged ubiquitin (His-Ub). 24 hours after transfection cells were infected with H5*pg*4100 virus and further incubated for 24 h. Mg132 (10 µM) was added to the cells 6 hours prior to harvesting as indicated. An aliquot of the cells was used to prepare total cell extracts. The protein levels of Usp7 and DBP were detected by 3D8 and B6-8 antibodies. β-actin was analyzed as a loading control. **(C)** The cells were lysed by the addition of 6M guanidine hydrochloride and ubiquitinated proteins were purified by Ni^{2+} - agarose beads as described in the Methods section. The eluted proteins were separated by SDS-PAGE. DBP and its ubiquitin conjugates (UB-conj.) were visualized by immunoblotting using B6-8 antibody. Ubiquitin conjugates of DBP: Distinct ubiquitinated bands are marked with arrowheads and a major ubiquitinated form with a triangle. The

unmodified 72K form (DBP) and the faster migrating splice-variants of DBP (s. v.) precipitated by Ni^{2+} - agarose beads were indicated. Shorter (short exp) and longer (long exp) exposures of the X-ray film are shown.

5.3 Usp7 is a critical regulator of adenovirus-mediated cell transformation

Adenovirus E1A and E1B-55K proteins can cooperatively transform primary human and rodent cells to a tumorigenic phenotype (Endter and Dobner, 2004). The role of E1A proteins in this process is well-established and involves the most critical step in cell transformation, which is the initiation of cell proliferation. Nevertheless, transformation by E1A is often inefficient and requires the functions of E1B-55K for complete transformation. It is generally considered that E1B-55K contributes to this event by antagonizing apoptosis and growth arrest, which primarily results from the induction and metabolic stabilization of the tumor suppressor p53. The transforming functions of E1B-55K are linked to its ability to act as a direct transcriptional repressor that is targeted to p53-responsive promoters by binding to p53. However, the mechanism underlying this event is not fully understood (Berk, 2005). In addition, it has been hypothesized that the mode of action of E1B-55K during transformation may involve additional functions and other protein interactions. Identification of Usp7 - a critical regulator of the p53 pathway - as a novel interaction partner of E1B-55K in this work prompted analysis of the potential functions of this protease in adenovirus-mediated cell transformation with regard to p53.

5.3.1 RNAi as a tool to study adenovirus-mediated cell transformation

5.3.1.1 The effect of Usp7 and p53 knockdown on E1A/E1B-55K induced focus formation

To clarify the potential role of Usp7 in cell transformation mediated by adenovirus E1A and E1B-55K proteins, and to better understand how p53 and its regulatory elements contribute to this process, RNAi was used as an experimental tool. Primary

baby rat kidney (BRK) cells were transfected with plasmids encoding E1A in combination with E1B-55K, shUsp7, and shp53 (Fig. 32A). Consistent with previous results (Debbas and White, 1993), E1A alone had very little focus forming activity, but co-transfecting the cells with E1B-55K expression plasmids increased the number of foci three to four-fold. However, surprisingly, in the presence of shUsp7 E1B-55K was completely inactive in cooperative focus formation. The number of foci in E1A/E1B/shUsp7 and E1A/shUsp7 transfected plates were similar, and both were lower than the foci induced by E1A alone, suggesting a strong requirement for Usp7 in E1A/E1B-55K mediated cell transformation.

Inclusion of p53 shRNAs in the assay introduced striking results. The co-transfection of E1A and shp53 yielded significantly more foci than with E1A/E1B-55K transfected cells. More importantly, the cells in the foci developed much more rapidly and to higher densities as judged by the size and intensity of the crystal violet staining (Fig. 32B). These observations showed for the first time that short-hairpin RNAs against p53 can cooperate with E1A to induce cell transformation and indicated that the major reason for requiring E1B-55K during E1A/E1B mediated cell transformation is related to its functions in inhibiting p53. However, interestingly, addition of E1B-55K to E1A/shp53 transfections further increased the number of transformed cells, suggesting that E1B-55K and shRNA-p53 can synergistically promote focus-formation in the presence of E1A. Of note, in the plates transfected with E1B-55K, shp53 or Usp7 alone, no single focus was observed, confirming the importance of E1A for initiating the transformation process.

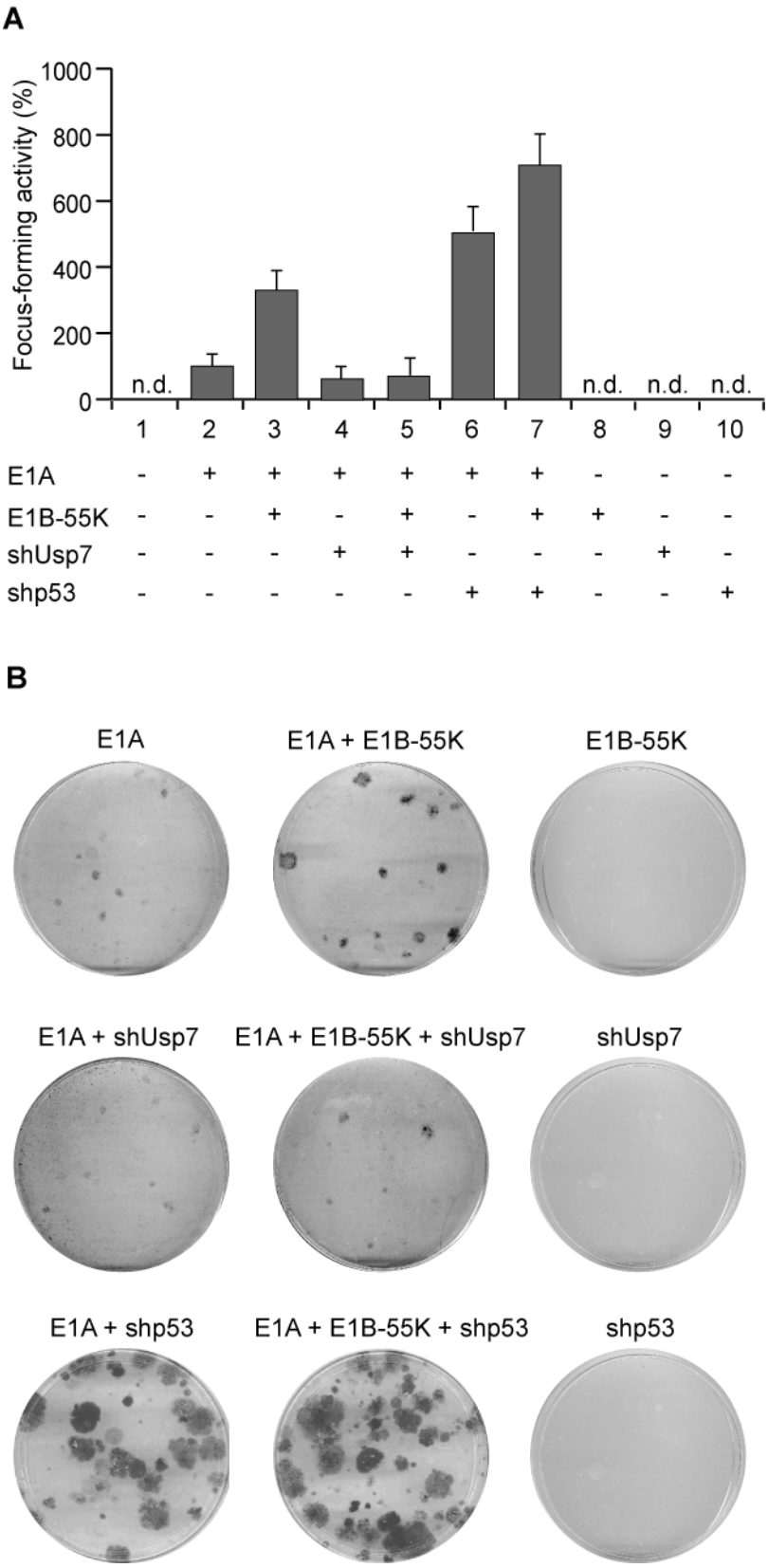

Figure 32. E1A and E1A/E1B-55K induced focus formation in the presence of shRNAs against Usp7 and p53. (A) Primary baby rat kidney cells were transfected with plasmids encoding E1A 12S (E1A), E1B-55K, Usp7 shRNAs (shUsp7), and p53 shRNAs (shp53) as indicated. Morphologically transformed colonies were scored 5 weeks after transfection.

Focus forming activity is represented as a percentage of E1A activity. The mean and standard deviation are presented for three independent experiments. The average number of foci for E1A 12S was 5. The n.d. stands for "not detected". **(B)** Representative crystal violet stained plates showing foci from each transfection are shown as an example.

5.3.2 Characterization of transformed cells

To investigate in detail how Usp7 shRNAs inactivate and p53 shRNAs promote cell transformation by adenovirus oncogenes, a panel of transformed monoclonal cell lines was established from E1A/E1B-55K (AB), E1A/shp53 (Ashp), E1A/E1B/shp53 (ABshp), and E1A/E1B/shUsp7 (ABshU) transformed foci. Although E1A/shUsp7 and E1A/E1B-55K/shUsp7 transfected cells initiated focus formation, most of the cells from these foci degenerated and died during their first passage in cell culture. Among ~30 trials, none of the E1A/shUsp7 transfected cells could be established as a cell line and only two of the isolated foci from E1A/E1B-55K/shUsp7 transfected cells could be grown for further passages. In contrast, nearly all of the isolated foci from both E1A/shp53 and E1A/E1B-55K/shp53 transfections were grown and established as permanent cell lines, highlighting the significance of p53 in the transformation process.

Figure 33 shows the immunoblot characterization of these shRNA transformed cell lines in comparison to the primary BRKs and the reference cell lines transformed with E1A/E1B-55K and the empty vector for shRNAs (AB718-720). In primary BRK cells p53 was present at background levels (panel A). As shown previously, adenovirus E1 transformed cells contain high levels of p53 due to the induction and metabolic stabilization of this protein by E1A (Debbas and White, 1993; Lowe and Ruley, 1993). It has also been shown that E1B-55K further increases the stability of p53 (van den Heuvel et al., 1993). Consistent with this, in the reference AB cells (AB718-720), p53 levels were found to be elevated. This E1A and E1B induced increase in p53 levels was fully eliminated in shp53 transfected cells. Both Ashp53 and ABshp53 cells exhibited undetectable levels of p53, as in the primary BRK cells, showing that the RNAi reduction of p53 is dominant over its induction by adenovirus oncogenes. Surprisingly, following the reduced p53 levels, accumulation

of E1B-55K was found to be defective in all of the three ABshp cell lines presented here (ABshp724- 726). The molecular basis for this effect is unknown but seems to be related to p53. Nevertheless, E1B-55K expression persisted in all of the monoclonals. These results raised the possibility that in the absence of p53, E1B-55K still contributes to the transformed phenotype and is not eliminated during the stages of transformation.

Unlike the consistent behavior of Ashp and ABshp cells in the presentation of E1B-55K and p53, the two cell lines that could be generated from shUsp7 transfections differed completely in this respect (Fig. 33B). In ABshU729 cells, the expression of E1B-55K was detected, but found to be reduced in comparison to reference AB cells, and p53 could not be detected. Inversely, ABshU730 cells exhibited elevated levels of p53 protein whereas the expression of E1B-55K was undetectable. It is known that the effect of Usp7 downregulation can lead to opposite results depending on the extent of knockdown. Partial reduction of Usp7 destabilizes p53 but nearly complete ablation stabilizes the tumor suppressor (Li et al., 2004). Therefore, these contradictory results can be linked to the differential levels of Usp7 in these cells, since it was found that the knockdown of Usp7 seems to be more efficient in ABshU730 than ABshU729.

In all of the established cell lines E1A protein was found to be presented in similar amounts, with the exception of ABshp726 cells expressing little of this protein. Thus, it can be concluded that the influence of shp53 and shUsp7 on the transformation process mainly affects the functions of E1B-55K.

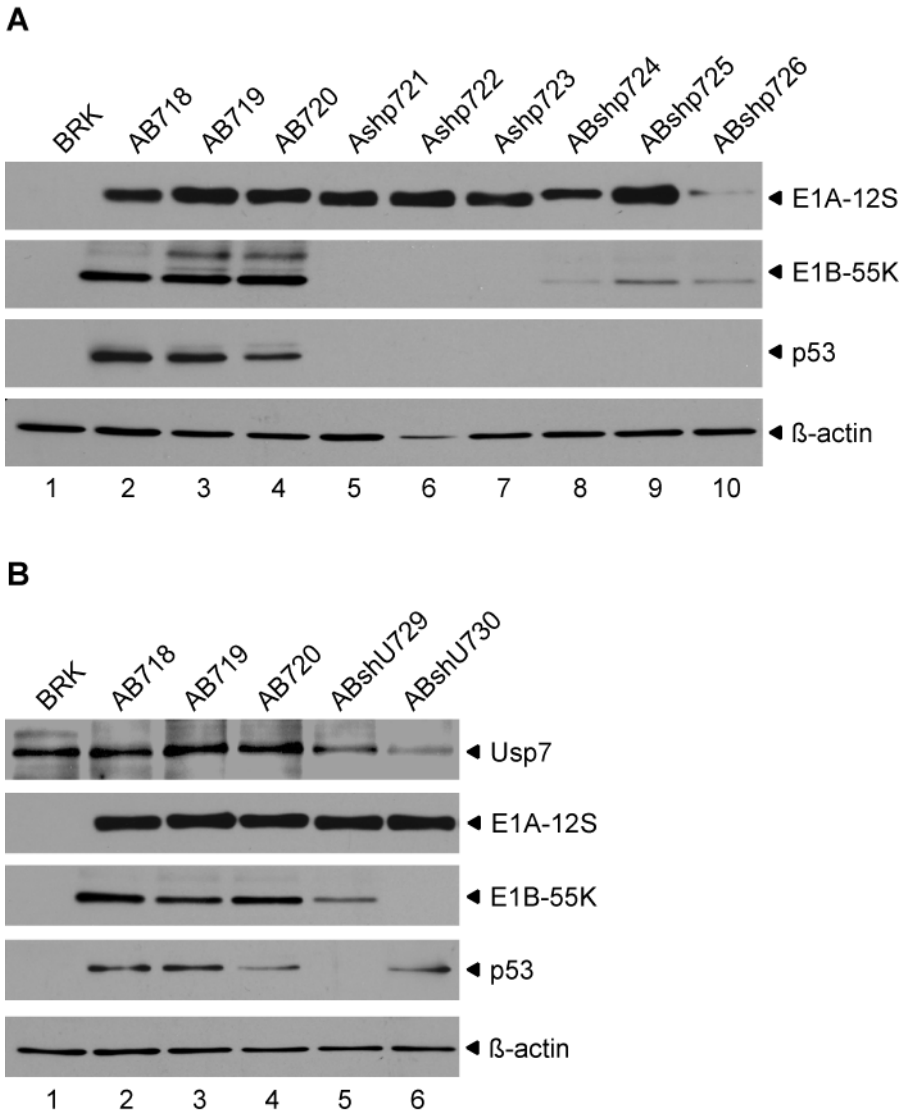

Figure 33. Protein analysis of selected AB, Ashp, ABshp, and ABshU cells (A) Total cell extracts were prepared from primary BRK, the reference E1A/E1B-55K/empty shRNA vector (AB718-720), E1A/shp53 (Ashp721-723), and E1A/E1B/shp53 (ABsh724-726) cells and subjected to immunoblotting by M73, 2A6, fl393 antibodies detecting the E1A-12S, and p53, respectively. β-actin was analyzed as a loading control. **(B)** Total cell extracts from E1A/E1B/shUsp7 (ABshU729 -730) were used instead of the Ashp and ABshp cells in panel A. Additionally, Usp7 was detected with a rat mab 6E6.

5.3.2.1 Subcellular localization of E1B-55K and p53 in transformed cells

It has been observed in several different studies that in adenovirus transformed cells p53 is bound to E1B-55K in large subcellular structures in the cytoplasm near the nucleus corresponding to aggrasomes (Liu et al., 2005). To investigate the effect of shRNAs on this particular localization of E1B-55K and p53, immunofluorescence

experiments were performed. In the spontaneously immortalized BRK line (BRK1), p53 was detected weakly in the nucleus (Fig. 34). The exclusive nuclear staining of p53 was altered in the reference AB718 line showing a typical co-localization of E1B-55K and p53 in large cytoplasmic aggregates. Consistent with the immunoblot analysis, both p53 and E1B-55K levels were low but the tiny amounts of these proteins were found to be co-localized in the cytoplasmic body in ABshp724 cells (panels g-i). Surprisingly, in the shUsp7 cell line with elevated p53 levels, localization of the tumor suppressor was nuclear. As a more sensitive method, IF detected the presence of E1B-55K in these cells, and a small amount of the 55K protein was found in the cytoplasmic aggregates (panels j-l). However, it was not co-localizing with p53. These results were striking since they suggest that Usp7 may play a role in the sequestration of p53 in adenovirus transformed cells, which is believed to be critical for the inhibition of p53.

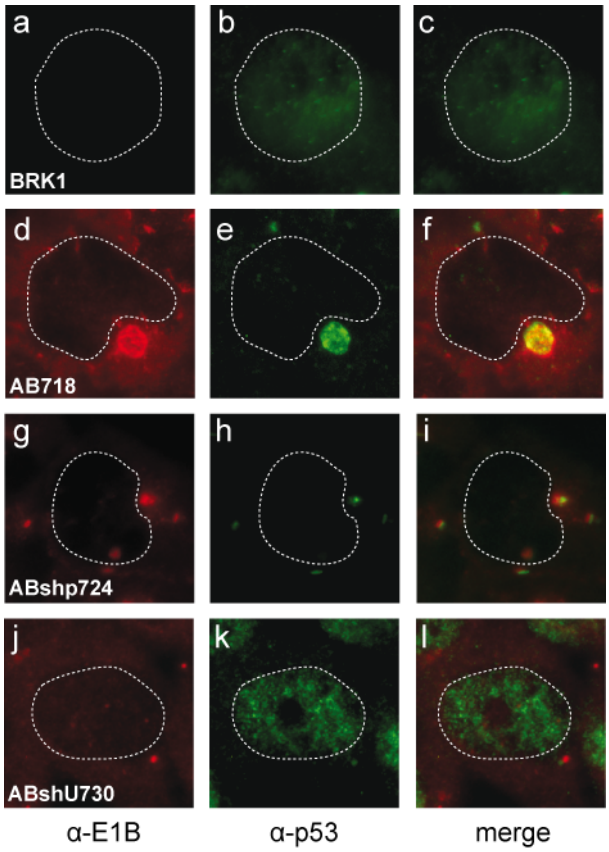

Figure 34. Steady state localization of E1B-55K and p53 in selected cells. Spontaneously immortalized BRK1, AB718, ABshp724, and ABshU730 cells were fixed and labeled with 2A6 (α-E1B) and fl393 (α-p53) antibodies. The proteins were visualized by Texas Red- and FITC-

conjugated secondary antibodies, respectively. Anti-E1B (red, panels a, d, g, and j) and anti-p53 (green, panels b, e, h, and k) staining patterns, and their overlay (merge, panels c, f, i, and l) are shown. In all panels, nuclei are shown by dotted lines.

5.3.2.2 **Growth characteristics of the transformed cell lines**

To reveal the effects of shUsp7 and shp53 expression on the transformed cell phenotype, the morphology and growth rates of shp53 and shUsp7 expressing lines were compared with those of primary BRK and AB cells. The data obtained for each set of AB, Ashp and ABshp lines was identical, therefore the growth rates of one clone for each set are presented. As shown in Figure 35, both Ashp and ABshp cells divide at higher growth rates than AB cells, which correlates with their rapid foci formation. Reproducible for each line, the growth rates of ABshp cells were higher than the Ashp cells, supporting the idea that E1B-55K enhances the transformed phenotype even with the nearly complete ablation of p53. For ABshU lines, as anticipated, cell growth was slower than that of AB cells, with a striking reduction observed for the ABshU730 line. Three days after plating, the number of cells in this line was as low as the non-dividing primary BRK cells. This can be explained by either the elevated p53 or reduced E1B-55K levels. Together, these results demonstrate that Usp7 depletion in general affects the transformation process negatively.

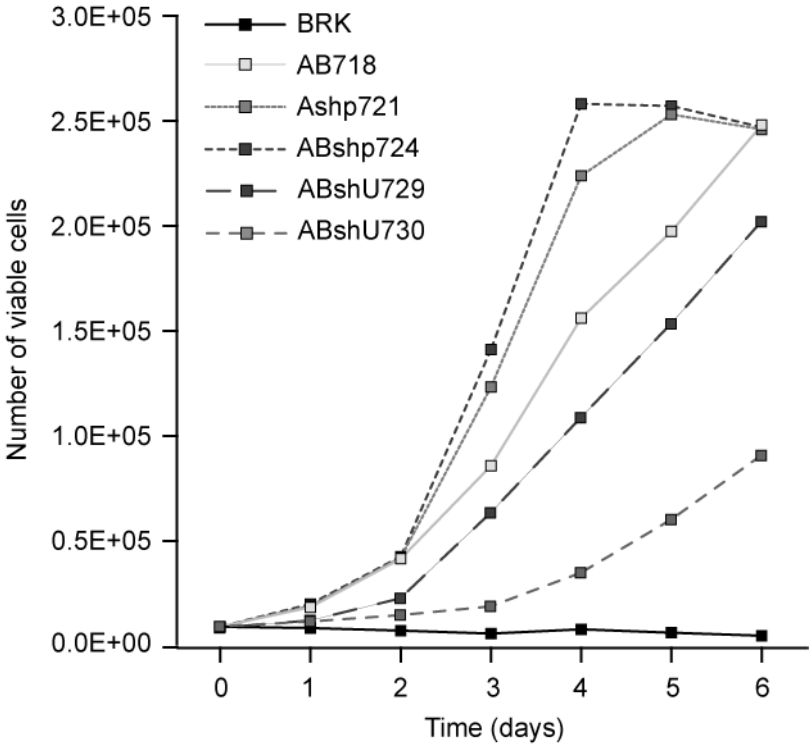

Figure 35. Growth characteristics of the selected cell lines. (A) Growth rate of Ashp721, ABshp724, ABshU729, and ABshU730 cells were compared to the primary BRK cells and the reference AB718 cell line. A total of 1 X 10^5 cells were plated on six-well dishes in culture medium, and viable cells were counted every day. The mean number of viable cells for duplicate dishes is shown.

5.3.2.3 **Morphology of the transformed cell lines**

As a general rule, adenovirus transformed cells can be distinguished from normal cells on the basis of morphology (Graham et al., 1984). To investigate the potential differences induced by the shRNAs in this respect, the morphology of the established cell lines were analyzed. An example from each different cell line is presented in Figure 36. As shown, in comparison to primary BRK cells all of the transformed lines exhibited altered morphology, being less stretched and much smaller. There were also minor differences between the transformed cell lines depending on the expression of shp53 or shUsp7. The reference AB cells were round in shape, however, Ashp and ABshp cells were smaller than these cells and had an elongated appearance. The morphology of ABshU729 resembled that of AB718 cells, but the ABshU730 cells were different in the way they tended to grow in colonies. As a conclusion, expression of shp53 or shUsp7 markedly affected the transforming

potential and the transformed phenotype.

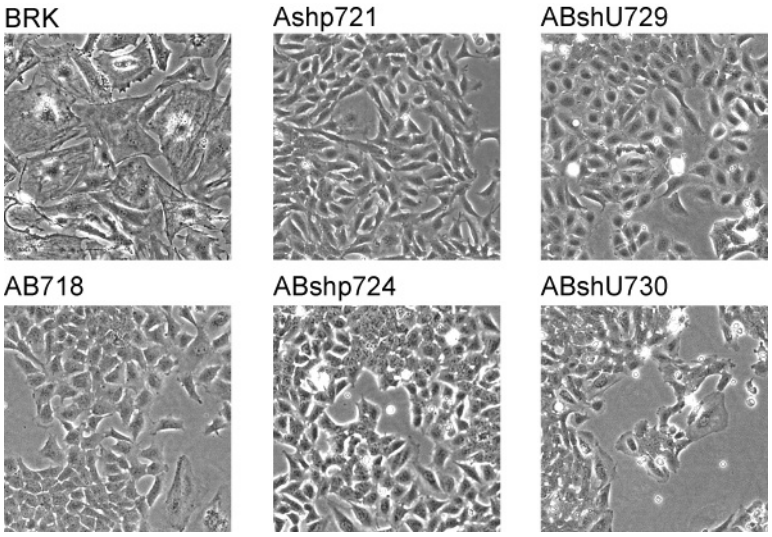

Figure 36. Morphology of primary BRK, AB718, Ashp721, ABshp724, ABshU729 and 730 cells at subconfluency. The cells were grown on cover-slips and analyzed by phase contrast microscopy. (Magnification: x1780)

Collectively the data described in this section suggest that the activity of Usp7 is required for efficient transformation of primary rat cells by adenovirus oncogenes. This requirement seems to be related to its activity in the p53 pathway and its association with the viral E1B-55K protein.

6 DISCUSSION

Protein ubiquitination has been identified as a critical regulatory mechanism in a number of cellular processes including cell cycle progression, apoptosis and DNA repair (Haglund and Dikic, 2005; Mukhopadhyay and Riezman, 2007). The most prominent role of ubiquitination is labeling proteins for proteolysis, which requires the covalent conjugation of a poly-ubiquitin chain to a target protein by a ubiquitin ligase. Viruses use this post-translational modification machinery to target cell signaling pathways and to inhibit cellular defense mechanisms (Shackelford and Pagano, 2004). Selective ubiquitination and degradation of cellular proteins using viral or cellular ubiquitin ligases is an important aspect of infection and cell transformation by tumor viruses. Thus, significant progress has been made in characterizing these ubiquitin ligases However, little is known about the enzymes counteracting the ubiquitination process: ubiquitin-specific proteases.

The extraordinary importance of ubiquitin-specific proteases came to attention when it was found that a component of this large family, Usp7 critically regulates the p53 pathway (Li et al., 2002). In cells, p53 is tightly regulated by the activities of the ubiquitin ligase Mdm2, and the transcriptional repressor MdmX (Haupt et al., 1997a; Migliorini et al., 2002; Momand et al., 2000; Momand et al., 1992). Interestingly, it has been shown that Usp7 acts as a de-ubiquitinase for both Mdm2 and MdmX under physiological conditions (Meulmeester et al., 2005a). Moreover, Usp7 directly de-ubiquitinates p53 and stabilizes this protein under stress environments (Li et al., 2002; Ronai, 2006; Tang et al., 2006). The critical role of Usp7 in this pathway can be highlighted by the example that Usp7 downregulation has been shown to inhibit cell proliferation and tumor growth mainly due to its actions on p53 (Becker et al., 2008; Cummins et al., 2004; Li et al., 2004).

Furthermore, Usp7 has been shown to be targeted by two different members of

herpes viruses. This ubiquitin-specific protease was first identified as an interaction partner of HSV-1 regulatory protein Icp0 (Everett et al., 1999; Everett et al., 1997). Shortly after this, EBV EBNA1 protein was shown to specifically interact with Usp7 (Holowaty et al., 2003a; Holowaty et al., 2003b). In both cases, critical functions have been assigned for these interactions. In the present study, two multifunctional regulatory proteins of adenovirus type 5 taking part in several processes in adenovirus infection and also adenovirus mediated cell transformation, E1B-55K and DBP were identified as novel interaction partners of Usp7. The interaction of Usp7 with these proteins, as well as the functions of this critical ubiquitin-specific protease in adenoviral infection and cell transformation processes were investigated in detail. The results of this investigation will provide a better understanding of the adenovirus infectious cycle and cell transformation induced by the oncogenes of this virus.

6.1 Functions of Usp7 – E1B-55K interaction during productive adenovirus infection

6.1.1 Usp7 binds to and stabilizes E1B-55K

The interaction between Usp7 and E1B-55K was first identified in yeast-two-hybrid screening performed in our group, where the N-terminal region of E1B-55K protein was used as the bait. These experiments suggested a direct interaction between the N-terminal region of the 55K protein and Usp7. In the present study, the interaction between these two proteins was analyzed in detail by combining both *in vitro* and *in vivo* binding experiments. The IP experiments performed in both directions, together with the GST pull-down assays carried out using different fragments of the 55K protein demonstrated that E1B-55K binds to Usp7 strongly and specifically in virus infected cells.

Having established the interaction between these two proteins, the contribution of this interaction to the functions of E1B-55K was investigated. Usp7 has been shown

to stabilize the majority of the proteins it interacts with by de-ubiquitinating them (Cheon and Baek, 2006). Two relevant examples for these proteins are cellular Mdm2 and viral Icp0 (Everett et al., 1999; Meulmeester et al., 2005a). Interestingly, both proteins have E3 ubiquitin ligase activity, are responsible for the proteolytic degradation of p53, and like several E3 ligases, ubiquitinate themselves (Canning et al., 2004; Fang et al., 2000). Usp7 acts as a de-ubiquitinase for both proteins. E1B-55K is also a major component of a virus-induced E3 ubiquitin ligase targeting p53 for ubiquitination (Harada et al., 2002; Querido et al., 2001). The high similarity between the functions of these proteins and the fact that they all interact with Usp7 pointed to the possibility that E1B-55K is also ubiquitinated during the process of p53 ubiquitination. However, there is no evidence so far showing the ubiquitination of the E1B-55K protein. The assays carried out in this work to show the ubiquitination of E1B-55K failed due to the aggregative behavior of this protein in SDS gels masking any ubiquinitated bands. However, a similar stabilizing effect of Usp7 on E1B-55K was detected. The first evidence for such an effect came from the inhibition experiments. Both the inhibition of general cysteine protease activity by E64 and specific down-regulation of Usp7 levels by RNAi resulted in the destabilization of E1B-55K protein. Similarly, the E1B-55K P70T/S73A mutant showing impaired binding to Usp7 was found to be defective in the maintenance of normal E1B-55K levels in virus infected and transiently transfected cells. Finally, blocking the proteasome restored the levels of both the wild-type E1B-55K in Usp7kd cells and the mutant E1B protein in normal cells. Altogether, these results strongly suggest that E1B-55K is subjected to protein turnover via ubiquitination and that Usp7 stabilizes E1B-55K by preventing its proteasomal degradation.

6.1.2 **Definition of the Usp7 binding site in E1B-55K**

One of the critical findings in the current study is the identification of the Usp7 binding motif in the E1B-55K protein. Previous investigations on the interaction of Usp7 with p53, Mdm2 and EBNA1 revealed the structural basis for these interactions and suggested two different consensus motifs: (Ø/E)G(Ø/G)S where Ø stands for a hydrophobic residue (Hu et al., 2006) and (P/A)XXS where X stand for any residue

(Sheng et al., 2006). Note, both reports implied the significance of the first and fourth residues of the motifs in regulating the interaction. Since the N-terminal 79 residues of E1B-55K protein was shown to be sufficient for binding to Usp7, the putative binding motifs within this region were screened and 4 candidate sites were found: AGFS (residues 13-16), AGGS (residues 51-54), EPES (residues 65-68), and PGPS (residues 70-73). Among these motifs, except EPES, the other three matched both proposed consensus sequences. However, the large F residue at the third position is unfavorable and according to Hu et al., the G at the third position has no interaction with the surface of Usp7, and therefore weakens the binding in comparison to a hydrophobic residue at the same position. Therefore, only the PGPS motif fits the criteria proposed by both reports and indeed, mutational analysis showed that this motif is the major Usp7 binding motif (UBM) in the E1B-55K protein. Moreover, alignment of the amino acid sequences of large E1B proteins from 16 different human serotypes showed that UBM has the highest level of conservation in the N-terminal region of the large E1B proteins, which highlights the importance of this interaction for the functions of 55K protein.

The defective binding of the P70T/S73A mutant to Usp7 was confirmed in both transient transfection and infection experiments. However, residual binding of this mutant to Usp7 was detected in these experiments. One possible explanation for this residual binding may be the presence of a mediator acting as a common interaction partner of Usp7 and E1B-55K. If this is the case, viral proteins and p53 can be excluded from the potential candidate list, since the initial binding experiments were conducted with transiently transfected p53-negative H1299 cells. Another possibility could be the presence of other Usp7-binding motifs in the C-terminus of E1B-55K. The C-terminal segments of this protein could not be included in the binding assays due to their toxicity when expressed in bacteria. Indeed, in the C-terminal part of E1B-55K, there are two additional putative Usp7 binding motifs fitting the (P/A)XXS consensus sequence that could accommodate alternative binding sites: PNFS (residues 244-247) and ASHS (residues 375-378). Although these sequences contain unfavorable residues at their third position (a large F residue in the former and a polar H residue in the latter), it is possible that they serve as alternative binding sites.

Moreover, the possible contribution of the other three putative N-terminal Usp7 binding sites to the interaction between Usp7 and E1B-55K should not be excluded. Mutating these sites one by one only resulted in binding deficiency with the PGPS motif. However, it is possible that the other sites still have a minor ability to bind to Usp7. It has been shown that Mdm2 contains several putative Usp7 binding sites and mutating one of the major binding sites enforces the use of an adjacent site for Usp7 binding (Sheng et al., 2006). It can be speculated that having more than one binding site is a common feature of the Usp7 interacting proteins and could be necessary for efficient de-ubiquitination of the lysine residues in different regions of the protein.

6.1.3 Usp7 contributes to the biological functions of E1B-55K

Identification of the PGPS motif in E1B-55K that is responsible for Usp7 binding allowed the construction of the virus mutant H5*pm*4185 expressing the minimally mutated version of E1B-55K protein (P70T/S73A) that was expected to be Usp7 binding deficient. Having verified the severely reduced Usp7 binding of this mutant E1B-55K in infected cells, the important features of this virus were investigated.

First, the effect of mutations on the subcellular localization and sumoylation of E1B-55K were analyzed. The close proximity of UBM, NES and SCM is noteworthy. Interestingly, the only serotypes that lack the UBM in their N-termini, Ad12 and Ad40, also present no NES or Sumo-1 conjugation site. This, together with the fact that the nucleocytoplasmic trafficking of E1B-55K is regulated by sumoylation (Kindsmuller et al., 2007) raises the obvious question of whether the adjacent UBM, NES, and SCM motifs modulate the functions of the E1B-55K protein in a concerted manner. However, in the experiments conducted in this work, no significant influence of the substitution mutations on the sumoylation or nucleocytoplasmic shuttling of E1B-55K was observed.

During wt H5*pg*4100 infection, Usp7 was observed to be translocated into the viral replication centers. This redistribution of Usp7 was retained in H5*pm*4185 infection, leading to the conclusion that Usp7 accumulation at the replication centers is

independent of E1B-55K. This conclusion was further supported by the E1B-deleted virus *dl*1520, which exhibited a similar localization of Usp7. On the other hand, inactivating the nuclear export of E1B-55K by LMB resulted in a perfect co-localization of 55K protein and Usp7 in replication centers. Therefore, it is still possible to think that E1B-55K contributes to this process. It is not clear whether the re-localization of Usp7 into viral replication centers is a process required by the virus in order to use or inhibit Usp7 functions. These two possibilities are not mutually exclusive. The virus may alter the localization of Usp7 and create a micro-environment in the nucleus so that the cellular proteins that react against the infection, such as p53, cannot be stabilized by Usp7; but at the same time adenovirus may use the activity of Usp7 for E1B-55K and other potential viral and cellular factors in the viral replication centers, as are required for efficient virus replication.

To characterize the H5*pm*4185 virus, two different cell lines were used. A549 cells were included in these experiments to test the potential effect of the mutation on p53 degradation. One of the major functions of E1B-55K during adenovirus infection is targeting p53 for proteolytic degradation (Berk, 2005), and it is possible that E1B-55K prevents the de-ubiquitination of p53 by binding to the same region in Usp7 and out-competing the tumor suppressor. Indeed, it has been shown that EBNA1 uses such a strategy to inhibit the stabilization of p53 by Usp7 (Holowaty et al., 2003a; Hu et al., 2002). The striking similarity of the PGPS binding motif in E1B-55K to the EGPS in EBNA-1 supports this idea, since EBNA1 has been shown to bind Usp7 with approximately 10-fold higher affinity than p53 and out-compete p53 (Holowaty and Frappier, 2004; Hu et al., 2006). However, unexpectedly, it was observed that in H5*pm*4185 infection the degradation of p53 is as efficient as with H5*pg*4100 virus.

The H5*pm*4185 virus was found to be defective in accumulating a late viral protein L4-100K and in virus production compared to wt H5*pg*4100 virus in H1299 cells. This defect can be attributed to E1B-55K functions, because in this cell line H5*pm*4185 also showed a defect in the maintenance of E1B-55K levels. In contrast, in A549 cells both viruses behaved similarly in terms of L4-100K accumulation and virus production. Interestingly, in this cell line, E1B-55K levels were also found to be

comparable in both virus infections. This striking difference regarding E1B-55K levels in these two cell types was complicated further by the finding that in Usp7 depleted APU6 cells derived from A549 cells, wt E1B-55K was even more defective in maintaining protein levels in infected cells. This phenomenon can be explained as follows: E1B-55K, Usp7, and p53 are present in a protein complex and the Usp7 dependent stabilization of E1B-55K does not require direct binding between these proteins but can be mediated by p53. Therefore, in p53 positive A549 cells, a Usp7 binding deficient mutant of E1B-55K can still be stabilized, whereas in p53 negative H1299 cells this stabilization does not occur. Moreover, in A549 derived Usp7kd cells (APU6), E1B-55K is not stabilized due to the lack of Usp7. Supporting this speculation, a similar mechanism has recently been shown between Mdm2, Usp7 and, p53. It has been shown that these proteins form a trimeric complex despite mutually exclusive binding, and Usp7 can still de-ubiquitinate a p53 mutant that lacks Usp7 binding by using Mdm2 as a bridge (Brooks et al., 2007). The presence of such a trimeric complex between E1B-55K, Usp7, and p53 should be analyzed in further studies.

In summary, the effect of the mutation in E1B-55K causing a defect in Usp7 binding is well-pronounced in terms of virus production, even at a high multiplicity of infection in H1299 cells. Therefore, it can be concluded that interaction with Usp7 is crucial for the biological functions of E1B-55K protein.

6.2 Usp7 is a factor required for efficient adenovirus replication

6.2.1 Usp7 knockdown cell lines as tools to study adenovirus infection

In this work, to analyze the functions of Usp7 in productive infection cycles in detail, stable Usp7kd cells were generated from H1299 and A549 cells. While choosing the parental lines for establishing the stable knockdown sub-lines two criteria were considered: They should be easily infected by Ad5, and since Usp7 is a critical component of the p53 pathway, they should antagonize in the presence of p53 to

allow a better interpretation of Usp7 functions in adenovirus infection. A549 and H1299 cells meet these requirements. First, lung epithelium is one of the primary targets of Ad5 infection and both of these cell lines were obtained from lung carcinomas. Second A549 cells express wt p53 (Lehman et al., 1991) whereas, H1299 lacks functional p53 (Mitsudomi et al., 1992). Having chosen these cells, stable Usp7kd clones were generated from each cell type and used in further experiments.

During the procedure of generating a stable cell line, new genes are randomly introduced into the host cell's genome and the cloned cell lines are grown from a single genetic background. Hence, at the end, the established monoclonal cell line may differ in some characteristics from the parental cell line and these differences may negatively affect virus infection. Three such parameters can be considered to be critical: cell growth, infectivity, and the random inactivation of an unknown factor that is required for adenovirus infection.

It is known that adenovirus infectivity varies greatly among different cell types (Goodrum and Ornelles, 1998). Therefore, to ensure the equivalent infectivity of the newly produced cell lines, the adenovirus transducing efficiency of each line was tested, and the amount of virus particles required to infect equivalent number of cells was found to be almost identical in the Usp7kd cells compared to their parental lines. Next, the growth properties of the established cell lines were investigated. Usp7 has growth regulatory functions basically due to its interactions with p53. It has previously been shown that disruption of the Usp7 gene stabilizes p53 and induces slow growth in HCT116 cells expressing wt p53, and it is not possible to obtain Usp7 knockout cells from SW48, a tumor cell line with intact p53 functions (Cummins et al., 2004). Similar results were obtained during the generation of Usp7kd lines from A549 cells in this study. Only a single stable clone (APU6) showing significant reductions in Usp7 levels could be established from these cells. Consistent with the previous report, APU6 cells exhibited a reduced growth rate compared to its parental line. To circumvent the potential negative effect of this reduced growth on virus infection, another A549-derived slow growing Usp7kd line (APU5), which presents comparable levels of Usp7 to the parental line, was used as an additional control.

Note, several clones with significantly reduced Usp7 levels could be obtained in p53 negative H1299 cells, and the selected HPU2 cells grew as efficient as the parental H1299 cells, emphasizing the critical role of this ubiquitin-specific protease in p53 dependent cell growth. As the third parameter, to be able to assign the obtained results specifically to Usp7 downregulation, a plasmid encoding an siRNA resistant form of the Usp7 gene was generated and ectopically expressed in the knockdown cells in order to rescue the RNAi effect, which is the ultimate control. Including all these controls, the generated cell lines provided effective tools to investigate the function of Usp7 in adenovirus infection in connection with the p53 pathway.

6.2.2 Usp7 operates at both early and late phases of the adenovirus infectious cycle

After establishing the Usp7kd cell lines, these were used to conduct a detailed investigation of adenovirus infection. The adenovirus lytic life cycle can be separated into two phases: an early and a late phase (Berk, 2007; Shenk, 2001). The early phase of infection is critical for the virus to establish an optimum environment for efficient viral DNA replication and subsequent expression of the late genes. The late phase starts with the onset of viral DNA replication and mainly involves structural protein synthesis and virus assembly. To understand the functions of Usp7 in adenovirus infection, the influence of this protease on the early and late phase of infection was assessed by analyzing the synthesis of early and late viral proteins, the formation of replication centers, and the production of progeny virions during wt virus infection in the various generated Usp7kd cells.

In this context, the synthesis of three multifunctional early phase proteins was investigated: E1A, E1B-55K, and DBP. Interestingly, in Usp7kd cells, the steady-state levels of all three proteins were found to be reduced in comparison to Usp7+ cells. This decrease in the levels of E1B-55K and DBP can be explained by reduced stability of these proteins in Usp7 depleted cells, since both proteins were shown to interact with, and be stabilized by Usp7 in this study. In contrast, the reduction in the levels

of E1A proteins (12S and 13S) was surprising. Being the first gene products in adenovirus infection, these proteins turn on the expression of other early genes (Berk, 2007). Therefore, it is logical that a reduction in E1A levels slows down the whole infection process. One possible explanation for such a reduction in E1A steady-state levels can be the missing stabilizing effect of Usp7, as seen with E1B-55K and DBP proteins. However, this was invalidated by the cycloheximide protein half-life experiments where E1A proteins were shown to be as stable in Usp7kd cells as in Usp7+ cells. Moreover, in ABshU729 and ABshU730 lines stably expressing the 12S splice-variant of E1A together with shUsp7, the steady-state levels of the small E1A protein were found to be identical to those in AB lines (718-720). Hence, the negative effect of Usp7 depletion on E1A levels does not seem to be due to a direct relation between these two proteins. Another and more prominent explanation is that impairment of an early function of Usp7 causes the delay in E1A protein expression. Such potential functions of Usp7 very early in adenovirus infection are discussed in Section 6.2.4.

It is known that adenoviruses can compensate for early phase defects by increasing the multiplicity of infection (Bridge et al., 1993; Huang and Hearing, 1989). The results of virus growth experiments showed that adenovirus can also compensate for the defects caused by depletion of Usp7 by increased numbers. For instance, at 48 h p.i., at a high moi, the virus production activity of wt virus was enhanced in Usp7kd cells. Since the previous experiments showed that Usp7 is essential for efficient initiation of replication center formation, it can be interpreted that Usp7 mainly influences the early phase of infection, and once the late phase is established the need for Usp7 is minimum or dispensable. However, this idea is contradicted by the observed maximal Usp7 accumulation in replication centers at 12 to 16 h p.i., when the late phase is assumed to start. Furthermore, the exclusive distribution of Usp7 in these structures late in infection, and the specific de-ubiquitinating activity of Usp7 on DBP during infection hints that Usp7 also functions in the late phase of infection.

Usp7 became the subject of this work by virtue of its binding to the E1B-55K protein. The Usp7-dependent stabilization of the 55K protein was shown to be critical for the

biological functions of E1B-55K in H1299 cells. One might think that in the absence of E1B-55K, adenovirus replication is equally defective in Usp7+ and Usp7kd cells. In sharp contrast, E1B-deleted *dl*1520 virus was found to be more defective than the wt virus in Usp7kd cells. These observations show that the interaction between these two proteins is more complicated than previously thought. Usp7 stabilizes E1B-55K but in turn, E1B-55K should utilize the functions of Usp7 for other aspects of the virus infection. Therefore, in the Usp7 depleted cells, the absence of E1B-55K further decreased the potential functions of Usp7 in other viral processes.

In summary, Usp7 plays critical regulatory roles throughout the adenovirus lytic cycle starting from the very early stages of infection. Apparently, Usp7 not only determines the localization of replication centers, but also is used as a stabilizer by at least two of the adenovirus regulatory proteins.

6.2.3 Correlation between cellular Usp7 levels and adenovirus replication efficiency

The characterization of wt and E1B-deleted virus in different Usp7kd cell lines demonstrated that Usp7 is a factor enhancing adenovirus replication regardless of the growth rate or p53 status of the host cell, or the functions of the viral E1B-55K protein. More importantly, exogenous expression of Usp7 in the knockdown cells elevated the early adenoviral protein expression levels and virus yield, not only confirming the specific effect of Usp7 on the infection, but also pointing to Usp7 as being a factor determining the rate of adenovirus replication. Supporting this hypothesis, in a Usp7 knockout cell line where the Usp7 gene is homozygously disrupted, adenovirus replication was found to be almost abortive.

Two conclusions can be derived from these results: First, blocking Usp7 activity could be used in the treatment of adenovirus infections. Adenovirus was previously not considered a major pathogen and no licensed anti-adenovirus drugs exist. However, transplantation coupled with strong immunosuppressive therapy has led to an increase in the incidence of severe adenovirus infections. Particularly pediatric

patients undergoing allogenic stem cell transplantation are vulnerable to disseminated adenovirus infections with a high rate of morbidity and mortality (Walls et al., 2003). There is a need for potent antiviral therapeutics against adenoviruses that allow suppression of the virus at different steps in the replication cycle (Naesens et al., 2005). Usp7, having enzymatic activity, represents a potent target for small molecule inhibitors. Indeed, one specific inhibitor of Usp7 has recently been identified in drug screening. In the light of the results presented here, such an inhibitor targeting Usp7 could be useful for treating adenovirus infections.

Second, the correlation between cellular Usp7 levels and the efficiency of adenovirus replication may provide further benefits for developing oncolytic adenoviral vectors. The oncolytic potential of adenoviruses has gained particular attention since it was suggested that the E1B-deleted *dl*1520 virus, which was also used in this study, can replicate selectively in tumor cells (Bischoff et al., 1996). Since the E1B-55K protein inhibits the functions of p53, it has been hypothesized that this virus can only replicate in tumor cells lacking a functional p53, and such selective replication has been shown in a number of tumor cell lines (Bischoff et al., 1996). Based on these findings, clinical trials were initiated with *dl*1520 for treating head and neck carcinomas lacking functional p53 (Khuri et al., 2000; Kirn, 2001b; Lamont et al., 2000; Nemunaitis et al., 2000). Contrary to these data, it was later shown in numerous different reports that *dl*1520 can replicate efficiently in several tumor cell lines and in some primary cultured human cells containing wt p53 (Goodrum and Ornelles, 1997; Harada and Berk, 1999). Today, the correlation between the p53 status of a cell and the replication competency of E1B-deleted virus remain controversial, and other factors such as regulators of the viral mRNA transport pathway were suggested to contribute to the selective replication of *dl*1520 (O'Shea et al., 2004). Nonetheless, adenoviruses have great potential as oncolytic vectors and identification of the host-range determinant for E1B-deleted virus growth would invaluable.

In this respect, the Usp7 levels of five different human tumor cell lines, 293, A549, C33A, RKO and Saos-2, were analyzed by immunoblotting. The results of this study were in absolute correlation with the adenovirus replication efficiencies determined

previously for these cell lines. Both wt and *dl*1520 viruses replicated efficiently in adenovirus transformed embryonic kidney cell line 293, in the lung carcinoma cell line A549, and in cervical carcinoma cell line C33A. In contrast, the replication of both viruses in colon carcinoma cell line RKO was modestly defective, whereas in the osteosarcoma cell line Saos-2 it was shown to be severely defective. As can be seen from the immunoblot (Fig. 26), the cell lines that express high levels of Usp7 supported efficient adenovirus growth, whereas less Usp7 expression resulted in limited adenovirus replication regardless of the cells' p53 status. This result is promising for pre-determining the efficiency of oncolytic therapy on a target tumor tissue.

6.2.4 Usp7-containing PML bodies as the sites of adenovirus replication centers

One of the striking observations in this work is that adenovirus replication centers begin to form adjacent to Usp7-containing PML bodies. It was previously observed that adenovirus genomes localize juxtaposed to specific PML bodies shortly after entering the nucleus (Ishov and Maul, 1996b). Indeed, this feature is not unique to adenovirus. Simian virus 40 (SV40), HCMV, and HSV-1 also deposit their genomes adjacent to PML bodies (Ishov and Maul, 1996b; Maul et al., 1996). These nuclear bodies contain several different proteins regulating numerous critical processes in the cell, including cell cycle regulation, transcriptional activation or repression and anti-viral defense (Borden, 2002; Ching et al., 2005; Everett, 2006). Thus, it has been controversially discussed in the literature whether the early localization of these DNA viruses' genomes adjacent to PML bodies inhibits or enhances viral replication. It is generally considered that when the lytic replication of DNA viruses occurs, PML bodies react to inhibit their replication (Ching et al., 2005; Everett, 2006). Supporting this phenomenon, HSV-1, HCMV, and adenovirus were shown to encode proteins that inactive these structures. For instance, while in HSV-1 and HCMV infection some PML body components including the PML protein itself are degraded (Ching et al., 2005), in adenovirus infection PML bodies are reorganized via the activity of the early protein E4orf3 (Tauber and Dobner, 2001). On the other hand, it has also

been proposed that the initial localization of HCMV parental genomes adjacent to PML bodies is highly beneficial for efficient early gene transcription (Ishov et al., 1997). These converse actions of PML bodies represent a bidirectional effect on the early phase of these viruses.

PML bodies within a nucleus differ from each other in their protein content and can be classified into subpopulations. Interestingly, Usp7 was identified as a component of a small subset of these bodies (Everett et al., 1997). In this work, adenoviral replication centers were observed to form adjacent to this specific subset of PML bodies containing Usp7. Interestingly, DBP levels were detectably lower in Usp7kd cells than in Usp7+ cells even at 6 hours after infection, and the formation of replication centers was found to be inefficient and delayed in such Usp7 depleted cells. These findings together with the fact that Usp7 is required for maximal adenovirus growth imply that this specific subset of PML bodies containing Usp7 is beneficial for adenovirus lytic infection. It can be hypothesized at this point that adenovirus genomes preferentially locate adjacent to Usp7-containing PML bodies, and that this is a prerequisite for efficient synthesis of early viral proteins and the formation of replication centers. Future investigations into other components of Usp7-containing PML bodies, as well as factors required for the specific localization of replication centers would help clarify the mode of action of these structures in adenovirus infection.

6.2.5 **The interaction between Usp7 and DBP and its consequences**

The exclusive localization of Usp7 at the viral replication centers late in infection together with the potential significance of this specific localization prompted the search for the viral factor responsible for this event. Since adenovirus DNA replication requires three viral elements (Bosher et al., 1990; Gounari et al., 1990; Santoro et al., 1988): Adenovirus DNA-polymerase (Pol), precursor- or pre-terminal protein (pTP), and single-stranded DNA binding protein (DBP), all of which accumulate in viral replication centers, the question was whether one of these factors stimulates accumulation of Usp7 at these centers. Indeed, GST pull-down

experiments found that DBP binds Usp7 specifically and strongly. Hence, in addition to E1B-55K, a second multifunctional early adenoviral protein, (DBP) was revealed to be a novel interaction partner of Usp7. Multiple functions have previously been assigned to this protein, including the activation of early gene transcription, DNA replication, viral assembly, and even cell transformation(Babich and Nevins, 1981a; Carter and Blanton, 1978a; Cleat and Hay, 1989; Lindenbaum et al., 1986; Rice et al., 1987b). Nonetheless, the major function of DBP is to increase the processivity of Ad Pol by unwinding the double-stranded DNA (Lindenbaum et al., 1986). DBP was found to alter the localization of Usp7 when transfected into H1299 cells, with these two proteins co-localizing in the DBP-induced structures. Since DBP, in the absence of any viral protein, was apparently sufficient for Usp7 redistribution in the nucleus, it was anticipated to be the factor responsible for bringing Usp7 to adenoviral replication centers during infection.

Interestingly, DBP was found to bind the TRAF-like domain of Usp7, which also interacts with E1B-55K. This binding was further confirmed by *in vivo* IP reactions in both directions, indicating the specificity of the interaction. The binding of both E1B-55K and DBP to the same region in Usp7 raised the question of whether the interaction of these proteins with Usp7 is mutually exclusive. One observation triggering this question was the elevated levels of DBP in virus infection with *dl*1520 lacking the 55K protein. DBP contains a single putative Usp7 binding motif suggested by Hu et al., which is VGFS (residues 119-122), and 4 of the less stringent motifs proposed by Sheng et al.: PSPS (residues 32-35), PRPS (residues 71-74), PSTS (residues 73-76), and PIVS (residues 176-179). Therefore, it will be of great interest to analyze these putative Usp7 binding motifs and the potential interplay between these three proteins in further studies.

DBP was found to interact with the N-terminal TD of Usp7, which raised the possibility that this protein is stabilized by Usp7. Confirming this hypothesis, protein half-life experiments detected substantially reduced levels of DBP in Usp7 depleted cells. Moreover, Usp7 was found to specifically de-ubiquitiante DBP, since a smear of poly-ubiquitinated DBP forms could only be observed in Usp7kd cells but not in

Usp7+ cells. Interestingly, a single dominant ubiquitinated form of this protein was detected, migrating around 250 kDa in both Usp7+ and Usp7kd lines, with enhanced accumulation in the latter. Presumably, this is a poly-ubiquitin chain conjugated to a single lysine residue of DBP that is inaccessible to Usp7. Strikingly, three additional ubiquitinated forms of DBP were detected almost exclusively in Usp7kd cells (Fig. 31; marked by arrowheads). These bands either correspond to the polyubiquitination of some specific lysine, or mono-ubiquitination of various lysine residues in DBP. More importantly, the near absence of these bands in Usp7+ cells led to the speculation that these specific, ubiquitinated, lysine residue(s) are rapidly de-ubiquitinated by Usp7. There are examples in the literature describing protein ubiquitination/de-ubiquitination cycles that are required for their functions (Vong et al., 2005). Therefore, it is plausible that this proceeds using the same machinery. If this is the case, it can be hypothesized that Usp7 regulates adenoviral DNA replication via continuously de-ubiquitinating DBP, a topic that requires detailed investigation.

6.3 Usp7 is a critical cellular factor regulating adenovirus mediated cell transformation

Since adenovirus can transform primary mammalian cells in culture to a tumorigenic phenotype, it provides an excellent tool to study the events in malignant cell growth. Discovering the transforming potential of human Ads stimulated extensive research on the adenoviral proteins that contribute to this process. Adenovirus mediated cell transformation is mainly a two step process (Endter and Dobner, 2004). The first step is induction of cell proliferation by inactivation of pRB. This most critical part of the adenoviral transformation is performed by the E1A proteins. However, the unprogrammed cell proliferation induces growth arrest and apoptosis. The expression of E1A induces and stabilizes p53 (Lowe and Ruley, 1993). Thus, for a complete transformation process, the growth suppression and apoptotic functions of p53 should be inactivated (Debbas and White, 1993; Lowe et al., 1994). E1B-55K alone has the ability to inactive p53. Indeed, p53 first came to attention due to its

interaction with SV40 large T antigen (Lane and Crawford, 1979) and two years later with adenovirus E1B-55K (Sarnow et al., 1982a). Several activities of the large E1B protein inhibit p53. First, E1B-55K binds to the N-terminal transactivation domain of p53, presumably inhibiting the functional activity of p53 (Kao et al., 1990). Another strategy used by the 55K protein is sequestration of the nuclear p53 protein to large cytoplasmic structures adjacent to the nucleus (perinuclear bodies), which are proposed to be aggresomes (Zantema et al., 1985b). More importantly, the repression domain in E1B-55K's C-terminus represses the p53 promoters, a function thought to be the most important action of the 55K protein in the transformation process (Martin and Berk, 1998; Yew et al., 1994). However, different reports show that each of these single activities is dispensable for the transforming functions of E1B-55K (Berk, 2005). Besides, it was recently proposed that E1B-55K has p53-independent functions during the transformation process (Hartl et al., 2008; Sieber and Dobner, 2007). In conclusion, although the contribution of E1B-55K to the cell transformation mechanism mainly involves inactivating p53 functions, which is still not well understood, it also requires other protein-protein interactions.

In cells p53 levels are regulated by a highly complicated system. Mdm2 regulates the levels of p53 by ubiquitinating this protein and targeting it to proteasomal degradation (Haupt et al., 1997b; Momand et al., 2000). Additionally, MdmX, which shows high sequence homology to Mdm2, inactivates the activity of p53 (Finch et al., 2002; Marine and Jochemsen, 2004). Interestingly, Usp7 is shown to de-ubiquitinate all of these proteins in a concerted manner to tightly regulate cell growth (Meulmeester et al., 2005a). The discovery of Usp7 as a novel interaction partner of E1B-55K led to the idea that the mode of action of E1B-55K in transformation processes may involve interactions between E1B-55K, p53, and Usp7 proteins. Therefore, the present study used RNA interference (RNAi) as an experimental tool to evaluate the role of Usp7 and p53 on E1A- plus E1B-mediated transformation of primary BRK cells.

6.3.1 E1B-55K and p53 shRNAs can synergistically cooperate with E1A to transform mammalian cells in culture.

The addition of p53 shRNAs to transformation assays including E1A and E1B-55K proteins gave surprising results. These experiments showed for the first time that p53 shRNAs can cooperate with E1A to completely transform rodent cells in culture. Interestingly, E1A/shp53 transfections yielded a greater number of foci than E1A/E1B-55K transfections. More importantly, these foci grew much larger and to higher densities, indicating that the E1A/shp53 transformed cells are growing faster than those transformed by E1A/E1B-55K. This was also confirmed by determining the growth rates of stably established cell lines derived from E1A/shp53 and E1A/E1B-55K transfected cells. These results led to the following conclusions: The main function of E1B-55K in the transformation process is to inhibit p53, since the lack of E1B-55K can be fully compensated by depletion of p53. Furthermore, the contribution of shRNAs against p53 to the transformation process was more profound than that of E1B-55K, suggesting that the 55K protein cannot fully inhibit p53 functions.

The analysis of E1A/E1B-55K/shp53 transfected primary cells added a further dimension to the transformation process. In such transfections, the focal transformation was even more efficient than with E1A/shp53 in terms of foci number and density. Moreover, the established cell lines grew even more rapidly than E1A/shp53 cell lines. This enhanced growth rate can be assigned to E1B-55K functions. E1B-55K expression persisted in all of these established lines. Therefore, it can be concluded that E1B-55K further enhances the transformed phenotype in the presence of p53 shRNAs. This can be explained by either functions of E1B-55K other than p53 inhibition, or absolute inhibition of p53 in the presence of both E1B-55K and shp53. In summary, E1B-55K and shp53 can synergistically cooperate with E1A to transform mammalian cells in culture.

An interesting observation was the correlation of E1B-55K and p53 levels in the transformed BRK cells. It is known that E1B-55K alone has a stabilizing effect on p53 in the transformed BRK cells (Levine, 1990). In E1A/E1B-55K transformed AB cells,

p53 accumulates to high levels (Lowe and Ruley, 1993). When the transformation assay was conducted in the presence of p53 shRNAs, in the transformed cell lines (ABshp) p53 is present at background levels. Surprisingly, E1B-55K protein levels were also fairly low in these lines compared to AB lines. Consistent with the immunoblot data, both these proteins were detected at very low concentrations in the ABshp cells when their subcellular localization was analyzed by immunofluorescence. Interestingly, as in AB cells, both E1B-55K and p53 proteins were found to co-localize in a single cytoplasmic body adjacent to the nuclei of the stained cells. However, in contrast to AB cells where these proteins accumulate in large and dense perinuclear bodies, the greatly reduced amounts of E1B-55K and p53 proteins in ABshp cells only formed a very small aggregate.

These results suggest that E1B-55K protein levels are highly dependent on p53 steady-states in transformed cells, or *vice versa*. As already mentioned above, sequestering p53, induced by unprogrammed cell proliferation, to cytoplasmic aggregates is one of the mechanisms E1B-55K uses to inactivate this tumor suppressor (Zantema et al., 1985b). While E1B-55K is promoting the aggregation of p53 in these bodies, it is also captured in these structures still bound to p53. This may explain the direct correlation between the levels of these proteins in the transformed cells. At the same time, co-localization of E1B-55K and p53 in the perinuclear body even in the ABshp53 cells may account in part for the further contribution of E1B-55K in the transformation process of these cells. If the limited amounts of p53 expressed by ABshp53 cells must still be inactivated by E1B-55K, this indicates that the level of p53 inactivation determines the aggressiveness of the adenovirus transformed cell phenotype.

6.3.2 The dependence of E1B-55K transforming potential on the activity of Usp7

Surprisingly, the efficient transformation of primary BRK cells induced by expressing E1A and E1B-55K proteins was almost completely inhibited by the co-expression of shRNAs against Usp7. In such a transformation assay, focus forming activity was

drastically reduced to background levels. In both E1A/shUsp7 and E1A/E1B-55K/shUsp7 transfected cells focus formation activity was observed to initiate, implying that E1A is still functional under these circumstances. Thus the strong inhibitory effect of Usp7 depletion can be assigned to its functional interaction with E1B-55K. Probably, downregulation of Usp7 leads to destabilization of E1B-55K, which is expected since the stability of this protein was shown to be highly dependent on Usp7. An alternative explanation for such a strong inhibitory effect may be that significant downregulation of Usp7 levels leads to the stabilization of p53, as shown in different reports (Becker et al., 2008; Cummins et al., 2004; Li et al., 2004).

The data obtained from analyzing ABshU729 and AB730 cells showed that these explanations are not mutually exclusive. While in ABshU729 cells Usp7 was found to be reduced ~50%, ABshU730 cells displayed a higher knockdown. Interestingly, E1B-55K levels followed exactly the same pattern: less in AB729 cells and almost no expression in ABshU730 cells, indicating that E1B-55K is also stabilized by Usp7 in the rat cells. Surprisingly, the low level of Usp7kd was accompanied by destabilization of p53 in AB729 cells, whereas the tumor suppressor accumulated to high levels in ABshU730 expressing even less Usp7, which was in correlation with previous reports (Becker et al., 2008; Cummins et al., 2004; Li et al., 2004).

Moreover, in ABshU730 cells showing highly efficient Usp7 knockdown and substantially reduced E1B-55K levels, the subcellur localization of p53 was exclusively nuclear, meaning this protein is active on its promoters. Apparently, the small amount of E1B-55K found in the perinuclear body was not enough to alter the localization of the p53 protein. Thus the growth arrested state of the ABshU730 cells, which divide very slowly, may also be explained by the presence of nuclear p53.

Altogether, these results strongly suggest that complete transformation requires inhibition of p53, and in adenovirus E1A/E1B-55K transformed cells, this is achieved by crosstalk between Usp7 – E1B-55K – p53 proteins. In the near absence of Usp7, E1B-55K loses its transforming functions. Altogether, these observations point to

Usp7 being a crucial factor required for adenovirus mediated cell transformation due to its influence on both E1B-55K and p53 proteins.

7 REFERENCES

Abe, S., Miyamura, K., Oba, T., Terakura, S., Kasai, M., Kitaori, K., Sasaki, T., and Kodera, Y. (2003). Oral ribavirin for severe adenovirus infection after allogeneic marrow transplantation. Bone Marrow Transplant *32*, 1107-1108.

Anderson, C. W. (1981). Spontaneous mutants of the adenovirus-simian virus 40 hybrid, Ad2+ND3, that grow efficiently in monkey cells. Virology *111*, 263-269.

Anderson, K. P., and Klessig, D. F. (1984). Altered mRNA splicing in monkey cells abortively infected with human adenovirus may be responsible for inefficient synthesis of the virion fiber polypeptide. Proc Natl Acad Sci U S A *81*, 4023-4027.

Andersson, M. G., Haasnoot, P. C., Xu, N., Berenjian, S., Berkhout, B., and Akusjarvi, G. (2005). Suppression of RNA interference by adenovirus virus-associated RNA. J Virol *79*, 9556-9565.

Ankerst, J., and Jonsson, N. (1989). Adenovirus type 9-induced tumorigenesis in the rat mammary gland related to sex hormonal state. J Natl Cancer Inst *81*, 294-298.

Ariga, H., Klein, H., Levine, A. J., and Horwitz, M. S. (1980). A cleavage product of the adenovirus DNA binding protein is active in DNA replication in vitro. Virology *101*, 307-310.

Aylon, Y., and Oren, M. (2007). Living with p53, dying of p53. Cell *130*, 597-600.

Babich, A., and Nevins, J. R. (1981a). The stability of early adenovirus mRNA is controlled by the viral 72 kd DNA-binding protein. Cell *26*, 371-379.

Babich, A., and Nevins, J. R. (1981b). The stability of early adenovirus mRNA is controlled by the viral 72 kd DNA-binding protein. Cell *26*, 371-379.

Baker, A., Rohleder, K. J., Hanakahi, L. A., and Ketner, G. (2007). Adenovirus E4 34k and E1b 55k oncoproteins target host DNA ligase IV for proteasomal degradation. J Virol *81*, 7034-7040.

Baker, S. J., Markowitz, S., Fearon, E. R., Willson, J. K., and Vogelstein, B. (1990). Suppression of human colorectal carcinoma cell growth by wild-type p53. Science *249*, 912-915.

Barker, D. D., and Berk, A. J. (1987). Adenovirus proteins from both E1B reading frames are required for transformation of rodent cells by viral infection and DNA transfection. Virology *156*, 107-121.

Baron, S. (1996). Medical Microbiology, Fourth Edition edn (Texas, University of Texas

Medical Branch at Galveston).

Becker, K., Marchenko, N. D., Palacios, G., and Moll, U. M. (2008). A role of HAUSP in tumor suppression in a human colon carcinoma xenograft model. Cell Cycle *7*, 1205-1213.

Beltz, G. A., and Flint, S. J. (1979). Inhibition of HeLa cell protein synthesis during adenovirus infection: restriction of cellular messenger RNA sequences to the nucleus. J Mol Biol *131*, 353-373.

Benkö, M., Elo, P., Ursu, K., Ahne, W., LaPatra, S. E., Thomson, D., and Harrach, B. (2002). First molecular evidence for the existence of distinct fish and snake adenoviruses. J Virol *76*, 10056-10059.

Benkö, M., and Harrach, B. (1998). A proposal for a new (third) genus within the family Adenoviridae. Arch Virol *143*, 829-837.

Berk, A. J. (2005). Recent lessons in gene expression, cell cycle control, and cell biology from adenovirus. Oncogene *24*, 7673-7685.

Berk, A. J. (2007). Adenoviridae: The viruses and their replication, 5 edn (New York, N. Y., Raven Press).

Bignell, G. R., Warren, W., Seal, S., Takahashi, M., Rapley, E., Barfoot, R., Green, H., Brown, C., Biggs, P. J., Lakhani, S. R., *et al.* (2000). Identification of the familial cylindromatosis tumour-suppressor gene. Nat Genet *25*, 160-165.

Bischoff, J. R., Kirn, D. H., Williams, A., Heise, C., Horn, S., Muna, M., Ng, L., Nye, J. A., Sampson Johannes, A., Fattaey, A., and McCormick, F. (1996). An adenovirus mutant that replicates selectively in p53-deficient human tumor cells. Science *274*, 373-376.

Blanchette, P., Cheng, C. Y., Yan, Q., Ketner, G., Ornelles, D. A., Dobner, T., Conaway, R. C., Conaway, J. W., and Branton, P. E. (2004). Both BC-box motifs of adenovirus protein E4orf6 are required to efficiently assemble an E3 ligase complex that degrades p53. Mol Cell Biol *24*, 9619-9629.

Blanchette, P., Kindsmuller, K., Groitl, P., Dallaire, F., Speiseder, T., Branton, P. E., and Dobner, T. (2008). Control of mRNA export by adenovirus E4orf6 and E1B55K proteins during productive infection requires E4orf6 ubiquitin ligase activity. J Virol *82*, 2642-2651.

Borden, K. L. (2002). Pondering the promyelocytic leukemia protein (PML) puzzle: possible functions for PML nuclear bodies. Mol Cell Biol *22*, 5259-5269.

Bosher, J., Robinson, E. C., and Hay, R. T. (1990). Interactions between the adenovirus type 2 DNA polymerase and the DNA binding domain of nuclear factor I. New Biol *2*, 1083-1090.

Boutell, C., and Everett, R. D. (2003). The herpes simplex virus type 1 (HSV-1) regulatory protein ICP0 interacts with and Ubiquitinates p53. J Biol Chem *278*, 36596-36602.

Boutell, C., Orr, A., and Everett, R. D. (2003). PML residue lysine 160 is required for the degradation of PML induced by herpes simplex virus type 1 regulatory protein ICP0. J Virol *77*, 8686-8694.

Boutell, C., Sadis, S., and Everett, R. D. (2002). Herpes simplex virus type 1 immediate-early protein ICP0 and is isolated RING finger domain act as ubiquitin E3 ligases in vitro. J Virol *76*, 841-850.

Bradford, M. M. (1976). A rapid and sensitive method for the quantitation of microgram quantities of protein utilizing the principle of protein-dye binding. Anal Biochem *72*, 248-254.

Bridge, E., Medghalchi, S., Ubol, S., Leesong, M., and Ketner, G. (1993). Adenovirus early region 4 and viral DNA synthesis. Virology *193*, 794-801.

Brooks, C. L., and Gu, W. (2004). Dynamics in the p53-Mdm2 ubiquitination pathway. Cell Cycle *3*, 895-899.

Brooks, C. L., Li, M., Hu, M., Shi, Y., and Gu, W. (2007). The p53--Mdm2--HAUSP complex is involved in p53 stabilization by HAUSP. Oncogene *26*, 7262-7266.

Brummelkamp, T. R., Nijman, S. M., Dirac, A. M., and Bernards, R. (2003). Loss of the cylindromatosis tumour suppressor inhibits apoptosis by activating NF-kappaB. Nature *424*, 797-801.

Bullock, W. O., Fernandez, J.M., und Short, J.M. (1987). XL1-Blue: A high efficiency plasmid transforming recA Escherichia coli strain with b-galactosidase selection. In Biotechniques, pp. 376-379.

Bunz, F., Hwang, P. M., Torrance, C., Waldman, T., Zhang, Y., Dillehay, L., Williams, J., Lengauer, C., Kinzler, K. W., and Vogelstein, B. (1999). Disruption of p53 in human cancer cells alters the responses to therapeutic agents. J Clin Invest *104*, 263-269.

Canning, M., Boutell, C., Parkinson, J., and Everett, R. D. (2004). A RING finger ubiquitin ligase is protected from autocatalyzed ubiquitination and degradation by binding to ubiquitin-specific protease USP7. J Biol Chem *279*, 38160-38168.

Carter, T. H., and Blanton, R. A. (1978a). Possible role of the 72,000 dalton DNA-binding protein in regulation of adenovirus type 5 early gene expression. J Virol *25*, 664-674.

Carter, T. H., and Blanton, R. A. (1978b). Possible role of the 72,000 dalton DNA-binding protein in regulation of adenovirus type 5 early gene expression. J Virol *25*, 664-674.

Chandar, N., Billig, B., McMaster, J., and Novak, J. (1992). Inactivation of p53 gene in human and murine osteosarcoma cells. Br J Cancer *65*, 208-214.

Chauvin, C., Suh, M., Remy, C., and Benabid, A. L. (1990). Failure to detect viral genomic sequences of three viruses (herpes simplex, simian virus 40 and adenovirus) in human and rat brain tumors. Ital J Neurol Sci *11*, 347-357.

Cheon, K. W., and Baek, K. H. (2006). HAUSP as a therapeutic target for hematopoietic tumors (review). Int J Oncol *28*, 1209-1215.

Ching, R. W., Dellaire, G., Eskiw, C. H., and Bazett-Jones, D. P. (2005). PML bodies: a meeting place for genomic loci? J Cell Sci *118*, 847-854.

Ciechanover, A., and Schwartz, A. L. (1998). The ubiquitin-proteasome pathway: the complexity and myriad functions of proteins death. Proc Natl Acad Sci U S A *95*, 2727-2730.

Ciechanover, A., and Schwartz, A. L. (2002). Ubiquitin-mediated degradation of cellular proteins in health and disease. Hepatology *35*, 3-6.

Cleat, P. H., and Hay, R. T. (1989). Co-operative interactions between NFI and the adenovirus DNA binding protein at the adenovirus origin of replication. Embo J *8*, 1841-1848.

Cleghon, V. G., and Klessig, D. F. (1986). Association of the adenovirus DNA-binding protein with RNA both in vitro and in vivo. Proc Natl Acad Sci U S A *83*, 8947-8951.

Cress, W. D., and Nevins, J. R. (1996). Use of the E2F transcription factor by DNA tumor virus regulatory proteins. Curr Top Microbiol Immunol *208*, 63-78.

Cummins, J. M., Rago, C., Kohli, M., Kinzler, K. W., Lengauer, C., and Vogelstein, B. (2004). Tumour suppression: disruption of HAUSP gene stabilizes p53. Nature *428*, 1 p following 486.

Cummins, J. M., and Vogelstein, B. (2004). HAUSP is required for p53 destabilization. Cell Cycle *3*, 689-692.

Debbas, M., and White, E. (1993). Wild-type p53 mediates apoptosis by E1A, which is inhibited by E1B. Genes Dev *7*, 546-554.

Diller, L., Kassel, J., Nelson, C. E., Gryka, M. A., Litwak, G., Gebhardt, M., Bressac, B., Ozturk, M., Baker, S. J., Vogelstein, B., and et al. (1990). p53 functions as a cell cycle control protein in osteosarcomas. Mol Cell Biol *10*, 5772-5781.

Dobner, T., and Kzhyshkowska, J. (2001). Nuclear export of adenovirus RNA. Curr Top Microbiol Immunol *259*, 25-54.

Duan, L., Reddi, A. L., Ghosh, A., Dimri, M., and Band, H. (2004). The Cbl family and other ubiquitin ligases: destructive forces in control of antigen receptor signaling. Immunity *21*, 7-17.

Endter, C., and Dobner, T. (2004). Cell transformation by human adenoviruses. Curr Top Microbiol Immunol *273*, 163-214.

Endter, C., Hartl, B., Spruss, T., Hauber, J., and Dobner, T. (2005). Blockage of CRM1-dependent nuclear export of the adenovirus type 5 early region 1B 55-kDa protein augments oncogenic transformation of primary rat cells. Oncogene *24*, 55-64.

Endter, C., Kzhyshkowska, J., Stauber, R., and Dobner, T. (2001). SUMO-1 modification required for transformation by adenovirus type 5 early region 1B 55-kDa oncoprotein. Proc Natl Acad Sci U S A *98*, 11312-11317.

Everett, R. D. (2000). ICP0, a regulator of herpes simplex virus during lytic and latent infection. Bioessays *22*, 761-770.

Everett, R. D. (2004). Herpes simplex virus type 1 regulatory protein ICP0 does not protect cyclins D1 and D3 from degradation during infection. J Virol *78*, 9599-9604.

Everett, R. D. (2006). Interactions between DNA viruses, ND10 and the DNA damage response. Cell Microbiol *8*, 365-374.

Everett, R. D., Meredith, M., and Orr, A. (1999). The ability of herpes simplex virus type 1 immediate-early protein Vmw110 to bind to a ubiquitin-specific protease contributes to its roles in the activation of gene expression and stimulation of virus replication. J Virol *73*, 417-426.

Everett, R. D., Meredith, M., Orr, A., Cross, A., Kathoria, M., and Parkinson, J. (1997). A novel ubiquitin-specific protease is dynamically associated with the PML nuclear domain and binds to a herpesvirus regulatory protein. Embo J *16*, 1519-1530.

Fallaux, F. J., Kranenburg, O., Cramer, S. J., Houweling, A., Van Ormondt, H., Hoeben, R. C., and Van Der Eb, A. J. (1996). Characterization of 911: a new helper cell line for the titration and propagation of early region 1-deleted adenoviral vectors. Hum Gene Ther *7*, 215-222.

Fang, S., Jensen, J. P., Ludwig, R. L., Vousden, K. H., and Weissman, A. M. (2000). Mdm2 is a RING finger-dependent ubiquitin protein ligase for itself and p53. J Biol Chem *275*, 8945-8951.

Finch, R. A., Donoviel, D. B., Potter, D., Shi, M., Fan, A., Freed, D. D., Wang, C. Y., Zambrowicz, B. P., Ramirez-Solis, R., Sands, A. T., and Zhang, N. (2002). mdmx is a negative regulator of p53 activity in vivo. Cancer Res *62*, 3221-3225.

Flint, S. J., and Gonzalez, R. A. (2003). Regulation of mRNA production by the adenoviral E1B 55-kDa and E4 Orf6 proteins. Curr Top Microbiol Immunol *272*, 287-330.

Frangioni, J. V., Beahm, P. H., Shifrin, V., Jost, C. A., and Neel, B. G. (1992). The nontransmembrane tyrosine phosphatase PTP-1B localizes to the endoplasmic reticulum via its 35 amino acid C-terminal sequence. Cell *68*, 545-560.

Gallimore, P. H., Byrd, P. J., and Grand, R. J. A. (1984). Adenovirus genes involved in transformation. What determines the oncogenic phenotype? In Viruses and Cancer. Symposium of the Society for General Microbiology, P. W. J. Rigby, ed. (Cambridge, Cambridge University Press), pp. 125-172.

Giard, R. J., Aaronson, S. A., Todaro, G. J., Arnstein, P., Kersey, J. H., Dosik, H., and Parks, W. P. (1973). *In vitro* cultivation of human tumors: establishment of cell lines derived from a series of solid tumors. J Natl Cancer Inst *51*, 1417-1423.

Gonzalez, R. A., and Flint, S. J. (2002). Effects of mutations in the adenoviral E1B 55-kilodalton protein coding sequence on viral late mRNA metabolism. J Virol *76*, 4507-4519.

Goodrum, F. D., and Ornelles, D. A. (1997). The early region 1B 55-kilodalton oncoprotein of adenovirus relieves growth restrictions imposed on viral replication by the cell cycle. J Virol *71*, 548-561.

Goodrum, F. D., and Ornelles, D. A. (1998). p53 status does not determine outcome of E1B 55-Kilodalton mutant adenovirus lytic infection. J Virol *72*, 9479-9490.

Goodrum, F. D., and Ornelles, D. A. (1999). Roles for the E4 orf6, orf3, and E1B 55-kilodalton proteins in cell cycle-independent adenovirus replication. J Virol *73*, 7474-7488.

Gounari, F., De Francesco, R., Schmitt, J., van der Vliet, P., Cortese, R., and Stunnenberg, H. (1990). Amino-terminal domain of NF1 binds to DNA as a dimer and activates adenovirus DNA replication. Embo J *9*, 559-566.

Graham, F. L., Rowe, D. T., McKinnon, R., Bacchetti, S., Ruben, M., and Branton, P. E. (1984). Transformation by human adenoviruses. J Cell Physiol Suppl *3*, 151-163.

Graham, F. L., Smiley, J., Russel, W. C., and Nairn, R. (1977). Characteristics of a human cell line transformed by DNA from human adenovirus type 5. J Gen Virol *36*, 59-72.

Graham, F. L., and van der Eb, A. J. (1973a). A new technique for the assay of infectivity of human adenovirus 5 DNA. Virology *52*, 456-467.

Graham, F. L., and van der Eb, A. J. (1973b). Transformation of rat cells by DNA of human adenovirus 5. Virology *54*, 536-539.

Groitl, P., and Dobner, T. (2007). Construction of adenovirus type 5 early region 1 and 4 virus mutants. Methods Mol Med *130*, 29-39.

Gustafsson, B., Huang, W., Bogdanovic, G., Gauffin, F., Nordgren, A., Talekar, G., Ornelles, D. A., and Gooding, L. R. (2007). Adenovirus DNA is detected at increased frequency in Guthrie cards from children who develop acute lymphoblastic leukaemia. Br J Cancer *97*, 992-994.

Hagglund, R., and Roizman, B. (2004). Role of ICP0 in the strategy of conquest of the host cell by herpes simplex virus 1. J Virol *78*, 2169-2178.

Hagglund, R., Van Sant, C., Lopez, P., and Roizman, B. (2002). Herpes simplex virus 1-infected cell protein 0 contains two E3 ubiquitin ligase sites specific for different E2 ubiquitin-conjugating enzymes. Proc Natl Acad Sci U S A *99*, 631-636.

Haglund, K., and Dikic, I. (2005). Ubiquitylation and cell signaling. Embo J *24*, 3353-3359.

Haglund, K., Sigismund, S., Polo, S., Szymkiewicz, I., Di Fiore, P. P., and Dikic, I. (2003). Multiple monoubiquitination of RTKs is sufficient for their endocytosis and degradation. Nat Cell Biol *5*, 461-466.

Hahn, W. C., Counter, C. M., Lundberg, A. S., Beijersbergen, R. L., Brooks, M. W., and Weinberg, R. A. (1999). Creation of human tumour cells with defined genetic elements. Nature *400*, 464-468.

Hall, A. R., Dix, B. R., O'Carrol, S. J., and Braithwaite, A. W. (1998). p53-dependent cell death/apoptosis is required for a productive adenovirus infection. Nat Med *4*, 1068-1072.

Hanahan, D. (1983). Studies on transformation of Escherichia coli with plasmids. J Mol Biol *166*, 557-580.

Harada, J. N., and Berk, A. J. (1999). p53-independent and -dependent requirements for E1B-55k in adenovirus type 5 replication. J Virol *73*, 5333-5344.

Harada, J. N., Shevchenko, A., Shevchenko, A., Pallas, D. C., and Berk, A. J. (2002). Analysis of the adenovirus E1B-55K-anchored proteome reveals its link to ubiquitination machinery. J Virol *76*, 9194-9206.

Harlow, E., Franza, B. R., Jr., and Schley, C. (1985). Monoclonal antibodies specific for adenovirus early region 1A proteins: extensive heterogeneity in early region 1A products. J Virol *55*, 533-546.

Harlow, E., and Lane, D. (1988). In Antibodies: A Laboratory Manual (New York, Cold Spring Harbor Laboratory), pp. 139-318.

Hartl, B., Zeller, T., Blanchette, P., Kremmer, E., and Dobner, T. (2008). Adenovirus type 5 early region 1B 55-kDa oncoprotein can promote cell transformation by a mechanism independent from blocking p53-activated transcription. Oncogene *27*, 3673-3684.

Hatt, J., Callahan, A., and Greener, A. (1992). Strategies *5*, 2-3.

Haupt, Y., Maya, R., Kazaz, A., and Oren, M. (1997a). Mdm2 promotes the rapid degradation of p53. Nature *387*, 296-299.

Haupt, Y., Maya, R., Kazaz, A., and Oren, M. (1997b). Mdm2 promotes the rapid degradation of p53. Nature *387*, 296-299.

Hicke, L. (2001). Protein regulation by monoubiquitin. Nat Rev Mol Cell Biol *2*, 195-201.

Holowaty, M. N., and Frappier, L. (2004). HAUSP/USP7 as an Epstein-Barr virus target. Biochem Soc Trans *32*, 731-732.

Holowaty, M. N., Sheng, Y., Nguyen, T., Arrowsmith, C., and Frappier, L. (2003a). Protein interaction domains of the ubiquitin-specific protease, USP7/HAUSP. J Biol Chem *278*, 47753-47761.

Holowaty, M. N., Zeghouf, M., Wu, H., Tellam, J., Athanasopoulos, V., Greenblatt, J., and Frappier, L. (2003b). Protein profiling with Epstein-Barr nuclear antigen-1 reveals an interaction with the herpesvirus-associated ubiquitin-specific protease HAUSP/USP7. J Biol Chem *278*, 29987-29994.

Howitt, J., Anderson, C. W., and Freimuth, P. (2003). Adenovirus interaction with its cellular receptor CAR. Curr Top Microbiol Immunol *272*, 331-364.

Hu, M., Gu, L., Li, M., Jeffrey, P. D., Gu, W., and Shi, Y. (2006). Structural basis of competitive recognition of p53 and MDM2 by HAUSP/USP7: implications for the regulation of the p53-MDM2 pathway. PLoS Biol *4*, e27.

Hu, M., Li, P., Li, M., Li, W., Yao, T., Wu, J. W., Gu, W., Cohen, R. E., and Shi, Y. (2002). Crystal structure of a UBP-family deubiquitinating enzyme in isolation and in complex with ubiquitin aldehyde. Cell *111*, 1041-1054.

Huang, M. M., and Hearing, P. (1989). Adenovirus early region 4 encodes two gene products with redundant effects in lytic infection. J Virol *63*, 2605-2615.

Ikeda, F., and Dikic, I. (2008). Atypical ubiquitin chains: new molecular signals. 'Protein Modifications: Beyond the Usual Suspects' review series. EMBO Rep *9*, 536-542.

Ishov, A. M., and Maul, G. G. (1996a). The periphery of nuclear domain 10 (ND10) as site of DNA virus deposition. J Cell Biol *134*, 815-826.

Ishov, A. M., and Maul, G. G. (1996b). The periphery of nuclear domain 10 (ND10) as site of DNA virus deposition. J Cell Biol *134*, 815-826.

Ishov, A. M., Stenberg, R. M., and Maul, G. G. (1997). Human cytomegalovirus immediate early interaction with host nuclear structures: definition of an immediate transcript environment. J Cell Biol *138*.

Javier, R. T., Raska, K., Jr., Macdonald, G. J., and Shenk, T. (1991). Human adenovirus type 9-induced rat mammary tumors. J Virol *65*, 3192-3202.

Jin, S., and Levine, A. J. (2001). The p53 functional circuit. J Cell Sci *114*, 4139-4140.

Jones, S. N., Roe, A. E., Donehower, L. A., and Bradley, A. (1995). Rescue of embryonic lethality in Mdm2-deficient mice by absence of p53. Nature *378*, 206-208.

Juven-Gershon, T., and Oren, M. (1999). Mdm2: the ups and downs. Mol Med *5*, 71-83.

Kamura, T., Burian, D., Yan, Q., Schmidt, S. L., Lane, W. S., Querido, E., Branton, P. E., Shilatifard, A., Conaway, R. C., and Conaway, J. W. (2001). Muf1, a novel Elongin BC-interacting leucine-rich repeat protein that can assemble with Cul5 and Rbx1 to reconstitute a ubiquitin ligase. J Biol Chem *276*, 29748-29753.

Kao, C. C., Yew, P. R., and Berk, A. J. (1990). Domains required for in vitro association between the cellular p53 and the adenovirus 2 E1B 55K proteins. Virology *179*, 806-814.

Khuri, F. R., Nemunaitis, J., Ganly, I., Arseneau, J., Tannock, I. F., Romel, L., Gore, M., Ironside, J., MacDougall, R. H., Heise, C., *et al.* (2000). A controlled trial of intratumoral ONYX-015, a selectively-replicating adenovirus, in combination with cisplatin and 5-fluorouracil in patients with recurrent head and neck cancer. Nat Med *6*, 879-885.

Kindsmüller, K. (2002) Molekularbiologische Charakterisierung von Mutanten des Adenovirus Typ 5 E1B-55kDa-Proteins, Diplomarbeit, Universität Regensburg.

Kindsmuller, K., Groitl, P., Hartl, B., Blanchette, P., Hauber, J., and Dobner, T. (2007). Intranuclear targeting and nuclear export of the adenovirus E1B-55K protein are regulated by SUMO1 conjugation. Proc Natl Acad Sci U S A *104*, 6684-6689.

Kirn, D. (2001a). Clinical research results with dl1520 (Onyx-015), a replication-selective adenovirus for the treatment of cancer: what have we learned? Gene Ther *8*, 89-98.

Kirn, D. (2001b). Oncolytic virotherapy for cancer with the adenovirus dl1520 (Onyx-015): results of phase I and II trials. Expert Opin Biol Ther *1*, 525-538.

Kitchingman, G. R. (1985). Sequence of the DNA-binding protein of a human subgroup E adenovirus (type 4): comparisons with subgroup A (type 12), subgroup B (type 7), and subgroup C (type 5). Virology *146*, 90-101.

Klein, H., Maltzman, W., and Levine, A. J. (1979). Structure-function relationships of the adenovirus DNA-binding protein. J Biol Chem *254*, 11051-11060.

Kosulin, K., Haberler, C., Hainfellner, J. A., Amann, G., Lang, S., and Lion, T. (2007). Investigation of adenovirus occurrence in pediatric tumor entities. J Virol *81*, 7629-7635.

Kovalenko, A., Chable-Bessia, C., Cantarella, G., Israel, A., Wallach, D., and Courtois, G. (2003). The tumour suppressor CYLD negatively regulates NF-kappaB signalling by deubiquitination. Nature *424*, 801-805.

Krätzer, F., Rosorius, O., Heger, P., Hirschmann, N., Dobner, T., Hauber, J., and Stauber, R. H. (2000). The adenovirus type 5 E1B-55k oncoprotein is a highly active shuttle protein and shuttling is independent of E4orf6, p53 and Mdm2. Oncogene *19*, 850-857.

Kruijer, W., van Schaik, F. M., and Sussenbach, J. S. (1981). Structure and organization of the gene coding for the DNA binding protein of adenovirus type 5. Nucleic Acids Res *9*, 4439-4457.

Kubbutat, M. H., Jones, S. N., and Vousden, K. H. (1997). Regulation of p53 stability by Mdm2. Nature *387*, 299-303.

Kzhyshkowska, J., Kremmer, E., Hofmann, M., Wolf, H., and Dobner, T. (2004). Protein arginine methylation during lytic adenovirus infection. Biochem J *383*, 259-265.

Kzhyshkowska, J., Schutt, H., Liss, M., Kremmer, E., Stauber, R., Wolf, H., and Dobner, T. (2001). Heterogeneous nuclear ribonucleoprotein E1B-AP5 is methylated in its Arg-Gly-Gly (RGG) box and interacts with human arginine methyltransferase HRMT1L1. Biochem J *358*, 305-314.

Laemmli, U. K. (1970). Cleavage of structural proteins during the assembly of the head of bacteriophage T4. Nature *227*, 680-685.

Lamont, J. P., Nemunaitis, J., Kuhn, J. A., Landers, S. A., and McCarty, T. M. (2000). A prospective phase II trial of ONYX-015 adenovirus and chemotherapy in recurrent squamous cell carcinoma of the head and neck (the Baylor experience). Ann Surg Oncol *7*, 588-592.

Lane, D. P., and Crawford, L. V. (1979). T antigen is bound to a host protein in SV40-transformed cells. Nature *278*, 261-263.

Lee, H. J., Kim, M. S., Kim, Y. K., Oh, Y. K., and Baek, K. H. (2005). HAUSP, a deubiquitinating enzyme for p53, is polyubiquitinated, polyneddylated, and dimerized. FEBS Lett *579*, 4867-4872.

Lehman, T. A., Bennett, W. P., Metcalf, R. A., Welsh, J. A., Ecker, J., Modali, R. V., Ullrich, S., Romano, J. W., Appella, E., Testa, J. R., and et al. (1991). p53 mutations, ras mutations, and p53-heat shock 70 protein complexes in human lung carcinoma cell lines. Cancer Res *51*, 4090-4096.

Levine, A. J. (1990). The p53 protein and its interactions with the oncogene products of the small DNA tumor viruses. Virology *177*, 419-426.

Li, M., Brooks, C. L., Kon, N., and Gu, W. (2004). A dynamic role of HAUSP in the p53-Mdm2 pathway. Mol Cell *13*, 879-886.

Li, M., Chen, D., Shiloh, A., Luo, J., Nikolaev, A. Y., Qin, J., and Gu, W. (2002). Deubiquitination of p53 by HAUSP is an important pathway for p53 stabilization. Nature *416*, 648-653.

Lim, S. K., Shin, J. M., Kim, Y. S., and Baek, K. H. (2004). Identification and characterization of murine mHAUSP encoding a deubiquitinating enzyme that regulates the status of p53 ubiquitination. Int J Oncol *24*, 357-364.

Lindenbaum, J. O., Field, J., and Hurwitz, J. (1986). The adenovirus DNA binding protein and adenovirus DNA polymerase interact to catalyze elongation of primed DNA templates. J Biol Chem *261*, 10218-10227.

Linne, T., and Philipson, L. (1980). Further characterization of the phosphate moiety of the adenovirus type 2 DNA-binding protein. Eur J Biochem *103*, 259-270.

Liu, Y., Shevchenko, A., Shevchenko, A., and Berk, A. J. (2005). Adenovirus exploits the cellular aggresome response to accelerate inactivation of the MRN complex. J Virol *79*, 14004-14016.

Lowe, S. W., Jacks, T., Housman, D. E., and Ruley, H. E. (1994). Abrogation of oncogene-associated apoptosis allows transformation of p53-deficient cells. Proc Natl Acad Sci USA *91*, 2026-2030.

Lowe, S. W., and Ruley, H. E. (1993). Stabilization of the p53 tumor suppressor is induced by adenovirus 5 E1A and accompanies apoptosis. Genes Dev *7*, 535-545.

Mackey, J. K., Green, M., Wold, W. S. M., and Ridgen, P. (1979). Analysis of human cancer DNA for DNA sequences of human adenovirus type 4. J Natl Cancer Inst *62*, 23-26.

Mackey, J. K., Rigden, P. M., and Green, M. (1976). Do highly oncogenic group A human adenoviruses cause human cancer? Analysis of human tumors for adenovirus 12 transforming DNA sequences. Proc Natl Acad Sci USA *73*, 4657-4661.

Marine, J. C., and Jochemsen, A. G. (2004). Mdmx and Mdm2: brothers in arms? Cell Cycle *3*, 900-904.

Martin, M. E., and Berk, A. J. (1998). Adenovirus E1B 55K represses p53 activation in vitro. J Virol *72*, 3146-3154.

Maul, G. G., Ishov, A. M., and Everett, R. D. (1996). Nuclear domain 10 as preexisting potential replication start sites of herpes simplex virus type-1. Virology *217*, 67-75.

McBride, W. D., and Wiener, A. (1964). In Vitro Transformation of Hamster Kidney Cells by Human Adenovirus Type 12. Proc Soc Exp Biol Med *115*, 870-874.

Meulmeester, E., Maurice, M. M., Boutell, C., Teunisse, A. F., Ovaa, H., Abraham, T. E., Dirks, R. W., and Jochemsen, A. G. (2005a). Loss of HAUSP-mediated deubiquitination contributes to DNA damage-induced destabilization of Hdmx and Hdm2. Mol Cell *18*, 565-576.

Meulmeester, E., Pereg, Y., Shiloh, Y., and Jochemsen, A. G. (2005b). ATM-mediated phosphorylations inhibit Mdmx/Mdm2 stabilization by HAUSP in favor of p53 activation. Cell Cycle *4*, 1166-1170.

Migliorini, D., Lazzerini Denchi, E., Danovi, D., Jochemsen, A., Capillo, M., Gobbi, A., Helin, K., Pelicci, P. G., and Marine, J. C. (2002). Mdm4 (Mdmx) regulates p53-induced growth arrest and neuronal cell death during early embryonic mouse development. Mol Cell Biol *22*, 5527-5538.

Mitsudomi, T., Steinberg, S. M., Nau, M. M., Carbone, D., D'Amico, D., Bodner, H. K., Oie, H. K., Linnoila, R. I., Mulshine, J. L., Minna, J. D., and Gazdar, A. F. (1992). p53 gene mutations in non-small-lung cell cancer cell lines and their correlation with the presence of ras mutations and clinical features. Oncogene *7*, 171-180.

Modrow, S., and Falke, D. (1997). Molekulare Virologie (Heidelberg, Spektrum Akademischer Verlag GmbH).

Momand, J., Wu, H. H., and Dasgupta, G. (2000). MDM2--master regulator of the p53 tumor suppressor protein. Gene *242*, 15-29.

Momand, J., Zambetti, G. P., Olson, D. C., George, D., and Levine, A. J. (1992). The mdm-2 oncogene product forms a complex with the p53 protein and inhibits p53-mediated transactivation. Cell *69*, 1237-1245.

Mukhopadhyay, D., and Riezman, H. (2007). Proteasome-independent functions of ubiquitin in endocytosis and signaling. Science *315*, 201-205.

Muller, S., Berger, M., Lehembre, F., Seeler, J. S., Haupt, Y., and Dejean, A. (2000). c-Jun and p53 activity is modulated by SUMO-1 modification. J Biol Chem *275*, 13321-13329.

Naesens, L., Lenaerts, L., Andrei, G., Snoeck, R., Van Beers, D., Holy, A., Balzarini, J., and De Clercq, E. (2005). Antiadenovirus activities of several classes of nucleoside and nucleotide analogues. Antimicrob Agents Chemother *49*, 1010-1016.

Nalepa, G., Rolfe, M., and Harper, J. W. (2006). Drug discovery in the ubiquitin-proteasome system. Nat Rev Drug Discov *5*, 596-613.

Nemunaitis, J., Ganly, I., Khuri, F., Arseneau, J., Kuhn, J., McCarty, T., Landers, S., Maples, P., Romel, L., Randlev, B., *et al.* (2000). Selective replication and oncolysis in p53 mutant tumors with ONYX-015, an E1B-55kD gene-deleted adenovirus, in patients with advanced head and neck cancer: a phase II trial. Cancer Res *60*, 6359-6366.

Nevels, M., Spruss, T., Wolf, H., and Dobner, T. (1999). The adenovirus E4orf6 protein contributes to malignant transformation by antagonizing E1A-induced accumulation of the tumor suppressor protein p53. Oncogene *18*, 9-17.

Nijman, S. M., Luna-Vargas, M. P., Velds, A., Brummelkamp, T. R., Dirac, A. M., Sixma, T. K., and Bernards, R. (2005). A genomic and functional inventory of deubiquitinating enzymes. Cell *123*, 773-786.

O'Shea, C. C., Johnson, L., Bagus, B., Choi, S., Nicholas, C., Shen, A., Boyle, L., Pandey, K., Soria, C., Kunich, J., *et al.* (2004). Late viral RNA export, rather than p53 inactivation, determines ONYX-015 tumor selectivity. Cancer Cell *6*, 611-623.

Ornelles, D. A., and Shenk, T. (1991). Localization of the adenovirus early region 1B 55-kilodalton protein during lytic infection: association with nuclear viral inclusions requires the early region 4 34-kilodalton protein. J Virol *65*, 424-429.

Parant, J., Chavez-Reyes, A., Little, N. A., Yan, W., Reinke, V., Jochemsen, A. G., and Lozano, G. (2001). Rescue of embryonic lethality in Mdm4-null mice by loss of Trp53 suggests a nonoverlapping pathway with MDM2 to regulate p53. Nat Genet *29*, 92-95.

Philipson, L. (1961). Adenovirus assay by the fluorescent cell-counting procedure. Virology *15*, 263-268.

Querido, E., Blanchette, P., Yan, Q., Kamura, T., Morrison, M., Boivin, D., Kaelin, W. G., Conaway, R. C., Conaway, J. W., and Branton, P. E. (2001). Degradation of p53 by adenovirus E4orf6 and E1B55K proteins occurs via a novel mechanism involving a Cullin-containing complex. Genes Dev *15*, 3104-3117.

Ramos, Y. F., Stad, R., Attema, J., Peltenburg, L. T., van der Eb, A. J., and Jochemsen, A. G. (2001). Aberrant expression of HDMX proteins in tumor cells correlates with wild-type p53. Cancer Res *61*, 1839-1842.

Reich, N. C., Sarnow, P., Duprey, E., and Levine, A. J. (1983). Monoclonal antibodies which recognize native and denatured forms of the adenovirus DNA-binding protein. Virology *128*, 480-484.

Reisman, D., and Sugden, B. (1986). trans activation of an Epstein-Barr viral transcriptional enhancer by the Epstein-Barr viral nuclear antigen 1. Mol Cell Biol *6*, 3838-3846.

Rice, S. A., Klessig, D. F., and Williams, J. (1987a). Multiple effects of the 72-kDa, adenovirus-specified DNA binding protein on the efficiency of cellular transformation. Virology *156*, 366-376.

Rice, S. A., Klessig, D. F., and Williams, J. (1987b). Multiple effects of the 72-kDa, adenovirus-specified DNA binding protein on the efficiency of cellular transformation. Virology *156*, 366-376.

Ronai, Z. (2006). Balancing Mdm2 - a Daxx-HAUSP matter. Nat Cell Biol *8*, 790-791.

Rothmann, T., Hengstermann, A., Whitaker, N. J., Scheffner, M., and zur Hausen, H. (1998). Replication of ONYX-015, a potential anticancer adenovirus, is independent of p53 status in tumor cells. J Virol *72*, 9470-9478.

Ruley, H. E. (1983). Adenovirus early region 1A enables viral and cellular transforming genes to transform primary cells in culture. Nature *304*, 602-606.

Salmena, L., and Pandolfi, P. P. (2007). Changing venues for tumour suppression: balancing destruction and localization by monoubiquitylation. Nat Rev Cancer *7*, 409-413.

Sambrook, J., Fritsch, E. F. and Maniatis, T. (1989). Molecular cloning: A laboratory manual, Vol 2 (Cold Spring Harbor, Cold Spring Harbor Laboratory Press).

Santoro, C., Mermod, N., Andrews, P. C., and Tjian, R. (1988). A family of human CCAAT-box-binding proteins active in transcription and DNA replication: cloning and expression of multiple cDNAs. Nature *334*, 218-224.

Sarnow, P., Ho, Y. S., Williams, J., and Levine, A. J. (1982a). Adenovirus E1b-58kd tumor antigen and SV40 large tumor antigen are physically associated with the same 54 kd cellular protein in transformed cells. Cell *28*, 387-394.

Sarnow, P., Sullivan, C. A., and Levine, A. J. (1982b). A monoclonal antibody detecting the adenovirus type 5-E1b-58Kd tumor antigen: characterization of the E1b-58Kd tumor antigen in adenovirus-infected and -transformed cells. Virology *120*, 510-517.

Scheffner, M., Munger, K., Byrne, J. C., and Howley, P. M. (1991). The state of the p53 and retinoblastoma genes in human cervical carcinoma cell lines. Proc Natl Acad Sci U S A *88*, 5523-5527.

Shackelford, J., and Pagano, J. S. (2004). Tumor viruses and cell signaling pathways: deubiquitination versus ubiquitination. Mol Cell Biol *24*, 5089-5093.

Sharma, R. C., and Schimke, R. T. (1996). Preparation of electrocompetent E. coli using salt-free growth medium. Biotechniques *20*, 42-44.

Shen, Y., Kitzes, G., Nye, J. A., Fattaey, A., and Hermiston, T. (2001). Analyses of single-amino-acid substitution mutants of adenovirus type 5 E1B-55K protein. J Virol *75*, 4297-4307.

Sheng, Y., Saridakis, V., Sarkari, F., Duan, S., Wu, T., Arrowsmith, C. H., and Frappier, L. (2006). Molecular recognition of p53 and MDM2 by USP7/HAUSP. Nat Struct Mol Biol *13*, 285-291.

Shenk, T. (2001). Adenoviridae: the viruses and their replication. In Virology, a. P. M. H. D. M. Knipe, ed. (New York, Lippincott-Raven), pp. 2265-2300.

Sieber, T., and Dobner, T. (2007). Adenovirus type 5 early region 1B 156R protein promotes cell transformation independently of repression of p53-stimulated transcription. J Virol *81*, 95-105.

Smith, D. B., Davern, K. M., Board, P. G., Tiu, W. U., Garcia, E. G., and Mitchell, G. F. (1986). Mr 26,000 antigen of Schistosoma japonicum recognized by resistant WEHI 129/J mice is a parasite glutathione S-transferase. Proc Natl Acad Sci U S A *83*, 8703-8707.

Smith, D. B. a. C., L. M. (1998). Protocols in Molecular Biology. In Current Protocols F. M. e. a. Ausubel, eds., ed. (New York, John Wiley and Sons, Inc.), pp. 16.17.11.

Stewart, P. L., Fuller, S. D., and Burnett, R. M. (1993). Difference imaging of adenovirus: bridging the resolution gap between X-ray crystallography and electron microscopy. Embo J *12*, 2589-2599.

Stracker, T. H., Carson, C. T., and Weitzman, M. D. (2002). Adenovirus oncoproteins inactivate the Mre11-Rad50-NBS1 DNA repair complex. Nature *418*, 348-352.

Stuiver, M. H., and van der Vliet, P. C. (1990). Adenovirus DNA-binding protein forms a multimeric protein complex with double-stranded DNA and enhances binding of nuclear factor I. J Virol *64*, 379-386.

Stuurman, N., de Graaf, A., Floore, A., Josso, A., Humbel, B., de Jong, L., and van Driel, R. (1992). A monoclonal antibody recognizing nuclear matrix-associated nuclear bodies. J Cell Science *101*, 773-784.

Tang, J., Qu, L. K., Zhang, J., Wang, W., Michaelson, J. S., Degenhardt, Y. Y., El-Deiry, W. S., and Yang, X. (2006). Critical role for Daxx in regulating Mdm2. Nat Cell Biol *8*, 855-862.

Tauber, B., and Dobner, T. (2001). Adenovirus early E4 genes in viral oncogenesis. Oncogene *20*, 7847-7854.

Telling, G. C., and Williams, J. (1993). The E1B 19-kilodalton protein is not essential for transformation of rodent cells in vitro by adenovirus type 5. J Virol *67*, 1600-1611.

Temperley, S. M., and Hay, R. T. (1991). Replication of adenovirus type 4 DNA by a purified fraction from infected cells. Nucleic Acids Res *19*, 3243-3249.

Teodoro, J. G., and Branton, P. E. (1997). Regulation of p53-dependent apoptosis, transcriptional repression, and cell transformation by phosphorylation of the 55-kilodalton E1B protein of human adenovirus type 5. J Virol *71*, 3620-3627.

Trentin, J. J., Yabe, Y., and Taylor, G. (1962). The quest for human cancer viruses: a new approach to an old problem reveals cancer induction in hamster hy human adenoviruses. Science *137*, 835-849.

Trompouki, E., Hatzivassiliou, E., Tsichritzis, T., Farmer, H., Ashworth, A., and Mosialos, G. (2003). CYLD is a deubiquitinating enzyme that negatively regulates NF-kappaB activation by TNFR family members. Nature *424*, 793-796.

Tsernoglou, D., Tsugita, A., Tucker, A. D., and van der Vliet, P. C. (1985). Characterization of the chymotryptic core of the adenovirus DNA-binding protein. FEBS Lett *188*, 248-252.

Turnell, A. S., Grand, R. J. A., and Gallimore, P. H. (1999). The replicative capacities of large E1B-null group A and group C adenoviruses are independent of host cell p53 status. J Virol *73*, 2074-2083.

van den Heuvel, S. J. L., van Laar, T., The, I., and van der Eb, A. J. (1993). Large E1B proteins of adenovirus types 5 and 12 have different effects on p53 and distinct roles in cell transformation. J Virol *67*, 5226-5234.

van der Eb, A. J., and Zantema, A. (1992). Adenovirus oncogenesis. In Malignant transformation by DNA viruses, W. Dörfler, and P. Böhm, eds. (Weinheim, VCH), pp. 115-140.

Voelkerding, K., and Klessig, D. F. (1986). Identification of two nuclear subclasses of the adenovirus type 5-encoded DNA-binding protein. J Virol *60*, 353-362.

Vong, Q. P., Cao, K., Li, H. Y., Iglesias, P. A., and Zheng, Y. (2005). Chromosome alignment and segregation regulated by ubiquitination of survivin. Science *310*, 1499-1504.

Walls, T., Shankar, A. G., and Shingadia, D. (2003). Adenovirus: an increasingly important pathogen in paediatric bone marrow transplant patients. Lancet Infect Dis *3*, 79-86.

Weitzman, M. D., and Ornelles, D. A. (2005). Inactivating intracellular antiviral responses during adenovirus infection. Oncogene *24*, 7686-7696.

Wilkinson, K. D. (2000). Ubiquitination and deubiquitination: targeting of proteins for degradation by the proteasome. Semin Cell Dev Biol *11*, 141-148.

Williams, J., Williams, M., Liu, C., and Telling, G. (1995). Assessing the role of E1A in the differential oncogenicity of group A and group C human adenoviruses. Curr Top Microbiol Immunol *199*, 149-175.

Wilson, J. B., Bell, J. L., and Levine, A. J. (1996). Expression of Epstein-Barr virus nuclear antigen-1 induces B cell neoplasia in transgenic mice. Embo J *15*, 3117-3126.

Wing, S. S. (2003). Deubiquitinating enzymes--the importance of driving in reverse along the ubiquitin-proteasome pathway. Int J Biochem Cell Biol *35*, 590-605.

Woo, J. L., and Berk, A. J. (2007). Adenovirus ubiquitin-protein ligase stimulates viral late mRNA nuclear export. J Virol *81*, 575-587.

Xirodimas, D., Saville, M. K., Edling, C., Lane, D. P., and Lain, S. (2001). Different effects of p14ARF on the levels of ubiquitinated p53 and Mdm2 in vivo. Oncogene *20*, 4972-4983.

Yew, P. R., and Berk, A. J. (1992). Inhibition of p53 transactivation required for transformation by adenovirus early 1B protein. Nature *357*, 82-85.

Yew, P. R., Kao, C. C., and Berk, A. J. (1990). Dissection of functional domains in the adenovirus 2 early 1B 55K polypeptide by suppressor-linker insertional mutagenesis. Virology *179*, 795-805.

Yew, P. R., Liu, X., and Berk, A. J. (1994). Adenovirus E1B oncoprotein tethers a transcriptional repression domain to p53. Genes Dev *8*, 190-202.

Zantema, A., Fransen, J. A., Davis, O. A., Ramaekers, F. C., Vooijs, G. P., DeLeys, B., and van der Eb, A. J. (1985a). Localization of the E1B proteins of adenovirus 5 in transformed cells, as revealed by interaction with monoclonal antibodies. Virology *142*, 44-58.

Zantema, A., Schrier, P. I., Davis, O. A., van Laar, T., Vaessen, R. T., and van der Eb, A. J. (1985b). Adenovirus serotype determines association and localization of the large E1B tumor antigen with cellular tumor antigen p53 in transformed cells. Mol Cell Biol *5*, 3084-3091.

Zapata, J. M., Pawlowski, K., Haas, E., Ware, C. F., Godzik, A., and Reed, J. C. (2001). A diverse family of proteins containing tumor necrosis factor receptor-associated factor domains. J Biol Chem *276*, 24242-24252.

Zheng, N., Schulman, B. A., Song, L., Miller, J. J., Jeffrey, P. D., Wang, P., Chu, C., Koepp, D. M., Elledge, S. J., Pagano, M., *et al.* (2002). Structure of the Cul1-Rbx1-Skp1-F boxSkp2 SCF ubiquitin ligase complex. Nature *416*, 703-709.

8 Publications

I. Publications in Scientific Journals

Koyuncu E., Haertl B. and Dobner T. Usp7 regulates the stability and the functions of adenovirus E1B-55K protein, EMBO J., manuscript in preparation.

Koyuncu E. and Dobner T. Usp7 is required for efficient cell transformation by adenovirus E1A/E1B-55K proteins, J Virol., manuscript in preparation.

II. Oral Presentations at Scientific Meetings

Koyuncu E., Haertl B. and Dobner T.: "The ubiquitin-specific protease Usp7 is a target of adenovirus E1B-55K oncoprotein". Adenovirus Workshop, Hamburg, Germany, 11 - 13 February 2009.

Koyuncu E., Haertl B. and Dobner T.: "The ubiquitin-specific protease Usp7 is a target of adenovirus E1B-55K oncoprotein". Molecular Biology of DNA Tumor Viruses Conference,Madison WI, USA, 22 - 27 July 2008.

Koyuncu E. and Dobner T.: "RNA interference as a tool to study adenovirus E1A/ E1B-mediated cell transformation". ICGEB DNA Tumor Virus Meeting, Trieste, Italy, 17 - 21 July 2007.

Koyuncu E. and Dobner T.: "Investigation of the secondary structure of Adenovirus Type 5 E4 ORF3 Protein by Fourier Transform Infrared Spectroscopy". XVI. National Biophysics Congress, Ankara, Turkey, 19 - 22 September 2004.

III. Poster Presentations at Scientific Meetings

Koyuncu E., Dirlik O. and Dobner T.: 13th Balkan Biochemical Biophysical Days and Meeting on Metabolic Disorders Congress, Kusadasi, Turkey, 12 - 15 October 2003 – Poster prize awarded.

9 Acknowledgements

I would like to thank Dr. Thomas Dobner for giving me the opportunity to work in his lab, in this beautiful country, and for introducing the great world of adenoviruses. Thank you for your guidance and your support. Thanks especially for the Christmas dinners, where I felt like I am home.

I would also like to thank Dr. Hans Wolf for his support in Institut für Medizinische Mikrobiologie und Hygiene der Universität Regensburg.

I would like to thank Peter Groitl for sharing me all the techniques and hints about cloning. It was a pleasure to work with you in the summer of 2000.

I would like to thank to my lab colleagues. I can describe the time I spent with you as: *Aba Heid ist Schi!*

I would further like to thank my friend Dr. Timo Sieber. Thank you Timo for your support and friendship and for being such a kind person.

I would like to thank Led Zeppelin for writing the great song "Since I've been loving you". Without this song, I could not have completed this thesis.

I thank to my family in Ankara. Nothing accounts for the time I spent far away from you. Please accept this thesis as a gift… I miss you a lot and I love you all.

I thank to my wife, Orkide Koyuncu. There is no word describing my love for you. Thank you for all your support, patience and love. You are my everything! You give meaning to this thesis and everything I do.